



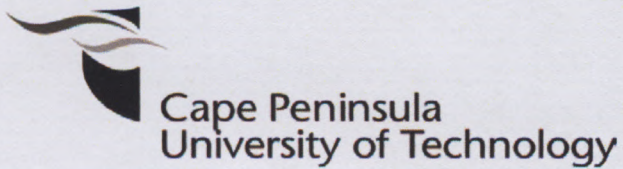
CAPE PENINSULA  
UNIVERSITY OF TECHNOLOGY



20160241

Not for loan

CPT ARC 628.12744 SHA  
(Green)



**AN INVESTIGATION INTO THE EFFECT OF DIFFERENT TYPES OF ANTI-  
SCALANT ON DESALINATION REVERSE OSMOSIS (RO) MEMBRANE FLUX**

by

**SHAMES ELHASHMI ADEL**

Thesis submitted in fulfilment of the requirements for the degree

Master of Technology: **Chemical Engineering**

in the Faculty of **Engineering**

at **Cape Peninsula University of Technology**

Supervisor: **Mr M. Aziz**

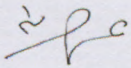
Co-supervisor: **Dr I. Goldie**

Cape Town

Data submitted: **September 2012**

***Declaration***

I, Adel Elhashmi Shames, declare that the contents of this thesis represent my own unaided work, and that the thesis has not previously been submitted for academic examination towards any qualification. Furthermore, it represents my own opinions and not necessarily those of the Cape Peninsula University of Technology.



.....  
**Signature**

Sept 2012

.....  
**Date**

## ***Acknowledgements***

I would like to express my deep and sincere appreciation to the strong influence of my supervisor Mr Aziz, for his valuable advice, enthusiasm, encouragement and patience throughout this study. I am gratefully indebted to him for his limitless supply of ideas, advice and support throughout this research.

A special thanks to Dr Ian Goldie, my co-supervisor, for his persistent guidance, and the friendly and patient manner in which he advised and assisted me in various ways during my research.

I also would like to express my gratitude to Prof Ron Sanderson for his assistance and time that he gave to me.

Thanks to Dr Margie Hurdall, for her time and help with the editing of my thesis. I would like to acknowledge Mr Akram Elkaseh and Mr Osama Bshena for their extensive experience in the membrane field and for helping me with my research.

I express my gratitude to my family. They provided me with support, enthusiasm and encouragement.

Thanking the Environmental Research Group in the Chemical Engineering Department for all their assistance.

Finally, I am extremely appreciative of the National Bureau of Research and Development in Libya for the financial support to do this research at the Cape Peninsula University of Technology.

## ***Abstract***

Recently much research and development has been done into the creation of desalination systems in South Africa, with particular emphasis on the commercialisation of desalination plants that serve local communities. This has been successful – there are currently plants running at Bitterfontien, Bushmans River Mouth and Robben Island – although membrane fouling and scaling remains a problem associated with membrane desalination, as it does worldwide

The aim of this study was to Investigate the performance of different type of antiscalants on artificially scaled membranes which we prepared inside the lab as well as on scaled membranes which were used in pilot plant. We used two type of anti-scalants in our research: Vitec 3000 and Zinc ions. The effects of these anti-scalants on the membrane were determind and the RO performances of the treated and untreated membrane compared.

A suitable autopsy procedure was established and was then used to autopsy the XLE 4040 membranes. The autopsied membranes were characterized by scanning electron microscopy (SEM) and optical microscopy (OM). The SEM and OM results clearly showed that scaling had taken place: deposits were observed for both the shell and core samples, which were not present in the images of the untreated membrane, especially when looking at high SEM images magnification.

Results also showed that the anti-scalants reduced the fouling and scaling on the membrane surface. As a result, the membrane rejection improved. Rejection and flux results indicated that commercial anti-scalant was more effective in preventing scaling than the Zinc ions. For Vitec anti-scalant case, the flux was in steady state at 36.8 l/h (5% less) after 5 hours compared to around 35 l/h (8% less) for zinc ions case. In addition; SEM images showed that less deposited particles are formed when the membrane was treated with commercial anti-scalant.

### ***List of symbols and abbreviations***

CaCO <sub>3</sub>	Calcium carbonate
CaSO <sub>4</sub>	Calcium sulphate
H	Hours
L/m <sup>2</sup> .h	Flux
MF	Microfiltration
OM	Optical microscopy
R%	Membrane retention/rejection
RO	Reverse osmosis
SEM	Scanning electron microscopy
TFC	Thin-film composite membrane
UF	Ultrafiltration
Zn <sup>2+</sup>	Zinc ions
Q <sub>p</sub>	Product water flow
Q	Volumetric flow rate
Q <sub>f</sub>	Feed flow rate

## Table of Contents

<i>Chapter 1 Introduction</i> .....	1
1.1 Introduction.....	1
1.1.1 <i>Background</i>	1
1.1.2 <i>Membrane separation processes</i>	1
1.1.3 <i>Reverse osmosis (RO)</i>	2
1.1.4 <i>Membrane fouling and scaling</i>	2
1.1.5 <i>Membrane autopsy</i>	3
1.2 Problem statement .....	3
1.3 Objectives.....	4
1.4 Methodology.....	5
1.5 Significance of this study .....	5
1.6 Delineation .....	6
<i>Chapter 2 Literature review</i> .....	7
2.1 Desalination.....	7
2.2 Membrane processes .....	7
2.3 RO and RO systems .....	8
2.3.1 <i>Reverse osmosis</i>	8
2.3.2 <i>RO systems</i>	8
2.4 RO membranes .....	9
2.4.1 <i>Historical development</i>	9
2.4.2 <i>Membrane geometries for RO Systems</i>	10
2.4.3 <i>RO membrane performance</i>	11
2.5 Membrane fouling.....	12
2.6 Membrane scaling .....	12
2.7 Prevention of membrane scaling .....	14
2.7.1 <i>General methods of inhibiting scale formation</i>	14
2.7.2 <i>Anti-scalants</i>	14



2.7.2.1	Overview	16
2.7.2.2	Chemicals	17
2.7.2.3	The use of trace metal ions as anti-scalants	19
2.7.2.4	Use of external magnetic fields	20
2.8	Membrane autopsy.....	20
2.8.1	Definition of a membrane autopsy	20
2.8.1.1	Fourier-transform infrared (FTIR) analysis	21
2.8.1.2	X-ray diffraction (XRD) analysis	22
2.8.1.3	X-ray fluorescence (XRF)	22
2.8.1.4	Scanning electron microscopy (SEM)	23
2.8.1.5	Optical microscopy (OM)	24
2.8.1.6	Atomic force microscopy (AFM)	25
2.8.1.7	Silt density index (SDI)	25
2.8.1.8	Melt flow index (MFI)	26
2.8.2	Selecting an appropriate methodology for a membrane autopsy	23
2.8.3	Membrane autopsy procedure	24

**Chapter 3 Materials and methods development of an autopsy procedure for scaled membranes ..... 30**

3.1	Introduction.....	30
3.2	Membranes .....	30
3.3	Autopsy procedure followed .....	31
3.3.1	External visual inspection	31
3.3.2	Preparation of samples for autopsy tests	31
3.3.3	Sample analysis	32
3.3.3.1	SEM analysis	32
3.3.3.2	Optical microscopy	32
3.3.3.3	Sample preparation	33
3.3.3.4	Preparation of the scaling solution	33
3.3.4	Membrane evaluation	33
3.4	RO pilot plant.....	33
3.5	RO test rig setup	35
3.5.1	Test equipment: laboratory scale	36

3.5.1.1	Experimental procedure	37
3.5.1.2	Generation of Zn <sup>2+</sup> ions	37
3.5.1.3	Constant flow Zn <sup>2+</sup> electrochemical cell generating Zn <sup>2+</sup> ions	39
<b>Chapter 4 Anti-scaling treatment of BW 30-4040 RO membranes</b>		<b>41</b>
4.1	Introduction	41
4.2	Objectives	41
4.3	Experimental	42
4.3.1	Autopsy procedure	42
4.3.2	Membranes used	42
4.3.3	Membrane element cell	42
4.4	RO results of scaled BW30-4040 membranes	42
4.4.1	Before anti-scaling treatment	42
4.4.2	After anti-scaling treatment with a commercial anti-scalant	44
4.4.3	After anti-scaling treatment with Zn <sup>2+</sup> ions (0.06 and 0.12 mg/L)	45
4.5	SEM and OM analyses of scaled BW30-4040 membranes	48
4.5.1	Without anti-scaling treatment	48
4.5.2	Anti-scaling treatment with a commercial anti-scalant	50
4.5.2.1	Experimental	50
4.5.2.2	Calculation of concentration of commercial anti-scalant	50
4.5.2.3	SEM analysis of scaled BW30-4040 membranes treated with commercial anti-scalant	51
4.6	SEM and OM analyses of scaled BW30-4040 membranes	53
4.6.1	Experimental	53
4.6.2	Calculations of zinc ion concentration	53
4.6.3	SEM results	53
4.7	Discussion	55
	Summary	59
<b>Chapter 5 Anti-scaling treatment of XLE 4040 RO membranes</b>		<b>60</b>
5.1	Introduction	60

5.2	Objectives.....	60
5.3	RO pilot plant.....	61
5.4	The Scaled XLE 4040 membrane .....	61
5.5	Experimental: Autopsy procedure .....	61
5.5.1	Membrane dissection	61
5.6	Autopsy results.....	64
5.6.1	Visual comparison	64
5.6.2	SEM results	66
5.6.2.1	Membrane treated with a commercial anti-scalant	67
5.6.2.2	Membrane treated with a commercial anti-scalant	68
5.6.2.3	Membrane terated with Zn <sup>2+</sup> ions	69
5.7	Discussion.....	70
	Summary.....	72
<b>Chapter 6 Conclusions.....</b>		<b>73</b>

## Table of Figures

Figure 2-1: Range of nominal membrane pore sizes (Alyson and Benny, 2002)	7
Figure 2-2: Schematic illustration of the RO process	8
Figure 2-3: Schematic representation of a TFC membrane	10
Figure 2-4: Spiral element construction showing feed and permeate flows, single leaf and feed spacer (Pearce, 2007) and a schematic representation of a spiral-wrap membrane (Nicolaisen, 2002)	11
Figure 2-5: (A) Amorphous and (B) crystal scale formation deposit on membrane surfaces (Dalton, et al., 2004)	15
Figure 2-6: Schematic diagram of SEM instrumentation, with an X-ray detector for chemical composition analysis. (Lindsay et al., 2000)	24
Figure 2-7: Tools used for membrane materials autopsies	25
Figure 3-1: Photograph of the membrane to be autopsied	31
Figure 3-2: Photograph of the membrane cut into four parts	31
Figure 3-3: Photograph of the autopsied part of the membrane	32
Figure 3-4: photograph of the spiral membrane RO test rig at Bitterfontein	34
Figure 3-5: Flow diagram of the RO test rig (shown Figure 3.4)	34
Figure 3-6: PFD of experimental set up when Vitec3000 was used	35
Figure 3-7: experimental set up when $Zn^{2+}$ ions was used	36
Figure 3-8: Flat cell used in RO experiments	36
Figure 3-9: A Multiparameter ion specific meter	38
Figure 3-10: Constant flow $Zn^{2+}$ electrochemical cell	39
Figure 4-1: Flux of scaled BW30-4040 RO membrane over time	43
Figure 4-2: Rejection of scaled BW30-4040 RO membrane over time	43
Figure 4-3: Flux of scaled BW30-4040 RO membrane treated with a commercial anti-scalant Vitec 3000	44
Figure 4-4: Rejection of scaled BW30-4040 RO membrane treated with a commercial anti-scalant	45
Figure 4-5: Fluxes of scaled BW30-4040 RO membranes treated with $Zn^{2+}$ ions (0.06 and 0.12 mg/L) as anti-scalant	46
Figure 4-6: Rejection of scaled BW30-4040 RO membrane treated with $Zn^{2+}$ ions (0.06 mg/L) and (0.12 mg/L)	48

Figure 4-7: SEM images of BW30-4040 membrane samples (A) after scaling and (B) untreated membrane (Mag 500x) .....	49
Figure 4-8: BW30-4040 membrane sample (A) after scaling and (B) untreated membrane (Mag. 750x).....	49
Figure 4-9: SEM images of (A) a membrane sample BW30-4040 after anti-scaling by 1m g/L Vitec 3000 commercial anti-scalant and (B) a untreated membrane (Mag. 200x).....	51
Figure 4-10: SEM images of (A) a membrane sample BW30-4040 after anti-scaling by 2 Vitec 3000 mg/L commercial anti-scalant and (B) untreated membrane (Mag. 200x).....	52
Figure 4-11: SEM images of (A) a membrane sample BW30-4040 after anti-scaling by 3 mg/L commercial anti-scalant and (B) untreated membrane (Mag. 500x).....	52
Figure 4-12: SEM images of (A) a BW30-4040 membrane after anti-scaling with 0.06 mg/L Zn <sup>2+</sup> and (B) untreated membrane (Mag. 1500x) .....	54
Figure 4-13: SEM images of (A) a BW30-4040 membrane sample after anti-scaling with 0.12 mg/L Zn <sup>2+</sup> and (B) untreated membrane (Mag. 1500x) .....	55
Figure 4-14: RO results (flux) results recorded for untreated (clean) membrane, a scaled membrane, and membranes treated with a commercial anti scalant and with Zn <sup>2+</sup> 0.12mg/L .....	56
Figure 4-15: RO results (rejection) results recorded for untreated (clean) membrane, a scaled membrane, and membranes treated with a commercial anti-scalant and with Zn <sup>2+</sup> ions at 0.12mg/L .....	57
Figure 4-16: SEM images of the surface of (A) a untreated membrane, (B) a scaled membrane, (C) membrane after using a commercial anti-scalant, and (D) membrane after using Zn <sup>2+</sup> ions at 0.12mg/L as anti-scalant (Mag. 500x) .....	59
Figure 5-1: Photograph of the membrane to be autopsied .....	62
Figure 5-2: Photograph of the membrane cut into three parts.....	62
Figure 5-3: A photograph of the autopsied part of the membrane .....	62
Figure 5-4: Photograph of the unravelled membrane sheets, cut into three parts: permeate, mid, and feed .....	63
Figure 5-5: Photograph of membrane (treated with Zn <sup>2+</sup> ions) cut into three parts .....	63

Figure 5-6: Photograph of membrane (treated with commercial anti-scalant) cut into three parts .....64

Figure 5-7: Comparison between three XLE 4040 membranes: one membrane was untreated, and the other two membranes were treated with different anti-scaling measures. ....65

Figure 5-8: An SEM image of the XLE 4040 unscaled membrane .....66

Figure 5-9: Comparison of SEM images of feed, middle and permeate side an untreated membrane (Mag. 1000x). ....67

Figure 5-10: Comparison of SEM images of feed side, middle and permeate side an membrane treated with a commercial anti-scalant (Mag. 1000x). ....68

Figure 5-11: Comparison of SEM images of feed side, middle and permeate of membrane treated with Zn<sup>2+</sup> ions (Mag. 1000x). ....69

Figure 5-12: Flux results for an untreated membrane and membranes treated with different anti-scalants (commercial anti-scalant and Zn<sup>2+</sup>) .....71

Figure 5-13: Rejection results for an untreated membrane and membranes treated with different anti-scalants (commercial anti-scalant and Zn<sup>2+</sup> ions) .....72

## **Chapter 1**

### **1.1 Introduction**

#### **1.1.1 Background**

The use of membranes has a long and noteworthy history in science. One of the earliest observers of membranes was Thomas Graham in 1861 (Michaels, 1976). Membranes became feasible for water purification in the 1960s due to the development of synthetic high-performance semi-permeable membranes. In the 1970s, exploration began into using membranes for sea water desalination due to their ability to separate water from salt water, by the pressure-driven separation process of reverse osmosis (RO). This was considered significant, particularly because increasingly high volumes of fresh water are needed in many parts of the world for agricultural, industrial and domestic use (Boubakri and Bouguecha, 2008). Subsequently, the use of RO and RO membranes has increased immensely. Today membranes can be considered as a foremost choice for water purification applications (Alyson and Benny, 2002). In reality, RO has now emerged as one of the promising large-scale processes for the economical removal of salts from sea water and brackish water, including the removal and recovery of valuable electrolytes from waste chemical process streams (Michaels, 1976; Scott and Hughes, 1996).

#### **1.1.2 Membrane separation processes**

There are several membrane processes used for water purification or desalination, e.g. reverse osmosis, nanofiltration (NF), ultrafiltration (UF) and microfiltration (MF) (Alyson and Benny, 2002). RO (or hyperfiltration) is a commonly used process for the desalination of brackish water or seawater, and advanced wastewater treatment (Michaels, 1976; Scott and Hughes, 1996; Thuy, et al., 2007).

#### **1.1.3 Reverse osmosis (RO)**

RO is the process whereby water molecules pass through a semi-permeable membrane, from the side with a low concentration of dissolved salts to the side with a higher concentration of dissolved salts, until equilibrium is reached. The semi-permeable membrane is permeable to the solvent, but not to the solute. In RO, water is forced, under

a pressure exceeding the osmotic pressure of the solution, across a semi-permeable membrane, leaving the impurities behind (Sourirajan, 1981).

#### **1.1.4 Membrane fouling and scaling**

One of the serious concerns associated with using membranes in water desalination or treatment is the presence of colloidal particles or salts, or deposits, in the feed waters, which may result in fouling (Stergios, et al., 2002) or scaling. This is the main obstacle in the performance and efficiency of RO systems (Thuy, et al., 2007).

According to the IUPAC system, fouling can be defined as follows: "The process that results in a decrease in performance of a membrane, caused by the deposition of suspended or dissolved solids on the external membrane surface, on the membrane pores, or within the membrane pores" (Koros and Shimizu, 1996). Membrane foulants are usually organic in nature.

Scaling means the deposition of particles on a membrane, causing it to plug. Typical scalants are calcium carbonate ( $\text{CaCO}_3$ ) and calcium sulphate ( $\text{CaSO}_4$ ) (Darton and Fazel, 2002). Membrane scalants are usually inorganic in nature.

Scaling of membranes can be controlled by adjusting the pH and/or adding anti-scalants, but the prevention of fouling is a much more difficult task that usually requires an intensive pre-treatment phase (Maxime et al., 2005).

The effective control of fouling or scaling requires a thorough diagnosis of the foulants because each foulant requires different means of removal (Hui et al., 2008). This is particularly important because only if the cause of the fouling can be identified can it then be effectively addressed; suitable steps can be taken to remedy it, and then recurrence of the problem can often be prevented (Ted et al., 2004). It is particularly important that researchers work on developing suitable systems to detect, and then minimise, membrane fouling and scaling, in order to obtain high quality desalinated water in the most cost-effective manner. Membrane autopsy plays an important role in the diagnosis of fouling.



### **1.1.5 Membrane autopsy**

Membrane autopsy is a destructive technique used to identify the cause of poor membrane performance caused by foulants/scalants. Researchers have performed membrane autopsies to identify these species, and also the mechanism of fouling (Butt et al., 1995; Dudley and Darton, 1996; Butt et al., 1997; Luo and Wang, 2001; Eun et al., 2003; Schneidel et al., 2005). The only way of knowing what is taking place within a membrane is to dissect it and examine/study (Ted et al., 2004) if there is any fouling/scaling.

Today, several advanced analytical techniques are also used to help scientists to be more accurate when determining the causes of fouling and the nature of membrane surface foulants (Ted et al., 2004; Boubakri and Bouguecha, 2008). These include Fourier transform infrared spectroscopy (FTIR), X-ray diffraction (XRD), X-ray photoelectron spectroscopy (XPS), energy dispersive X-ray spectroscopy (EDX), X-ray fluorescence (XRF), scanning electron microscopy (SEM), optical microscopy (OM), atomic force microscopy (AFM), silt density index (SDI) determination and melt flow index (MFI) determination.

## **1.2 Problem statement**

Membrane fouling and scaling are considered to be the main causes of membrane system failure. Membrane fouling is caused by a number of different foulants, including organic and inorganic matter. Scaling occurs when the membranes become blocked due to the increase in concentration of dissolved salts (normally carbonate salts).

Anti-scaling material can be used to improve the performance of membrane systems and reduce the cleaning frequencies, and subsequently extend the life of the system.

Membrane autopsy is considered as one of the procedures to identify the type of fouling in a membrane system, after which possible solutions can be considered.

### 1.3 Objectives

The overall objectives of this study are:

1. Develop a membrane autopsy procedure for the membranes under test conditions.
2. Generate  $Zn^{2+}$  ions in a laboratory at two different concentrations by using an electrochemical cell to be evaluated as anti-scalants.
3. Analyse membrane surfaces using scan electron microscopy (SEM) and optical microscope (OM) in order to study the morphology of the membrane surface before and after scaling, and after treatment of the scaled membranes with the anti-scalants under investigation.
4. The RO performances of the membranes (flux and rejection) are to be determined in the presence and absence of two anti-scalants, a commercial Vitec 3000 (Avista Technologies, 2004) and  $Zn^{2+}$  ions (generated in the laboratory using an electrochemical cell) (Yuan et al., 2009). Anti-scaling performance on the membrane surface, rejection and flux measurements are to be compared.
5. Using a laboratory-scale flat cell to Investigate the efficiency of the two anti-scalants: (Vitec 3000) and  $Zn^{2+}$  ions) on the BW30-4040 polyamide membrane after causing its scaling by a feed solution containing  $CaCl_2$ ,  $MgSO_4$  and  $NaHCO_3$ . The investigation is to be done by carrying out membrane autopsies on treated and untreated BW30-4040 polyamide membrane
6. To study the severity of scaling of three XLE 4040 polyamide membranes that were used in a pilot plant at Bitterfontein by carrying out membrane autopsies. One of these membranes was to be treated with a commercial anti-scalant and one with  $Zn^{2+}$  ions. The third one is an untreated membrane. After the autopsies SEM and OM were to be used to determine any differences between these membranes, in terms of the type of scaling and the efficiency of the respective anti-scalants.

### 1.4 Methodology

1. Two different concentrations of  $Zn^{2+}$  ions generated in the laboratory were used to create an artificial scale on the membranes surface.
2. Thereafter a comparison of the surface and performance of one type of membrane (BW 30-4040) in the laboratory using a synthetic feed with a flat cell configuration with untreated, commercial anti-scalant and  $Zn^{2+}$  ions was evaluated.

3. Additionally, to compare the performance of one type of membrane using a pilot plant on site (existing brackish water desalination plant) over a 3 month period using raw water (underground water) to investigate and study the efficiency of the membrane.

### **1.5 Significance of this study**

A membrane autopsy was used in this study to identify the cause of fouling/scaling problems caused by different organic and inorganic matter on membrane surfaces during RO. Knowledge of the type of foulants or scalants enables researchers to suggest suitable recommendations for further, plant modifications or various cleaning procedures, to improve membrane performance.

The target of this study, however, was to compare between the efficiency of two anti-scalants. The first is an existing commercial Vitec 3000 and the second is a Laboratory generated  $Zn^{2+}$  ions, which has good anti-scalant properties as reported by (Yuan et al., 2009).

The mechanisms used to quantify the examination of antiscalant effects, based on the membrane performance and topology, were membrane autopsy, (eg. SEM and OM), rejection and flux.

### **1.6 Delineation**

This research project focus on 2 types of antiscalant:  $Zn^{2+}$  ions & Vitec, using TFC polyamide RO membrane with brackish water using XLE 4040 and BW3040. All other are delineated.

## Chapter 2

### Literature review

#### 2.1 Desalination

Desalination refers to a process of water purification by removing excess salts and minerals from water. Water desalination processes to produce potable water may be divided into three principal categories: membrane technologies, thermal technologies and chemical approaches. Membrane technology has become the common separation technology because it does not require the addition of chemicals, the energy used is relatively low, and process conditions are easy and efficient (Mulder, 1996).

#### 2.2 Membrane processes

The different pressure-driven membrane processes of reverse osmosis, nanofiltration, ultrafiltration and microfiltration differ in several features, including the membrane pore diameter, as shown in Figure 2-1 (Alyson and Benny, 2002).

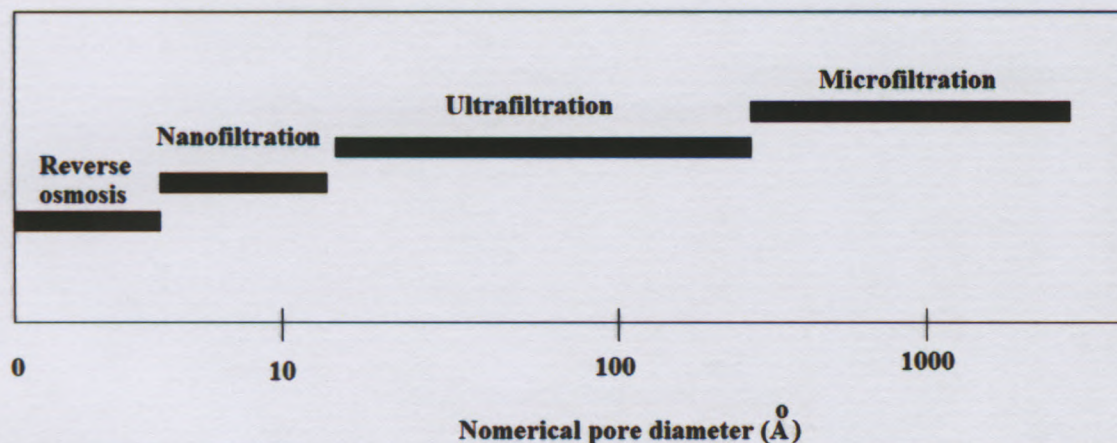


Figure 2-1: Range of nominal membrane pore sizes (Adopted from Alyson and Benny, 2002)

RO is increasingly used in water treatment (including desalination and advanced wastewater treatment) because it offers a reliable and efficient production of high quality water, in an environmentally friendly manner (Hilal et al., 2003; Roever and Huisman, 2007; Trana et al., 2007).

## 2.3 RO and RO systems

### 2.3.1 Reverse osmosis

According to Johnson et al. (2002), RO is the process whereby water molecules pass through a semi-permeable membrane, from the side with a low concentration of dissolved salts to the side with a higher concentration of dissolved salts, until equilibrium is reached. In RO the normal osmotic flow of water across a permselective membrane is reversed by exerting an applied pressure. The semi-permeable membrane is permeable to the solvent, but not to the solute. Water is forced under a pressure exceeding the osmotic pressure of the feed solution, across a semi-permeable membrane, leaving the salts behind. A schematic diagram of the RO process is shown in Figure 2.2. The process is able to remove the salts in one step. Due to the high osmotic pressure of seawater, usually the operating pressures required for RO desalination systems are very high (up to 100 bars).

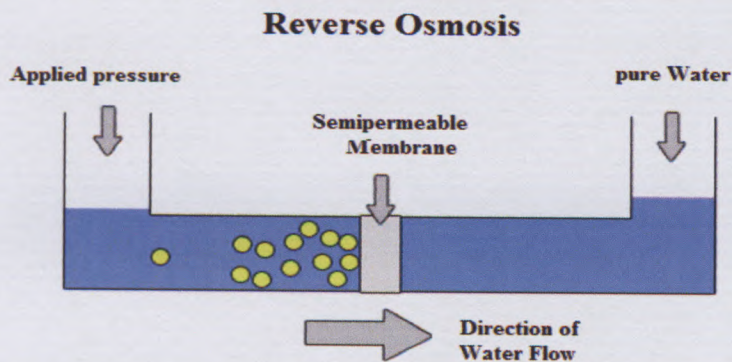


Figure 2.2: Schematic illustration of the RO process

### 2.3.2 RO systems

RO systems typically comprise the following elements: a feed tank, a high-pressure pump, tubing, a pre-treatment system, the membrane assembly, a post-treatment system, and brine disposal.

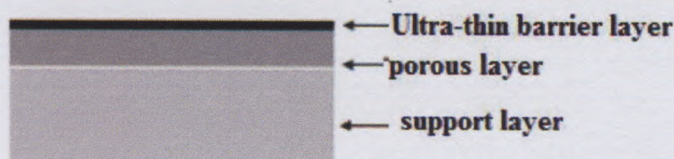
## 2.4 RO membranes

### 2.4.1 Historical development

The osmotic phenomenon has been known for a very long time. The breakthrough in RO was indebted to the development of the Loeb-Sourirajan asymmetric cellulose acetate (CA) membrane in 1960 (Loeb and Sourirajan, 1963; Masahiko et al., 1997; Menlo, 1997). As a result of this development, water desalination using these membranes became a potentially practical process. Asymmetric CA membranes were the industry standard through the

1960s to the mid-1970s (Cadotte, 1981). In 1972, an interfacial polymerisation method was developed at North Star Research, USA, by Rozelle and Cadotte, for producing composite membranes (Cadotte and Rozelle, 1972; Cadotte and Petersen, 1975; Cadotte, 1981). RO Membranes with high RO performances were made from cross-linked aromatic polyamide composites. These were widely used in sea water and brackish water desalination and in the production of ultra pure water during the 1990s (Masahiko et al., 1997). Since then, researchers have focused on further improving the performance and efficiency of these membranes, in order to meet the world's increasing demands and for high-quality water. RO, NF, MF, UF and electrodialysis are currently established separation processes, with large plants installed worldwide (Menlo, 1997).

The most widely used type of RO membrane today is the thin-film composite (TFC) polyamide membrane. TFC membranes comprise an ultra-thin (20–200 nm) permselective layer of polymer deposited and insolubilised on the surface of a microporous substrate membrane, typically polysulphone (Figure 3-3). The latter acts only as a support for the very thin film; it does not contribute to the salt retention and performance of the thin skin active layer. Interfacial polycondensation is widely used to create polyamide TFC membranes (Cadotte and Petersen, 1975; Cadotte, 1985).



**Figure 2.3: Schematic representation of a TFC membrane**

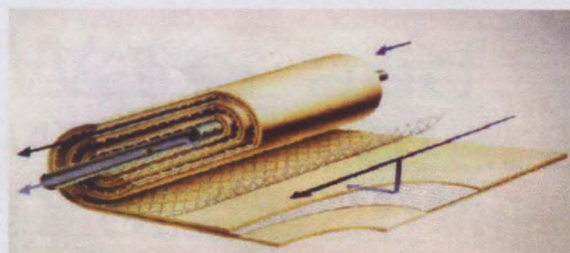
A summary of features of RO membranes is tabulated in Table 2:1.

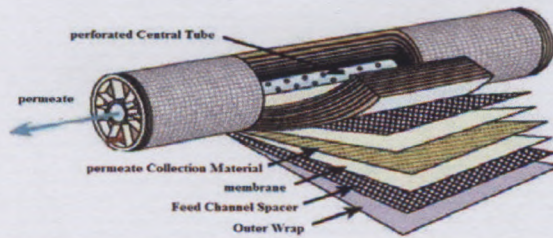
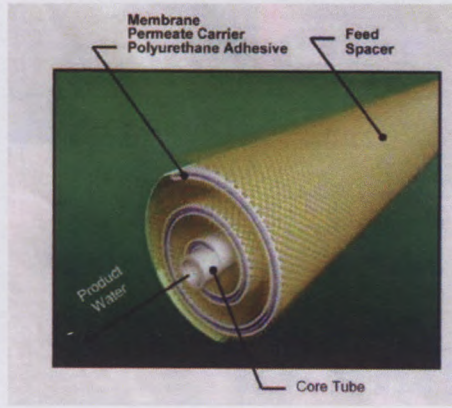
**Table 2.1: Features of RO membranes (Mulder,1996)**

<b>Membrane type</b>	Asymmetric or composite
<b>Thickness</b>	Sub layer 150 $\mu\text{m}$ ; top layer 1 $\mu\text{m}$ (asymmetric)
<b>Pore size</b>	< 2 nm
<b>Driving force</b>	Pressure: brackish water 15-25 bar Sea water 40-80 bar
<b>Separation principle</b>	Solution–diffusion
<b>Membrane material</b>	Cellulose triacetate, aromatic polyamide, polyamide and poly(ether urea) (interfacial polymerisation)
<b>Main applications</b>	Desalination of brackish water and sea water Desalination of ultra-pure water (electronic industry) Concentration of food juice and sugars (food industry)

#### 2.4.2 Membrane geometries for RO Systems

There are several different types of membrane geometries: flat-sheets, tubes, capillaries and spiral-wraps. The spiral-wrap membrane element configuration is widely used due to its high packing density and relatively low price (Nicolaisen, 2002). Spiral-wrap membranes consist of two layers of membrane, placed onto a permeate collector. This membrane envelope is wrapped around a centrally placed permeate drain. The feed channel is placed at moderate height, to prevent plugging of the membrane unit. Photographs of spiral-wrap modules, illustrating the geometry, are shown in Figure 2.4: below.





**Figure 2-4: Spiral element construction showing feed and permeate flows, single leaf and feed spacer (Pearce, 2007) and a schematic representation of a spiral-wrap membrane (Nicolaisen, 2002)**

### 2.4.3 RO membrane performance

The three most important RO membrane performance parameters are; salt rejection, flux/productivity and recovery. RO membranes are typically defined in terms of the solute retention, or rejection (Scott and Hughes, 1996). Rejection is the percentage of solids removed from the system feed water by the membrane. The desalination of seawater is more challenging than brackish water because rejection must be approximately 98% in order to obtain a suitable product. Rejection (R) can be determined by the following equation:

$$R\% = 100 \left( 1 - \frac{C_p}{C_r} \right) \quad \text{Equation 2.1}$$

where R is the percent rejection, and  $C_r$  and  $C_p$  are solute concentrations in the feed and permeate, respectively (Zazouli et al., 2008).

According to Odhav, (2004), membrane flux is the volume of solvent transported through the membrane per unit time and is directly proportional to the effective pressure, normally expressed in terms of  $L/m^2 \cdot h$  (Lmh). An increase in pressure leads to an increased flux



(output). Flux can be calculated from the ratio between the permeate flux (Q) and the membrane surface area (A), as follows:

$$Flux = \frac{Q}{A}$$

Equation 2.2

The permeate flux decline (PFD) is defined as the percentage of reduced permeate flux compared to initial permeate flux, calculated as follows (Zazouli et al., 2008):

$$PFD(\%) = \left(1 - \frac{J}{J_0}\right) \times 100$$

Equation 2.3

Where:  $J_0$  is the initial permeate flux at filtration start time and  $J$  is the permeate flux at filtration time  $t$ .

Permeate flux is important because higher fluxes mean requiring shorter operation times, which reduces the cost of operating a RO system (Cengeloglu et al., 2008). On the other hand, the higher the flux is, the sooner the membrane surface will become coated with fouling material (Norman et al., 2008). Recovery can be defined as the percentage of a membrane system's feed water that emerges from the system as product water or "permeate". Membrane system design is based on expected feed water quality, and recovery is fixed through the initial adjustment of valves on the concentrate stream. Recovery is often fixed at the highest level that maximises permeate flow while preventing precipitation of supersaturated salts within the membrane system (Shun, 2007). Water recovery for most RO plants is designed in the range of 75–90% for brackish water and 30–50% for seawater (Shun, 2007).

$$Recovery = \frac{Q_p}{Q_f} \times 100$$

Equation 2.4

Where:  $Q_p$  is the product water flow rate and  $Q_f$  is the feed water flow rate.

Operating parameters such as operating pressure, temperature, feed concentration and pH can affect the performance of RO membranes. For example, as the water temperature increases the water flux increases almost linearly, due primarily to the higher diffusion rate of water through the membrane. Higher pH values may cause a lower permeate flux. On the other hand, the higher the operating pressure the greater will be the permeate flux (Myzairah, 2007).

## 2.5 Membrane fouling

Membrane fouling can significantly increase the cost of a membrane system as well as reduce its reliability. Therefore, fouling is costly and leads to a much shorter life of the membrane elements. This limitation has been the cause of a much recent development in membrane science. Several approaches have been used to try and minimise the effects of fouling.

Polymer chemists are developing many new membranes that have “low fouling” characteristics. Several techniques are used, such as altering the zeta potential or amount of ionic charge of the membrane surface. Another method is modifying the thermodynamic potential of the membrane surface by using low surface energy materials that reduce the chemical free energy change upon absorption of foulants (Norman, 2008)

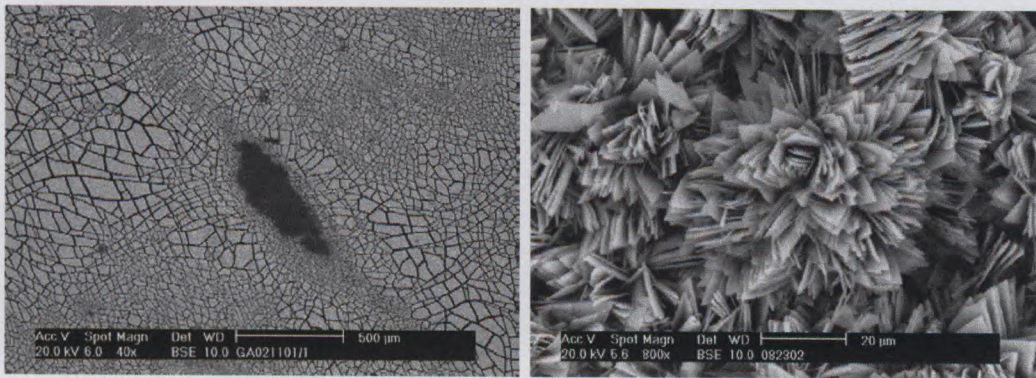
Another method of combating fouling is by affecting the fluid dynamics at or near the membrane surface. Membrane systems use aggressive tangential flow in order to help reduce the thickness of diffusion polarisation layers of foulants, as well as colloidal films that can form on the membrane. Since static dead-end media will simply retain particles or ions left behind as the water is removed, it is only a matter of time until the rejected material must be physically removed (Mulder, 1996).

Membrane fouling is a process that results in a decrease in membrane performance, caused by the deposition of suspended or dissolved solids on the external membrane surface, on the membrane pores, or within the membrane pores (Koros, 1996). Fouling results in the need for frequent cleaning of a membrane. Careful attention must therefore be given to the problem of membrane fouling. Several approaches have been used to try and minimize the effects of fouling. Membrane autopsies (see Section 2.8) were carried out in this study, to identify fouling occurrence.

## 2.6 Membrane scaling

Scaling means the deposition of particles on a membrane surface and in the pores, causing it to become blocked. Scale formation is one of the major factors limiting the application of RO membranes. A high recovery is needed in membrane separation processes, such as RO, because high conversion means a high percentage of feed water will be converted to the desired product. Scaling causes the nominal flux and the process efficiency to decrease, and consequently, the process needs higher energy, and an increased cleaning frequency, resulting in the membrane water treatment process becoming more expensive (Johnson and Culkin. 2002). Scaling not only reduces membrane flux and retention, but also shortens the membrane life. It has always been recognised as a serious constraint in designing and operating RO systems. Membrane scaling is caused as a result of the build

up of dissolved salts on the membrane surface (Chesters et al., 2007). Figure 2.5 shows SEM images of scale formation deposits on membrane surfaces (Dalton, et al., 2004). RO processes typically concentrate dissolved salts on the feed side by permitting the water molecules to pass through the membrane, while retaining the salt molecules. When the brine concentration is very high, the solubility limits of these salts may be exceeded when the water is further concentrated. This results in precipitation of the dissolved salts. According to Johnson et al. (2002) the most common forms of minerals scale are: calcium carbonate, calcium sulphate, calcium phosphate, barium sulphate, iron hydroxide silicon dioxide (silica).



**Figure 2.5: (A) Amorphous and (B) crystal scale formation deposit on membrane surfaces (Dalton, et al., 2004)**

Concentration polarization can occur due to the accumulation of retained species at the membrane surface which is a consequence of the membrane separation. In the low-pressure membrane processes the retained species will be particulate, colloidal, and macromolecular, depending on the membrane pore size. The localized accumulation on the membrane is polarization; either particle polarization or concentration polarization (applies to dissolved species).

In general, it is agreed upon that the concentration polarization depends strongly on fluid dynamics, membrane characteristics, and temperature. These parameters can be reduced by increasing the flow rates of the fluids (i.e., feed and/or permeate velocities), with the inclusion of turbulence promoters in the membrane module channels, by decreasing the section of fluid channels, by using spacer-filled channels. To prevent excessive concentration polarization mass transfer rates at the feed boundary layer must be sufficient that can lead to membrane wetting by scaling and building up of salt crystals or minerals on the membrane surface. Some authors considered the use of spacer-filled channels of the plate-and-frame membrane modules in both the feed or permeate side of the

membrane. However, this may lead to a decrease of the membrane surface area and therefore to the flux (Mulder, M., 1996).

## **2.7 Prevention of membrane scaling**

### **2.7.1 General methods of inhibiting scale formation**

There are several ways of inhibiting scale formation, such as: ion exchange, increasing the fluid velocity; pH control, acidification by addition of sulphuric acid or hydrochloric acid to precipitate and prevent  $\text{CaCO}_3$  scale formation and to remove low solubility solutes (e.g. calcium, barium, and silica) from the feed water and anti-scalant chemical addition to keep the solutes in a supersaturated state. A difficulty associated with using anti-scalants is however, finding the most suitable anti-scalant for a specific scaling mineral, and then the associated increased cost of the water processing system.

### **2.7.2 Anti-scalants**

Anti-scalants are surface active materials that interfere with one of the crystal growth stages in three primary ways:

- Threshold effect: amounts of anti-scalants prevent the precipitation of salts that have exceeded their solubility products, e.g. the commercial anti-scalant, Vitec 3000 (Drak et al., 2000; Avista Technologies, 2004).
- Crystal distortion effect: anti-scalants interfere with the normal crystal growth to produce an irregular crystal structure with poor scale-forming ability, e.g.  $\text{Zn}^{2+}$  ions, (Goldie et al., 2008).
- Dispersions: a surface charge is placed on the crystal. Comparable charges cause the crystals to repel one other.

An ideal anti-scalant for RO membranes should offer the following features (Goldie et al., 2008):

- Compatible with the RO membrane, and should not foul it.
- Approved by institutional agencies and drinking water authorities.
- Provide effective control of  $\text{CaCO}_3$ , calcium sulphate, barium sulphate, strontium sulphate, calcium fluoride and silica.
- Exhibit good tolerance to aluminium, iron and manganese oxides.

- Its use should result in the maintenance of membrane surfaces by dispersing particulate foulants.
- Effective in feed water over a wide pH range.
- Exhibit high stability in the feed water over a wide temperature range.
- Effective for bio-growth control, within its formulation, to protect against biological fouling.
- Compatible with coagulants and/or coagulant aids (polyelectrolytes) used in the pre-treatment stage because incompatible materials may cause membrane fouling.

### 2.7.2.1 Chemicals

Anti-scalant chemicals are generally added to the RO feed water to prevent precipitation and scaling in the RO system. Although anti-scalant chemicals are effective, it is difficult to predict the maximum concentrations of the sparingly soluble solutes in excess of recorded solubility limits that can be tolerated with anti-scalant chemicals.

Anti-scalants with broad activity are currently available. The industry standard for scale control treatment is the inorganic phosphate sodium hexametaphosphate (SHMP). It acts by inhibiting the growth of  $\text{CaCO}_3$  crystals. Carbonate-based scales can be controlled by  $\text{H}_2\text{SO}_4$  injection and maintaining the saline feed pH in the range 4–6, whereas sulphate-based scales are prevented by the addition of SHMP (Chesters, 2007). Other anti-scalants include sodium tripolyphosphate and sodium polyacrylate (Goldie et al., 2008). However, the use of these chemicals has certain drawbacks which include acid-induced corrosion in the system and biofouling of the system. Furthermore, these chemicals act as a breeding ground for bacteria.

Advanced organic anti-scalants have recently been developed and tested. They are non-corrosive, have a long shelf-life, and are claimed to be technically and economically competitive with traditional anti-scalant treatments. Different anti-scalants are selected on the basis of the simultaneous control of calcium, strontium and barium sulphate, calcium fluoride, reactive silica, iron, aluminium, and heavy metal scales, where acidification of feedwater is not necessary (Goldie et al., 2008).

Vitec 3000 (Avista Technologies) is a liquid anti-scalant used to inhibit silica, sulphate, and carbonate scales and disperse colloidal particles in RO and nanofiltration membrane systems. It has a different scale control ranges which can be changed from one type of

mineral to another, such as  $\text{CaCO}_3$ ,  $\text{CaSO}_4$ , barium sulphate, and calcium fluoride (Nkosikho, 2008).

Vitec 3000 anti-scalant offers a variety of critical performance and application benefits (Avista Technologies, 2004):

- Powerful inhibitor against a variety of carbonate and sulphate scale.
- Highly effective in a wide range of feed water types and pH ranges.
- Crystal modification properties which effectively distorts inorganic salt crystal growth, reducing system fouling.
- Compatible with polyelectrolyte coagulants.
- Threshold scale inhibition at low dosage rates allows economical system operation. The formulation has been certified by the National Sanitation Foundation (NSF) under ANSI/NSF Standard 60 for use in potable water production. This formulation is compatible with organic coagulants. Coagulants may be indirectly present in municipal feed waters or directly present as a result of coagulation or flocculation treatments upstream of the RO system. Vitec 3000 can be injected as is or diluted and can be used in a wide array of feed water sources (Avista Technologies, 2004; Nkosikho, 2008).

There are two further possible methods of scale prevention: the use of trace amounts of metal ions in the feed and the use of external magnetic fields.

#### 2.7.2.2 The use of trace metal ions as anti-scalants

It has been shown, on laboratory and pilot plant scale, that the use of specific concentrations of  $\text{Zn}^{2+}$  ions can inhibit scale formation in RO feed water by changing the scale crystal structure (Goldie et al., 2008; Coetzee et al., 1998). The presence of  $\text{Zn}^{2+}$  ions induces scale suppression effects substantially similar to those of organic anti-scalants.

Zinc ions generated from electrochemical was done by immersing zinc metal into sodium chloride solution ( $\text{NaCl}$ ), where zinc metal quickly becomes covered with small bubbles. This was achieved through oxidation and reduction process zinc metal and sodium chloride solution.

Based on findings at higher voltages zinc concentration in increased solution. The higher the voltage, the sooner saturation occurs or process comes to halt. Continuation of process

(zinc ion generation), at higher voltages, generates more metal attacks rather than zinc ions. (Coetzee et al.1998).

Scale formation can be suppressed by adding metallic ions. For instance, dissolved copper ions inhibit the growth of  $\text{CaCO}_3$  crystals. The active growth sides of  $\text{CaCO}_3$  are blocked by dominated  $\text{CaCO}_3$  complex. Iron ions in other hand cause the formation of  $\text{CaCO}_3$  in the aragonite crystal form. Magnesium ions adsorbing at the growth sites of the crystal surface and formation of different polymorphs within the precipitation of calcium carbonate carbonate may also be affected by the presence of impurities on the kinetics of the crystal growth.

According to Yang et al. (2005), metallic ion impurities, notably  $\text{Zn}^{2+}$  ions, can hinder  $\text{CaCO}_3$  precipitation from hard water and alter crystal morphology. This study has also shown that  $\text{Zn}^{2+}$  causes a substantial increase in induction time and induces the formation of  $\text{CaCO}_3$  in the aragonite form rather than the calcite form.

The main advantages of using  $\text{Zn}^{2+}$  ions are that they can be conveniently dosed (e.g. as Cu–Zn alloy), they are environmentally friendly they are much lower running cost, availability of  $\text{Zn}^{2+}$  metal, easy and cheap to generate  $\text{Zn}^{2+}$  ions with different concentrations and do not raise a problem in concentrate waste disposal. Additionally the product water meets drinking water criteria with upper limit of 5 ppm in drinking water due to a taste the ions impart to water when above 5 ppm.( Yang et al., 2005).

### 2.7.2.3 Use of external magnetic fields

It has also been shown that physical water conditioners treat water using magnetic, electrolytic, or other electromagnetic processes. These devices 'stabilise' the hardness in minerals, which leads to a reduction or prevention of the build-up of hard scale. In actual fact, the generation of magnetic fields to prevent  $\text{CaCO}_3$  scalants through the use of magnetic treatment devices on the feed line to the RO membrane is a controversial science. On a laboratory scale a distinct improvement in the prevention of flux-limiting scale was achieved, but this was not observed on a pilot plant scale (Goldie et al., 2008).

## 2.8 Membrane autopsy

### 2.8.1 Definition of a membrane autopsy

Membrane autopsy is a technique used to identify the cause of poor membrane performance. The idea of membrane autopsy is as old as membranes themselves. The

only way of knowing what is taking place inside the membrane is to perform an autopsy (Koros and Shimizu, 1996) to determine whether there is fouling, scaling and any other operational problems. Membrane autopsy is considered an accurate method available to analyse foulants on a membrane surface in order to identify the causes of fouling or scaling (Chesters, 2007).

Membrane autopsies are offered by most membrane manufacturers, and by water treatment companies, e.g. Nalco, at its PermaCare Centre, Mfg (Canadian) (Lisitsin et al., 2005). Generally, an autopsy includes observation of the degree of fouling, collection of deposits for chemical and microbiological analysis, and evaluates the integrity of the membrane surface.

A statistical review of 150 membrane autopsies was reported by Dalton et al., 2004. Their conclusions indicated three features: (i) although every membrane has a biofilm, it is seldom a problem when bacteria are present at  $<10^4$  cfu/cm<sup>2</sup> of membrane surface; (ii) the use of chlorination and dechlorination has no discernable benefit on membrane performance in terms of reduced biofilm; (iii) the most common foulant is an organic biofilm followed by iron and silica which is invariably associated with aluminium and to a lesser extent iron.

Membrane autopsy requires that a used membrane be removed from the desalination plant and then analysed, to determine the nature of membrane fouling, i.e. the foulant present on the membrane surface. An autopsy investigation usually involves dissecting of the membrane – hence it is a destructive process. Foulant samples are obtained from the membrane surface and used in further analytical procedures, which include chemical and microbiological analyses. Sophisticated analytical techniques such as Fourier transmission infrared (FTIR), X-ray photoelectron spectroscopy (XPS), energy dispersive X-ray (EDX), scanning electron microscopy (SEM) and Optical Microscopy (OM) are used to characterise membrane surface foulant (Koros, 1996; Chesters, 2007). Other techniques such as X-ray diffraction (XRD), X-ray fluorescence (XRF), atomic force microscopy (AFM), silt density index (SDI) determination and melt flow index (MFI) determination can be used.

Autopsy analysis results, can be used to make correlations between fouling and the resultant membrane performance, and then recommendations can be made to RO plant operators, with specific regards to the process engineering aspects of the plant, e.g. pre-treatment required and/or plant modification.



### 2.8.1.1 Fourier-transform infrared (FTIR) analysis

FTIR analysis involves scanning a sample by IR radiation. FTIR is a common tool used to analyse the chemical composition of a product. FTIR spectroscopy can be used to identify the functional groups of organic material depositing on a membrane surface. To obtain an infrared spectrum a sample has to be prepared in a translucent film or be physically mixed with a salt that when pressed will give a translucent window through which an infrared beam can be passed and the absorbance of this beam can be measured.

According to Leenheer et al. (2000), when a membrane is fouled the FTIR peaks of the clean membrane change in their absorbance intensity, indicating the covering of the original clean surface by the functional groups of foulants. The resulting spectra can be compared with a library of spectra of numerous organic compounds, in efforts to identify the chemical functionalities present in the foulant.

### 2.8.1.2 X-ray diffraction (XRD) analysis

The advantage of using the XRD analysis is to determine the chemical nature and relative amounts of the scales deposited on the membranes, such as  $\text{CaCO}_3$ ,  $\text{CaSO}_4$  and  $\text{SrSO}_4$ . X-ray diffraction (XRD) determines the geometry or shape of a molecule using X-rays. X-ray diffraction techniques are based on the elastic scattering of X-rays from structures that have long-range order. The most comprehensive description of scattering from crystals is given by the dynamical theory of diffraction. XRD is a technique used to characterise the crystallographic structure, crystallite size (grain size), and preferred orientation in polycrystalline or powdered solid samples. It is commonly used to identify unknown substances, by comparing diffraction data against a database maintained by the International Centre for Diffraction Data. It may also be used to characterize heterogeneous solid mixtures to determine relative abundance of crystalline compounds.

Shon et al (2009) used SEM/EDX analysis to identify inorganic membrane fouling on membrane SR Aromatic polyamides. A SEM image of a cross-section of the RO membrane indicated a fouling thickness of approximately 0.1  $\mu\text{m}$ . Detailed elemental analysis results showed that the clean membrane consisted of carbon (C), oxygen (O) and sulphur (S) originating from the components of the polyamide membrane polymer and polysulphone support, but EDX results of fouled membranes showed different elements on the fouled membrane surface. The relative fraction of the carbon decreased, while sodium (Na), magnesium (Mg), chlorine (Cl) and iron (Fe) elements were found in the foulants on the fouled membrane surface. Wilf (2007) reported that the decrease of carbon content, as

observed by EDX, was due to the foulant layer, while the increase of oxygen content was due to a component of oxides (Si, Al) and iron hydroxides.

#### 2.8.1.3 X-ray fluorescence (XRF)

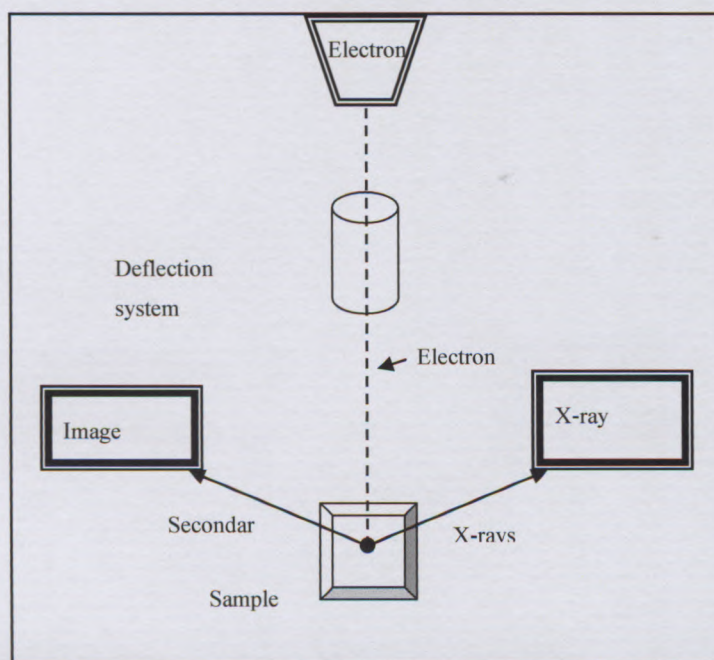
In XRF the inner shell electrons are transferred to an outer shell or removed completely. The empty inner shell that remains is 'filled' with electrons from an outer shell of the atom. During the de-excitation process, an electron moves from a higher energy level to fill the vacancy. The energy difference between the two shells appears as an X-ray, emitted by the atom. The X-ray spectrum acquired during the above process reveals a number of characteristic peaks. The energy of the peaks leads to the identification of the elements present in the sample (qualitative analysis), while the peak intensity provides the relevant or absolute elemental concentration (semi-quantitative or quantitative analysis).

Butt et al., (1997) conducted an autopsy of fouled membranes using visual inspection, OM, SEM, XRD, and XRF. They found that XRF was a very helpful technique to identify the scaling. Pontie et al., (2005) have used XRF to reveal thick deposits of calcium/magnesium phosphonate on stage 1 permeator fibres formed by the reaction of the inhibitor with  $\text{Ca}^{2+}$  ions of the brine.

#### 2.8.1.4 Scanning electron microscopy (SEM)

Topography or morphology is an important surface characteristic that influences the physical properties of materials, such as wettability, adhesibility and biocompatibility. SEM provides valuable information about the three-dimensional microstructure of surfaces. Any type of dry specimen can be analysed by this technique (Fay et al., 2005).

SEM uses electrons as a source, to produce high resolution images. Figure 2-6 shows a typical SEM setup. Samples are placed in a vacuum chamber, which contains an electron gun. The emitted electrons travel through a series of magnetic lenses designed to focus the electrons on a very fine spot on the sample. As the electron beam hits the sample, secondary electrons are released that can be detected (Lindsay 2000). Due to the shallow penetration depth of the primary electrons, only the secondary electrons generated near the surface can escape and are detected. A detector counts these electrons and sends the signal to an amplifier and the final image is built from the number of electrons emitted from each scanned point. Samples have to be electrically conductive to be suitable for SEM imaging. The surfaces of non-conductive samples, such as polymers, need to be coated with a thin layer of gold to minimise negative charge accumulation from the electron beam.



**Figure 2.6: Schematic diagram of SEM instrumentation, with an X-ray detector for chemical composition analysis. (Lindsay et al., 2000)**

Butt et al. (1995) used SEM and XRD analyses to show the bulk of the scale deposits to be amorphous in nature. John et al. (1997) used SEM; Laser Ionisation Mass Analysis (LIMA) and Matrix-assisted Laser Desorption/Ionisation (MALDI) techniques in four case studies to identify inorganic and organic foulants on the surfaces of the membranes.

### 2.8.1.5 Optical microscopy (OM)

OM can identify many foulants by their colour, size, crystalline structure, or other characteristic. Well-known examples of foulants that can be recognized by optical microscopy are iron oxide (by its colour, size, and agglomerate nature) and bacteria (by their shape, size, and movement). The use of OM for membrane autopsy is limited by the fact that a transparent sample is required. The latter can be obtained by removing the foulants from the membrane and mounting them on a glass slide.

OM produces images of solid samples at magnification levels much lower than the levels achieved with SEM. There is no need for the sample to be coated. The objective lens is, at its simplest, a very high powered magnifying glass, i.e. a lens with a very short focal length. This is brought very close to the specimen being examined so that the light from the specimen comes to focus about 160 mm inside the microscope tube. This creates an enlarged image of the subject. This image is inverted and can be seen by removing the eyepiece and placing a piece of tracing paper over the end of the tube. By carefully

focusing a rather dim specimen, a highly enlarged image can be seen. It is this real image that is viewed by the eyepiece lens that provides further enlargement.

Butt et al., (1997) used many techniques including OM to identify scales on a commercial RO desalination plant. Although, this analytical technique is qualitative in nature, they found a predominance of iron sludge. OM showed that foulant/scaling deposits are overwhelmingly amorphous in nature.

#### 2.8.1.6 Atomic force microscopy (AFM)

AFM is one of the most powerful techniques for surface analysis. It is a member of the family of scanning probe microscopes which can be used to study a wide variety of material surfaces, e.g. coatings, ceramics, composites, glasses, synthetic and biological membranes, metals and polymers. AFM is a rich information technique, which provides images of the surface topography and morphology on a nanometre scale. It can also be used to study properties such as hardness, adhesion, abrasion, friction and many other physical properties.

To obtain an AFM image, a fine tip is raster-scanned across a surface with a feedback control that enables the determination of inter-atomic forces acting between the tip and the sample surface. A topographical image is acquired by keeping this force at a constant value. The tips are mainly manufactured from silicon nitride or silicon, and mounted on the end of a soft, flexible cantilever. A laser beam is focused onto the back of this cantilever and reflected by a mirror into a segmented photo detector. As the tip traces the surface of the sample, moving up and down, it follows the surface features, depending on the attractive or repulsive forces, and the voltage measured in the photo detector varies.

#### 2.8.1.7 Silt density index (SDI)

The SDI is a commonly used indicator to predict a feed water's potential to foul a membrane, by colloidal particles smaller than 0.45  $\mu\text{m}$ . It is however, only a guide for pre-treatment (not an indication of adequate pre-treatment). The SDI is a static measurement of resistance, which is determined for samples taken at the beginning and at the end of the test (Baker, 2004). SDI values of less than one means that the RO systems can run for several years without colloidal fouling. Brackish water will typically have an SDI less than three, whereas sea water will have significantly high SDI with values of 6-20. SDI values  $<3$  means that the system can run for several months between cleanings. SDI values of 3-5 means that particulate fouling is likely to be a problem and frequent, regular cleaning will be

needed. SDI values  $>5$  are unacceptable, and it indicates that additional treatment is needed to make the water feed acceptable.

#### 2.8.1.8 Melt flow index (MFI)

The MFI is determined using the same apparatus and procedure as used for SDI determination (Schippers and Verdouw, 1980). The MFI is based only on the cake filtration mechanism, and has a linear relation with colloidal matter concentration. MFI relies strongly on the pore size of the membrane, and particle diameter and particle concentration (Baker, 2004). MFI increases with decreasing particle and pore diameter, and increasing particle concentration.

### 2.8.2 Selecting an appropriate methodology for a membrane autopsy

Problems in a membrane plant can occur anywhere in the system, but in general will either be prominent on the lead or concentrate elements. Problems occurring due to material being carried into the system, such as colloidal or particulate materials will be trapped on the lead element. Problems that occur within the system, such as scaling, will be prevalent depending on the concentration of these elements, as this is where the salt concentrations are highest. There are two techniques that can be used to solve this problem: destructive tests which require the membrane casing to be opened, and non-destructive tests which are carried out without opening the membrane. The advantage of a non-destructive autopsy is the element may be re-used, with the disadvantage that the range of analytical techniques used to analyse scaling/fouling is much smaller. This may indicate that non-destructive testing is not able to identify the problems with sufficient certainty (Jefferies and Champion, 2009).

Visually inspecting the elements from these positions may be sufficient to identify which elements to select for autopsy. Failing this, it is recommended to select an element from the feed position and one from the concentrate position for inspection. Based on the non-destructive testing, the element which best reflects the problems seen on site can then be autopsied. However, the only accurate method of determining the organic, mineral and microbiological deposits within the membranes is to carry out destructive autopsy procedures to analyse foulants on the membrane surface (Boubakri and Bouguecha, 2008).

### 2.8.3 Membrane autopsy procedure

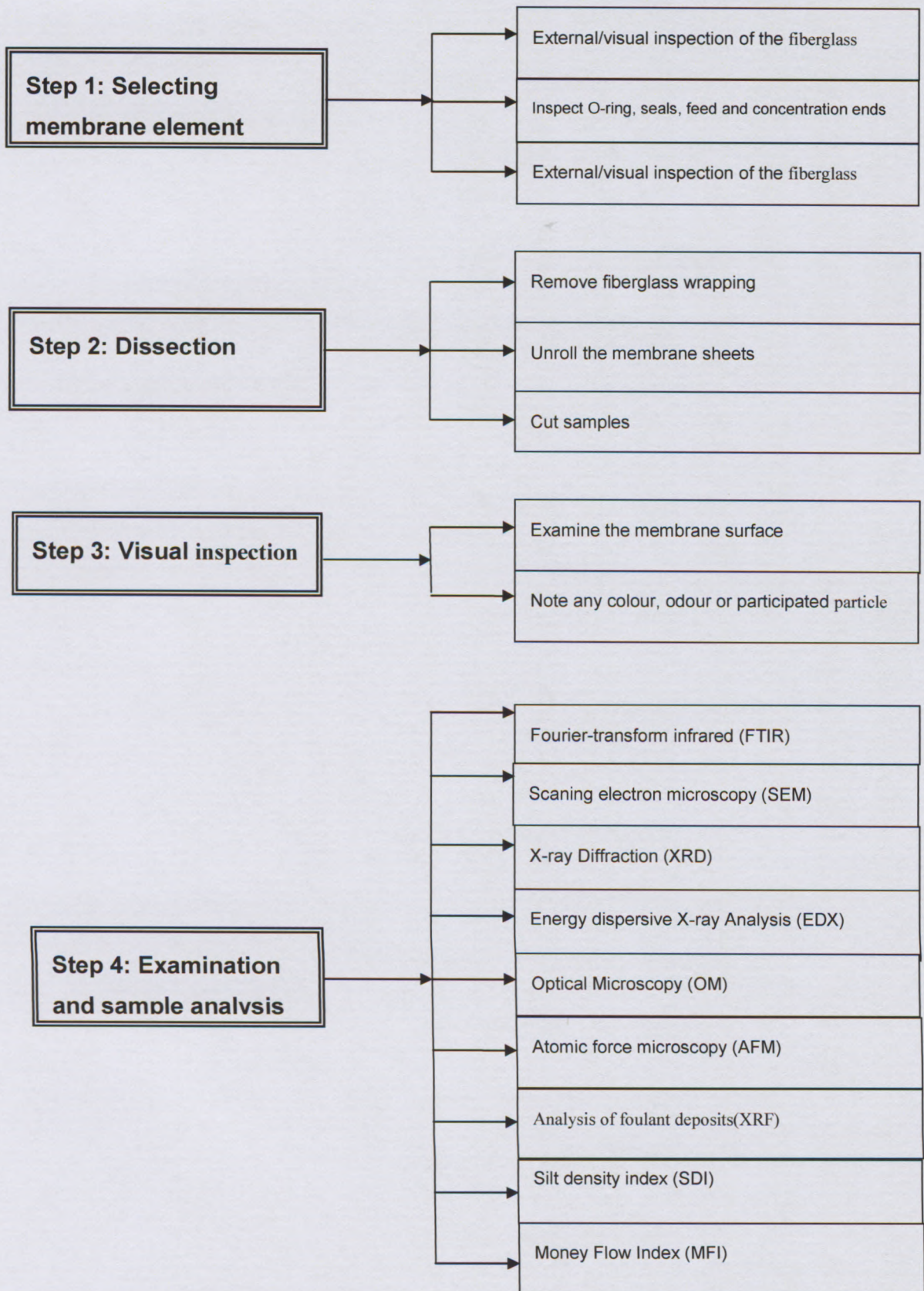
A membrane autopsy comprises numerous steps and procedures. Before any physical dissection is carried out the membrane element must be visually examined. The following steps should be followed:

1. Examine the membrane element visually, by external and internal inspection;
2. Remove the fibreglass wrapping;
3. Use a power saw to remove the ends and slice through the fibreglass sleeve;
4. Unroll the membrane sheets;
5. Carry out a visual inspection of the unrolled membranes to examine the glue lines and the membrane surface, and note any colouring, precipitated material or odour. For an efficient inspection, a comparison must be made between the fouled membrane and an unused one. The fouled material with foulant is then collected for further analysis.

The following additional steps can be used to identify foulants and membrane integrity:

1. Loss of ignition testing (LOI): This procedure is used to obtain an indication of organic versus inorganic fouling material.
2. Dye testing: Dye can be used to mark damaged areas of membranes, and detect pinholes. It can also mark the uptake of chlorine (used in pre-treatment).
3. Summarising test results – identifying foulants and likely causes of the problem – and making recommendations for remedial action, e.g. what cleaning agents to use and any structural modifications required to the RO plant itself.

The tools used for membrane materials autopsies are illustrated below:



**Figure 2-7: Tools used for membrane materials autopsies**

## Chapter 3

### Materials and methods development of an autopsy procedure for scaled membranes

#### 3.1 Introduction

The maximum recovery of the feed water mainly depends on the salinity and scaling potential of the source water. As described in Chapter 2, scaling occurs when the minerals (such as dissolved salts) left behind on the rejection side of the membrane are concentrated to a level at which they begin to form crystalline compounds on the membrane surface, which in turn plug the membrane pores and interfaces. Scaling can make the treatment processing expensive and shorten the operation life of a membrane.

In South Africa, RO desalination systems are being used to treat groundwater in several areas, for example, along the West Coast and at Bitterfontein (Southern Cape). Scale formation is a problematic issue, and anti-scaling chemicals are required to reduce or prevent scaling on the membrane surface in these desalination systems. This in turn increases the costs.

Membrane autopsies were carried out on membranes, in the laboratory and in the field, after being used in a RO pilot plant at Bitterfontein. SEM and OM analysis were used to analyse the membrane surfaces because of their high significance and availability.

The experimental details of an autopsy procedure for the scaled membranes are described in this chapter.

#### 3.2 Membranes

Scaling was caused in a untreated BW30-4040 polyamide membrane by a synthetic feed solution containing  $\text{CaCl}_2$ ,  $\text{MgSO}_4$  and  $\text{NaHCO}_3$ , using a laboratory-scale flat cell.

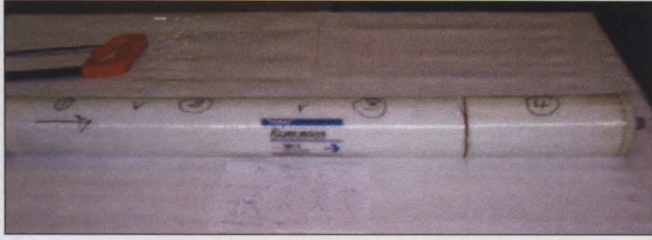
#### 3.3 Autopsy procedure followed

##### 3.3.1 External visual inspection

External visual inspection of the BW30-4040 polyamide membranes (before removing the fibre glass wrapping) was carried out to observe any damage or defects of the O-rings and the brine seal. The external inspection also included inspecting the feed, the concentrate



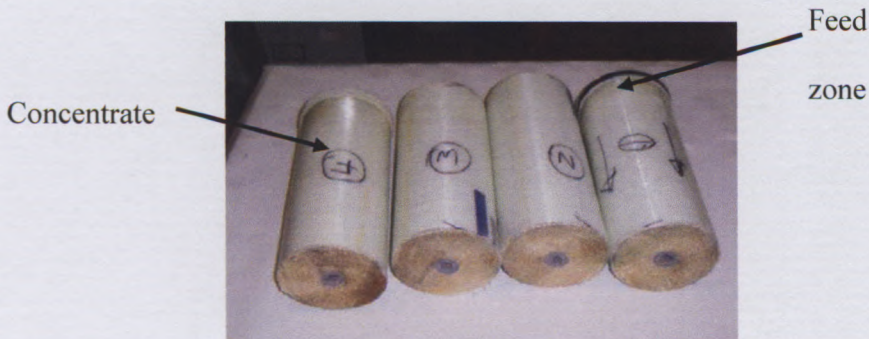
ends, and the outer fibreglass wrapping to identify the deposits on the membrane surface. A photograph of the membrane to be autopsied is shown in Figure 3.1.



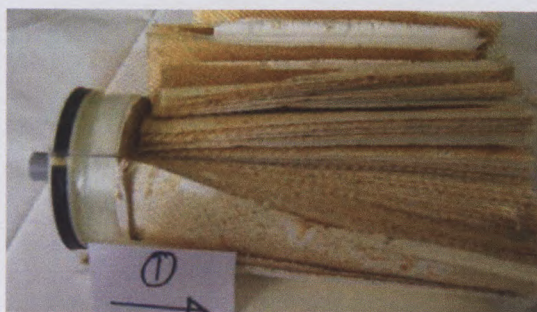
**Figure 3.1: Photograph of the membrane to be autopsied**

### 3.3.2 Preparation of samples for autopsy tests

The membrane element was cut, using a saw, into four zones; each zone was 20 cm long. Each zone was opened by slicing the ends and removing the fibreglass housing. Then each zone was unrolled and the spacer was carefully removed. The four zones are shown in Figure 3-2. Two samples were taken from each zone: one sample was taken close to the membrane shell and one was taken close to the core (see Figure 3-3). Both sides of the membrane were analysed. OM and SEM images of all the cut samples were recorded.



**Figure 3-2: Photograph of the membrane cut into four parts**



**Figure 3-3: Photograph of the autopsied part of the membrane**

A total of eight samples were analysed and labelled to distinguish between the membrane samples. Labelling was such that the code 1S was given to the sample taken closest to the shell side (S) in Zone 1.

### **3.3.3 Sample analysis**

SEM and OM were used to analyse the samples in order to determine the nature of the scalants and foulants.

#### **3.3.3.1 SEM analysis**

SEM analysis was carried out to obtain a qualitative assessment of the types of the foulants deposited on the membrane surface. Four different magnifications were used: 500x, 700x, 900x and 1500x. Imaging of the samples and analysis of the phase compositions was accomplished using a Leo® 1430VP SEM apparatus at Stellenbosch University. Prior to imaging or analysis, the samples were sputter-coated with gold.

#### **3.3.3.2 Optical microscopy**

The light microscope used in this study was a Carl Zeiss model, Axiolab, connected to a CCD-IRIS SONY type digital camera to capture the images. Two different magnifications were used: 470x and 2660x to compare each sample.

#### **3.3.3.3 Sample preparation**

Samples were prepared by cutting small pieces (2 cm x 2cm) from the membrane sheet. A total of eight samples were cut for each membrane: four from the shell side and four from the core side along the four zones (see Figure 3-2). The samples were dried at room temperature for 24 h, before analysis.

The samples were mounted on a small stub with double-sided carbon tape make handling easier, and then the sempleces were mounted on the SEM stage. The samples were then coated with a thin layer of gold which did not change the shape or hide any openings or details on the sample. This made the sample surface electrically conductive so that the negative electrons can be conducted to the stage of the microscope.

#### 3.3.3.4 Preparation of the scaling solution

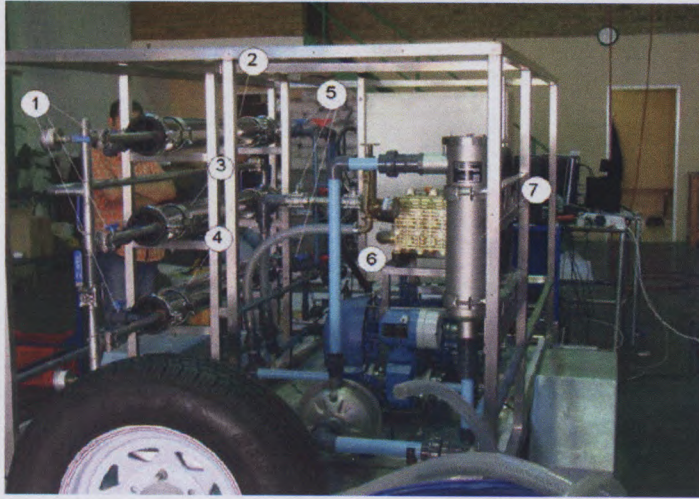
A synthetic scaling solution was prepared by adding  $\text{CaCl}_2$  (61mg/L),  $\text{MgSO}_4$ , (5mg/L) and  $\text{NaHCO}_3$  (51mg/L) to 100 L water in the feed tank and stirring for at least one hour, before use. This combination of this solution mainly generates  $\text{CaCO}_3$  crystals (Lisitsin et al., 2005).

### 3.3.4 Membrane evaluation

#### 3.4 RO pilot plant

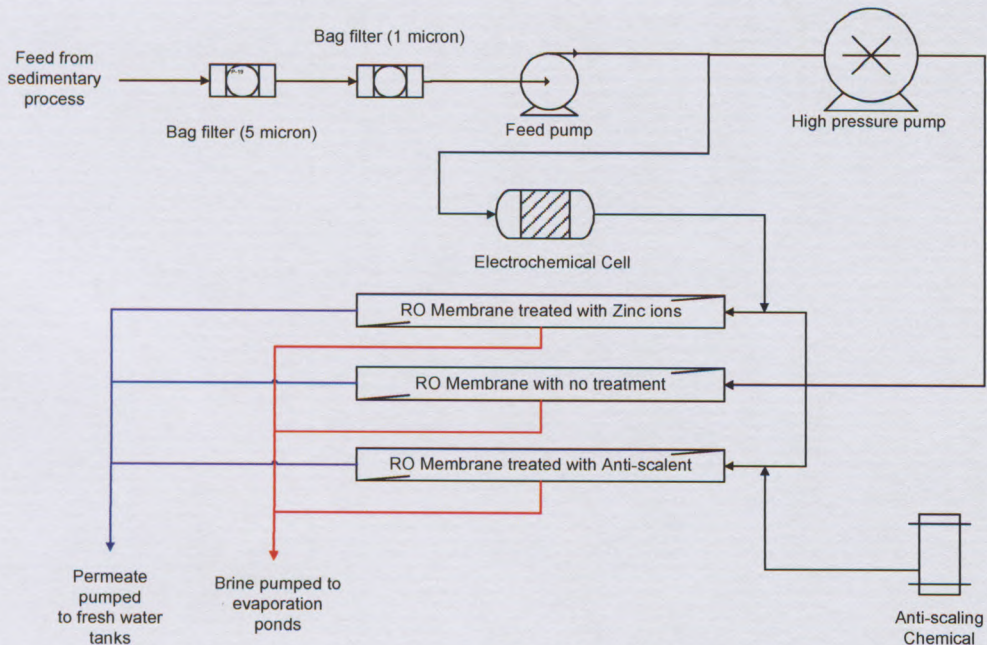
The required experiments to evaluate the performance and effectiveness of the spiral wrap membrane elements and the evaluation of the anti-scaling chemicals were undertaken on a mobile pilot RO plant. A pilot plant with three XLE4040 membranes was used in the investigation, one membrane was (unused), and the other two membranes were treated with different anti-scaling measures (a commercial anti-scalant and  $\text{Zn}^{2+}$  ions).

A photograph of the spiral membrane test rig that was used to evaluate membrane performance in terms of salt retention and permeate flux at Bitterfontein is shown in Figure 3.3, and the flow diagram of the plant is shown in Figure 3.4.



**Figure 3-4: Photograph of the spiral membrane RO test rig at Bitterfontein**

- |                                      |                       |
|--------------------------------------|-----------------------|
| 1: Feed valves                       | 5: Reject valves      |
| 2: XLE 4040 membrane (untreated)     | 6: High pressure pump |
| 3: XLE 4040 membrane (Vitec treated) | 7: Cartridge filter   |
| 4: XLE 4040 membrane (Zn treated)    |                       |



**Figure 3-5: Flow diagram of the RO test rig (shown in Figure 3.4).**

### 3.5 RO test rig setup

The RO test rig setup comprised a feed tank, RO cell body, feed spacer, permeate carrier, shim, electrical stirrer and the membrane. Experiments were conducted in a continuous process. Two filters were linked to the tap water, to reduce the amount of dissolved salts on the tap water. The hydraulic hand kit pump was prepared, where permeate carrier, membrane element, feed spacer and shim, were cut to fit the membrane element cell. The pressure was 25 bar on the cell holder and 10 bar at the hydraulic. The feed flow control valve and the bypass flow control valve were open. The pump speed was 25 volts and the flow rate was 2800 mL/min. The flow rate was measured by using the concentrator and permeates as both outlet of the cell, to give the input of the cell. The RO test results were recorded every 30 minutes for 5 hours. A schematic of the RO test rig is shown in Figure 3.5.

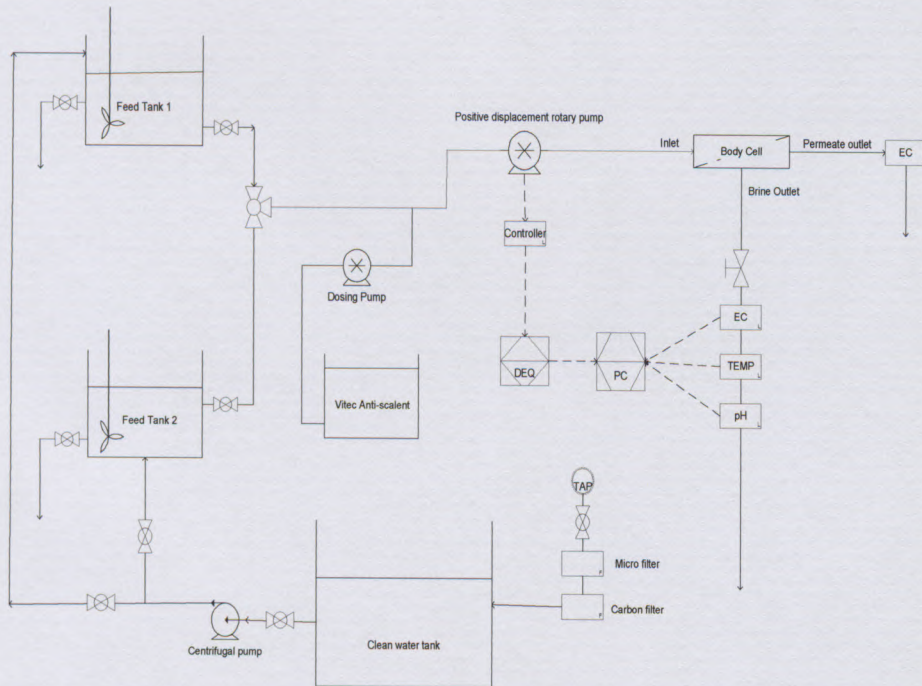
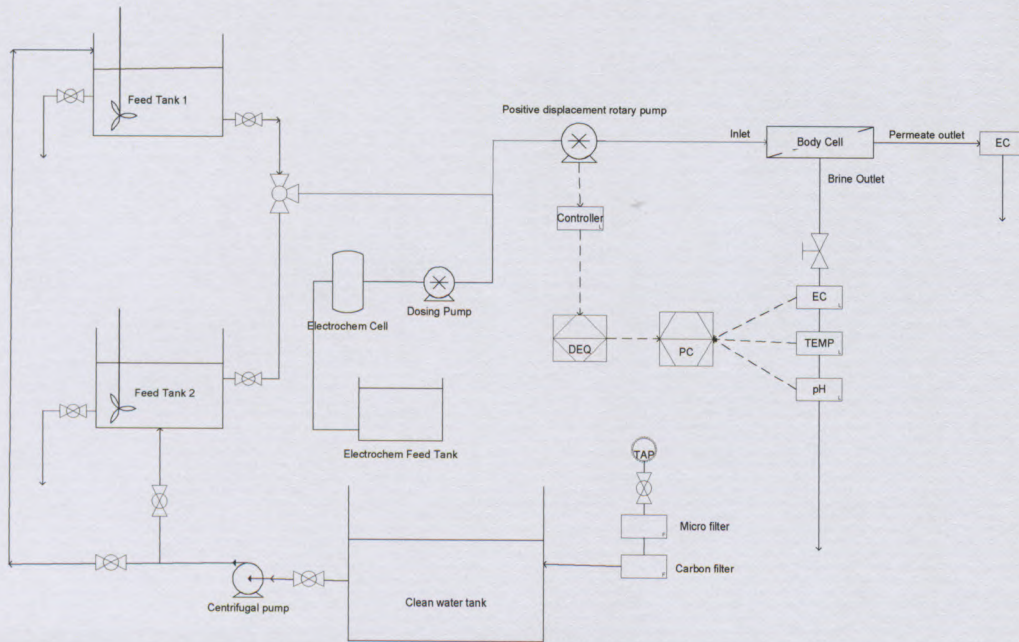


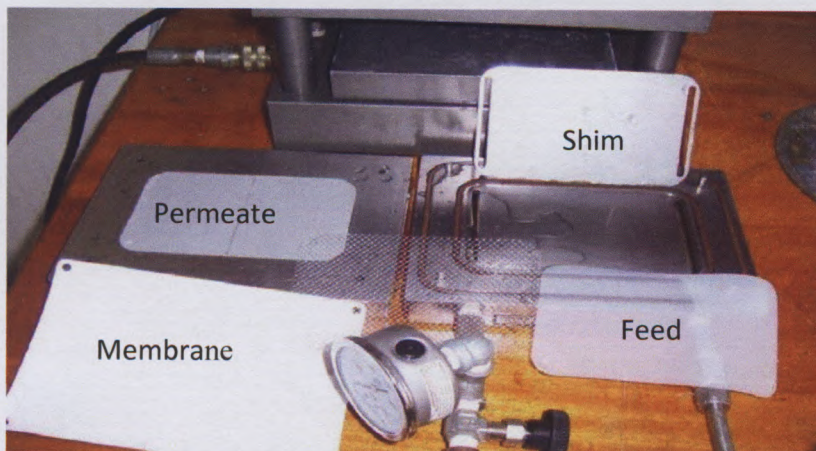
Figure 3-6: PFD of experimental set up when Vitec 3000 was used



**Figure 3-7: experimental set up when  $Zn^{2+}$  ions was used**

### 3.5.1 Test equipment: laboratory scale

A laboratory scale investigation was performed to monitor and quantify the occurrence of the scaling in brackish water BW30-4040 polyamide membranes. The feed solution contained three types of scalants:  $CaCl_2$ ,  $MgSO_4$  and  $NaHCO_3$ . A flat RO test cell was used to determine the flux and rejection rate of the above membranes (see Figure 3.5). The purpose of the test cell was to see the performance of the membrane with Vitec 3000 and  $Zn^{2+}$  ions anti-scalant and not in terms of water or brine recovery.



**Figure 3-8: Flat cell used in RO experiments**

### 3.5.1.1 Experimental procedure

The following procedure was followed to first cause scaling of the BW30-4040 membrane in a flat cell.

- The feed tank was filled with 95 L water. Specific quantities of  $\text{CaCl}_2$  (61g),  $\text{MgSO}_4$  (5 g) and  $\text{NaHCO}_3$  (51g) were added to a 5 L of water in a container and was shaken for 2 mins till all the salts were dissolved in water then added to the feed tank to increase the salt water concentration to 2000 mg/L.
- The membrane element, feed spacer and shim, were cut as the same membrane element cell dimensions. The sample and the spacer were placed on top of the wetted shim and then sealed.
- The hydraulic pump was set at 25 bar to seal the element cell.
- The mixture in the tank was allowed to mix for an hour before feeding the cell.
- The pump speed was set to 25 volts and the flow rate was adjusted for different flow rates.
- A dosing pump was used to dose the Vitec3000 and  $\text{Zn}^{+2}$  ions as seen in figure 3.6.
- A dosing pump was used to dose the  $\text{Zn}^{+2}$  ions before the high pressure pump as can see in figure 3.7.
- The results were recorded every 15 minutes for 5 hours.

For each operational period the flux and rejection data were logged by a computer and recorded in an Excel spreadsheet for analysis.

### 3.5.1.2 Generation of $\text{Zn}^{2+}$ ions

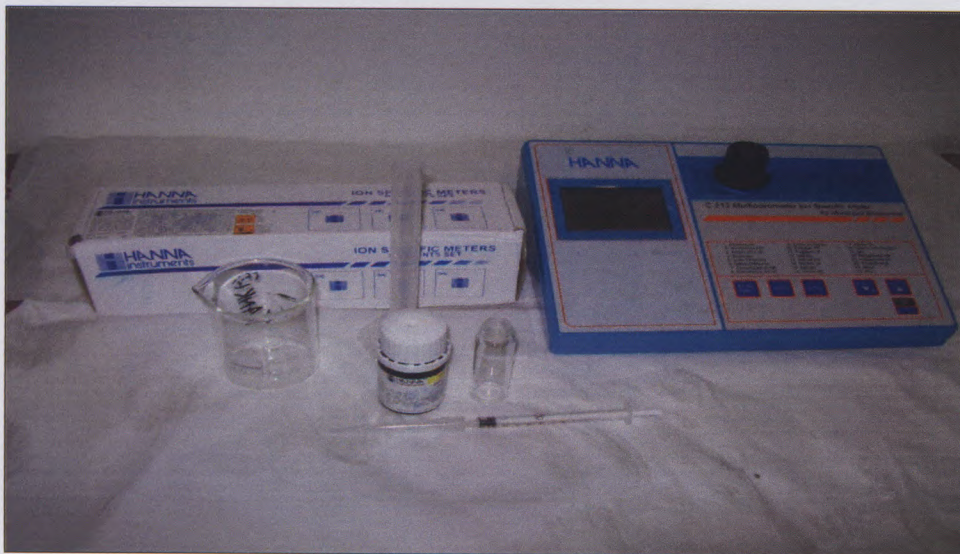
Measurement of  $\text{Zn}^{2+}$  ions in solution

The following apparatus and reagents were used to measure the  $\text{Zn}^{2+}$  ions in solution:

A Multi-parameter ion specific meter (see Figure 3-8), 10 mL syringe, 50 mL beaker, cuvette with stopper, soft cloth, 'Reagent A', 'Reagent B', and cyclohexanone.

- A 20 mL sample was poured into a beaker, followed by the addition of one packet of Reagent A.

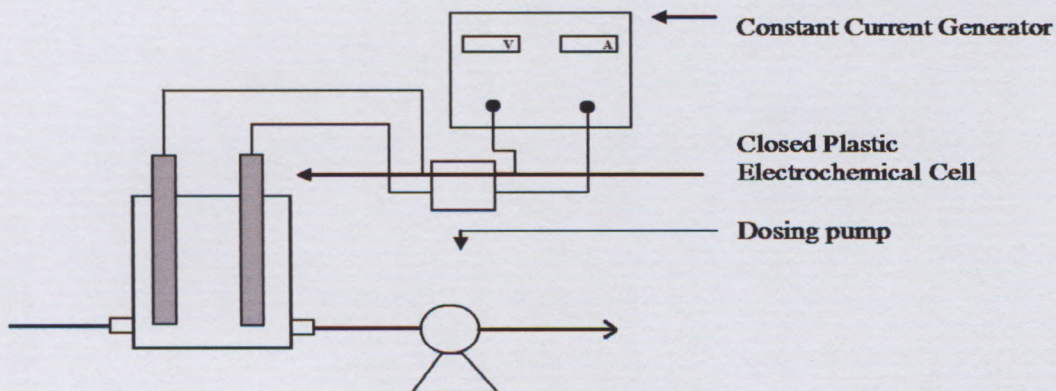
- The content turned orange. The beaker was slowly swirled until all the solids were dissolved.
- The multiparameter ion specific meter was switched on and the appropriate program was selected to read  $Zn^{2+}$  ions. (This program is the mechanism that adjusts the appropriate wavelength to read  $Zn^{2+}$  ion concentration.)
- A 10 mL sample was poured into a clean cuvette, which was then covered with a secure stopper, and then inserted into the ion specific meter. The validation took a few seconds.
- The cuvette was then removed and 0.5 mL Reagent B was added, using a measuring syringe.
- The sealed cuvette was reinserted into the meter. A measured concentration was displayed after approximately



**Figure 3-9: A Multiparameter ion specific meter**



### 3.5.1.3 Constant flow $Zn^{2+}$ electrochemical cell generating $Zn^{2+}$ ions



**Figure 3-10: Constant flow  $Zn^{2+}$  electrochemical cell**

Apparatus:

- Plastic electrochemical housing,
- 2 x  $Zn^{2+}$  bars,
- relay switch,
- dosing pump,
- connecting wires,
- Stopwatch.

Method:

The dosing pump feed pipe was inserted into real brackish water and the pump started. The flow of water through the electrochemical cell was then calculated. After this the volts and amps were then set on the Constant current generator and the stopwatch started. A sample was taken every 10 minutes and the  $Zn^{2+}$  concentration measured by according to the procedure described in

Section 3-9.

The volts, amps, flow rate and  $Zn^{2+}$  concentration were recorded for every 10 min. This experiment was repeated by using different volt and amp settings to determine the optimum point for  $Zn^{2+}$  generation

In this study, two different concentrations of  $Zn^{2+}$  ions (0.06 mg/L and 0.12 mg/L) were used to treat the scale that was formed on the membrane surfaces.

These concentrations of  $Zn^{2+}$  ions showed that they can slow down the nucleation rate of calcium carbonate and also promote its crystallisation in the aragonite rather than the calcite form even under conditions where calcite would be the preferred crystal form as reported by Coetzee et al 1998. On the other hand Vitec 3000 was used as received from Avista Technologies, 2004.

## Chapter 4

# Anti-scaling treatment of BW 30-4040 RO membranes

### 4.1 Introduction

This chapter describes research carried out on the scale formation on the surface of scaled BW 30-4040 RO membranes and then the removal of the scale, on a laboratory scale. Membrane autopsies are described. An anti-scaling feed solution was used to artificially scale the membrane surface. A commercial anti-scalant (Vitec 3000) and Zn ions ( $Zn^{2+}$ ) were used as anti-scalants, in separate experiments. The RO performances of untreated and treated membranes, before and after the use of an anti-scalant, respectively, were determined.

The impact of (surface crystallization, i.e., crystallization takes place directly on the membrane surface) was characterized via flux decline measurements and by both optical and high-resolution scanning electron microscopy (SEM) (Shih et al, 2005).

### 4.2 Objectives

1. Treating the membrane with synthetic scaling solution as prepared in section 3.3.3.4
2. Treatment of the fouled membranes with two types of anti-scaling materials namely  $Zn^{2+}$  and Vitec 3000.
3. Comparison between the effect of  $Zn^{2+}$  and Vitec 3000 by observing the rejection and Flux.
4. Analyzing the treated membrane surface using SEM and OM techniques, then compare these results to a surface of an untreated membrane.

### 4.3 Experimental

#### 4.3.1 Autopsy procedure

Before any physical dissection, the membrane element was visually examined (see Section 3.3.1). This included examination of the glue lines and the membrane surface. Any colouring, precipitated material or odour was noted. For an efficient inspection a

comparison must be made between the fouled membrane and an unused one. The fouled material (foulant) was then collected for further analysis.

#### 4.3.2 Membranes used

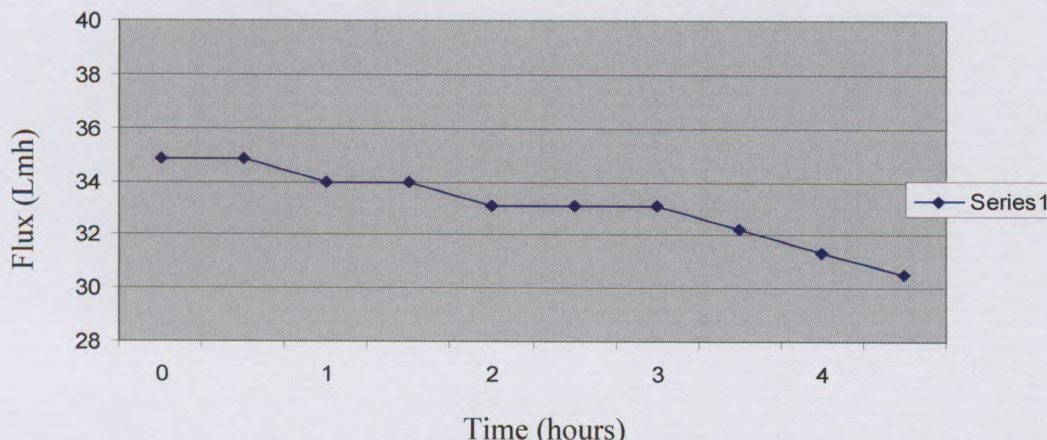
#### 4.3.3 Membrane element cell

A SEPA CF II membrane element cell (Osmosis) (see Figure 3.8) was used in this part of the study. This cell is a laboratory-scale cross flow filtration unit that provides fast and accurate performance. It has flexibility to vary the operating conditions and fluid dynamics over broad ranges.

### 4.4 RO results of scaled BW30-4040 membranes

#### 4.4.1 Before anti-scaling treatment

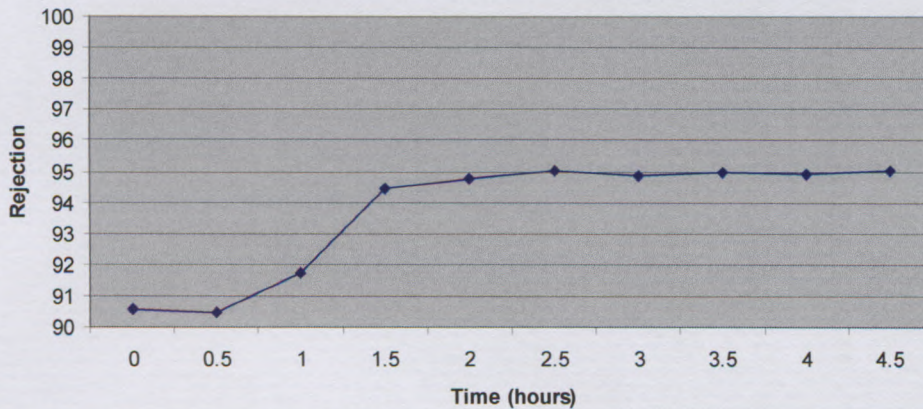
RO results obtained from the flat cell experiments for the membrane flux and rejection are shown in Figure 4.1 and Figure 4.2, respectively (the experiment was done several times and all the results were comparable). The extent of surface scale formation was evaluated by flux decline monitoring and optical imaging of scaled membranes.



**Figure 4.1: Flux of scaled BW30-4040 RO membrane over time**

The initial flux did not decrease over the first 30 min of operation, followed by a gradual decrease until 4 h of operation. This rapid decline in permeate flux is due to the deposition of particulates followed by the build-up of scale formation on the membrane surface which resulted in the membrane pores becoming blocked. The molecular deposition of these dissolved particles and ions at the membrane surface create a local concentrated layer.

Due to the relatively high local concentration, this accumulation tends to reduce the permeate flux through the membrane and hence resulting in a more significant flux decline (Sheikhholeslami and Tan,1999). Here,  $\text{CaCO}_3$  and  $\text{CaSO}_4$  precipitations were the main reason of the flux decline. However, the flux decline could also be due to an increase in ionic concentration and osmotic pressure during the RO process

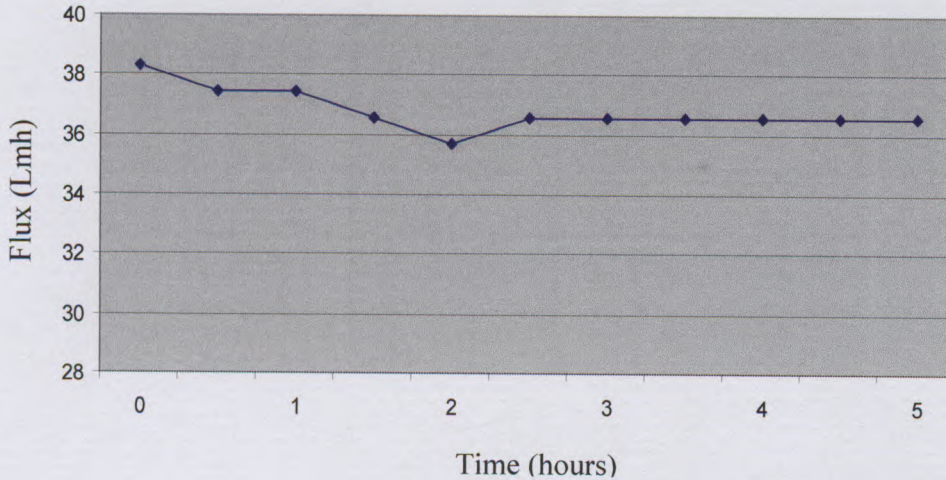


**Figure 4.2: Rejection of scaled BW30-4040 RO membrane over time**

Similarly, the rejection did not change over the first 30 min of operation. This could be as results of wetting and swelling of the membrane before it reflects on the rejection performance. On the other hand compaction causes an increase in the time required for the reflection from the membrane surface, since compression moves the membrane–fluid interface away from the transducer. This was noticed by the gradual increase until 2.5 h of operation. The rejection thereafter becomes constant again until 4.5 h of operation. (see Appendix A).

#### **4.4.2 After anti-scaling treatment with a commercial anti-scalant**

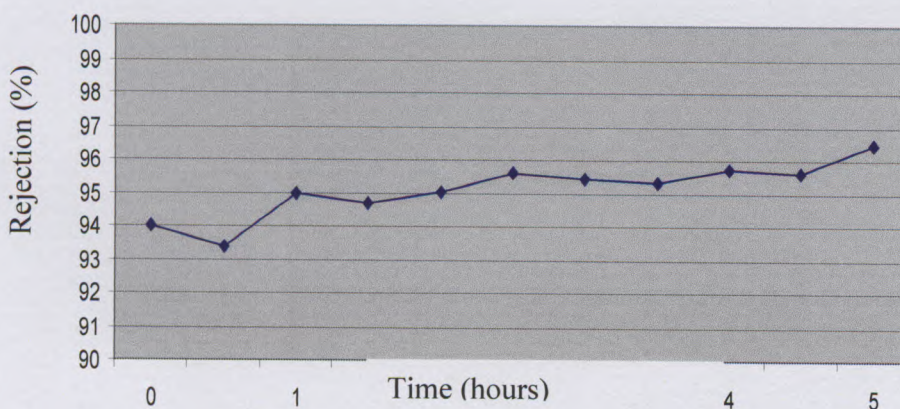
RO results obtained from the flat cell experiments for the flux and rejection after using a commercial anti-scalant (Vitec 3000) are shown in Figure 4.3 and Figure 4.4 respectively.



**Figure4-3: Flux of scaled BW30-4040 RO membrane treated with a commercial anti-scalant Vitec 3000**

Figure 4-3 shows that the flux decline was reduced to just 5%. The initial flux decreased until it reached the point where it stabilized (after 2 h). This was because the anti-scalant was added at this point. The anti-scalant enhanced the flux rate immediately, and then, the flux rate remained at steady state for the remainder of the experiment time. Limited flux decline was noted after adding the anti-scalant. This gave an indication that the use of the commercial anti-scalant modifies parts of the membrane surface from deposited particles, surface crystallization and deposition of salt crystals. This included the retardation or prevention of the deposition of particles and bulk crystallization on the membrane surface, consequently preventing the membrane pores from blockage. The rejection also showed a clear improvement, as shown in Figure 4-4.

This inhibition of flux decline suggests either a complete retardation of the onset of surface crystallization or extremely slow growth of salt crystals on the membrane surface.



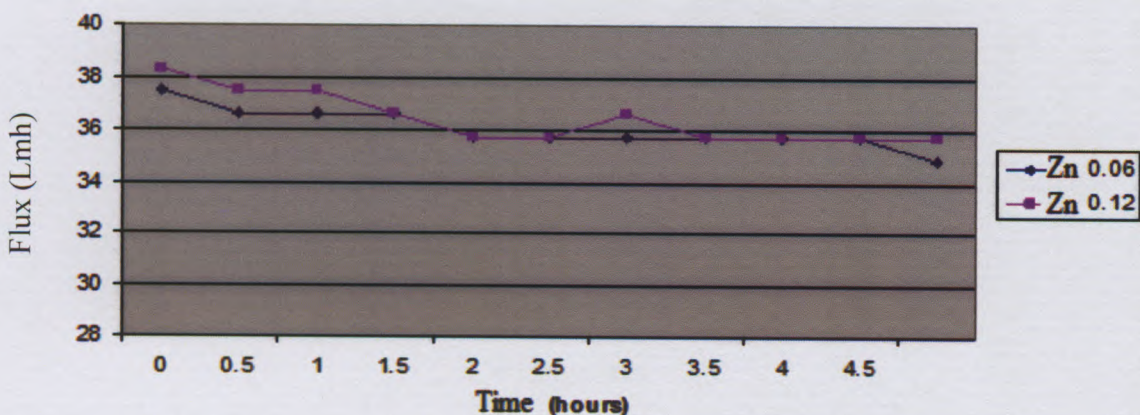
**Figure 4.4: Rejection of scaled BW30-4040 RO membrane treated with a commercial anti-scalant**

#### **4.4.3 After anti-scaling treatment with $Zn^{2+}$ ions (0.06 and 0.12 mg/L)**

Coetzee et al. (1998) reported that  $Zn^{2+}$  and other metal ions released from surfaces in certain magnetic and other physical water treatment (PWT) devices used for anti-scalant treatment were primarily responsible for the observed scale reduction effects. They found that these effects can cause reduction in the scaling of membranes in a simple laboratory application. They also found that the effects produced by other metal ions (e.g. Mg, Cu and Fe) released from PWT devices were much less effective than for  $Zn^{2+}$ . It was further found that an increase in concentration of  $Zn^{2+}$  ions to above 2 ppm reduces the scale inhibition effect, resulting in a faster drop in flux (Goldie et al., 2008).

The upper limit of zinc in drinking water is 5 mg/L. This is not because of associated health hazard but due to the astringent taste that  $Zn^{2+}$  ions impart to water (Lisitsin et al., 2005).

Following on from the findings of Coetzee et al. (1998) regarding the observation that  $Zn^{2+}$  can substantially inhibit the scaling. In this study two different concentration of  $Zn^{2+}$  ions 0.06 mg/L and 0.12 mg/L were used as mentioned in Section 3.5.1.3. Flux results obtained from the flat-cell experiments using  $Zn^{2+}$  ions as anti-scaling treatment are shown in Figure 4-5. In both cases the initial flux decreased until it reached the point where the flux stabilized. This gives an indication that zinc as anti-scalant prevents the deposition of particles on the membrane surface, and consequently, prevents the membrane pores from blockage.



**Figure 4.5: Fluxes of scaled BW30-4040 RO membranes treated with  $Zn^{2+}$  ions (0.06 and 0.12 mg/L) as anti-scalant**

It is evident from the above figure that trace amounts of  $Zn^{2+}$  can substantially inhibit the nucleation rate of calcium carbonate crystallization by inducing increases in nucleation times. In addition the predominant crystal structure of the calcium carbonate formed changed to aragonite instead of calcite. Both these effects can lead to less scale formation. The presence of  $Zn^{2+}$  ions in solution, at very low concentrations, may adsorb onto the crystallization surface causing to delay nucleation, reduce the precipitation rate and modify the surface of those crystals which do form and block the energetically favorable growth positions on the surface thus completely inhibiting further precipitation (Zeppenfeld, 2010).

However, the mechanisms behind metal ions has received some attention although it is not clear if the metal ion is enhancing bulk nucleation (Pernot et al., 1999), inhibiting crystal growth (Meyer, 1984) or forming competitive zinc carbonate species (Coetzee et al., 1996). Performance is dependent on the metal ion concentration where a minimum Zn/Ca mass ratio of 0.06 E03 was reported to be required for zinc to cause a measurable effect.

In the solution-diffusion mechanism that happened (Figure 4-6), it is assumed that each permeating molecule dissolves. In other words, it is believed that the membrane is not necessary to be selective as required in other membrane processes such as pervaporation. The solution-diffusion flow through the nonporous portion of the membrane is not considered in spite of the possible existence of a high "affinity" (i.e., close solubility parameters) between the species to be separated and the membrane material.

In thin-film composite types, the transport of molecules through the membrane matrix (i.e., surface diffusion) is neglected due to the fact that the diffusion area of the membrane matrix is small compared to the pore area. For thin-film membranes, the "affinity" between water and the membrane material is very low, and it may be allowed to neglect the contribution of transport through the membrane matrix, especially for porous membranes with large pore sizes and high porosities. Nevertheless, when other compounds are present in the feed solution, especially for compounds having strong affinity with the membrane material, the transport mechanism through the matrix of the membrane may have a significant effect.(Norman, 2008).

RO rejection results obtained from the flat cell experiments using  $Zn^{2+}$  ions (0.06 and 0.12 ppm) as anti-scalant are shown in Figure 4-6. There was a slight improvement in the rejection 0.12 mg/L.



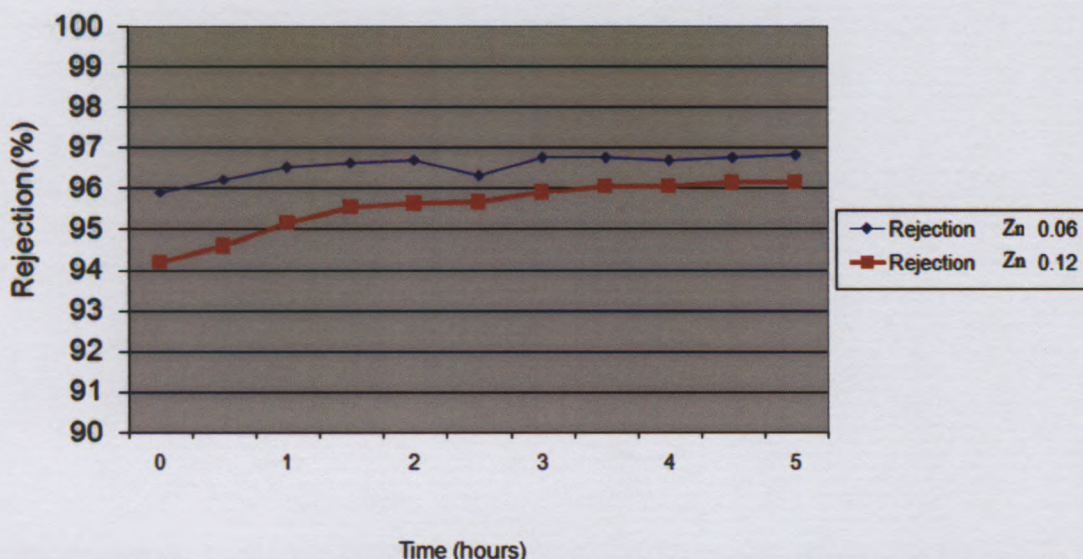


Figure 4.6: Rejection of scaled BW30-4040 RO membrane treated with Zn<sup>2+</sup> ions (0.06 mg/L) and (0.12 mg/L)

#### 4.5 SEM and OM analyses of scaled BW30-4040 membranes

##### 4.5.1 Without anti-scaling treatment

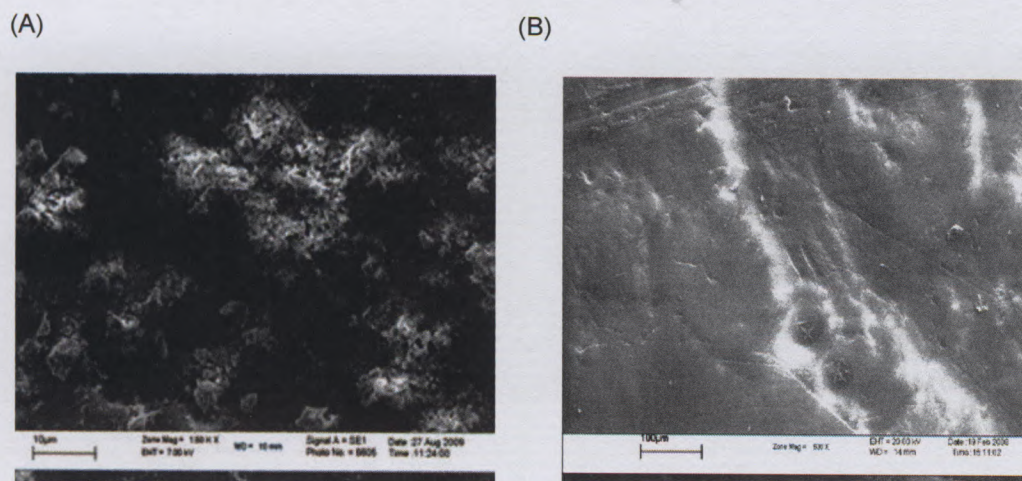
SEM and OM images were recorded of scaled and unsealed BW30-4040 membranes, without anti-scaling treatment. Figure 4-7 shows SEM images of a scaled BW30-4040 membrane and an unscaled membrane (Mag. 500x). A similar image of crystals has been shown by Tzotzi et al. (2007).

The visible cracks in the SEM images of the untreated membrane were not present in the SEM images of the scaled membrane. Deposits of CaCO<sub>3</sub> scalant were evident as small white clusters on the surface of the membrane sample, as shown in Figure 4-7A. It seems that both calcite crystals and aragonite clusters are observed in this membrane (see Tzotzi et al., 2007).

The crystal growth was seen laterally as well as vertically with a pattern of fluent rooted on the water. Some loose crystals were randomly arranged. These crystals tend to increase in size with a deformed shape compared to the initial rhombohedra phase, as they grow with time in all directions; they “coalesce” with each other, forming a coherent blocking layer of tenacious CaCO<sub>3</sub> deposits which are difficult to clean.

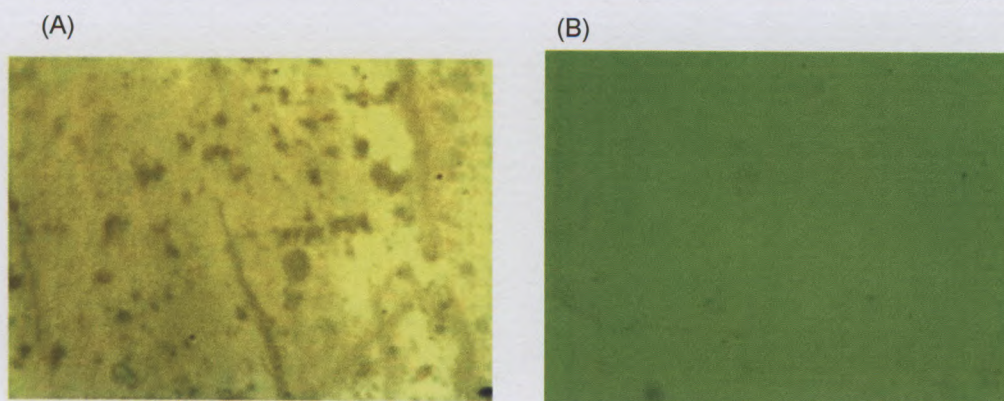
The pure calcium carbonate crystals deposit in calcite phase where the aggregated structures are composed of regular rectangular plate and rhombohedra like structures. However, magnesium normally influences much on the calcium carbonate precipitation. At low concentration, it settles within the calcite lattice; while at high concentration (Mg/Ca > 1), it induces aragonite precipitation.

Figure 4-7 also revealed that the calcite crystals coagulated in round shapes tendency of combining and forming a cluster of round crystallize balls. This is the characteristics of  $\text{CaCO}_3$  resulting in a continuous fouling layer on the membrane which is adherent and hard to remove by simply cleaning.



**Figure 4-7: SEM images of a BW30-4040 membrane sample (A) after scaling and (B) untreated membrane (Mag 500x)**

On the other hand, in the OM image of used scaled BW30-4040 membrane a dark brown/black layer was seen on the membrane surface, as shown in Figure 4-8 A.



**Figure 4.8: BW30-4040 membrane sample (A) after scaling and (B) untreated membrane (Mag. 750x)**

These dark spots indicate the formation of scaling. No dark spots can be seen in OM image of untreated BW30-4040 membrane, as shown in Figure 4.8 B.

## 4.5.2 Anti-scaling treatment with a commercial anti-scalant

### 4.5.2.1 Experimental

Different concentrations of a commercial anti-scalant (Vitec 3000) were used to investigate the effect on scaled membrane surfaces. Quantities of 1, 2 and 3 g of commercial anti-scalant Vitec 3000 were added to the 100 L of water in the feed tank, in separate experiments. The same RO test system with flat cells was used as shown in Figure 4.1, except that the feed solution included the commercial anti-scalant in the feed tank. The feed conductivity was 1562  $\mu\text{s}/\text{cm}$  and the feed temperature was at room temperature (about 25 °C).

### 4.5.2.2 Calculation of concentration of commercial anti-scalant

The concentration of Vitec 3000 was determined by means of a mass balance on the system RO experimental system. Samples were taken from the brine and permeate, and with mass balance the concentration on the membrane side could be calculated.

A summary of the calculated concentrations is as follows:

Dose rate of Vitec solution (before pumping commences) = 0.12 L/h (2mL/min)

Permeate flux rate = 0.00048 L/h (0.48% x 0,40%)

Brine flow rate = 0.11952 L/h (99,60%)

The concentration of Vitec in the brine was found to be 2 mg/L.

By means of a mass balance the amount of Vitec on the membrane was 0.057mg/L. (see Appendix A 4.6.2).

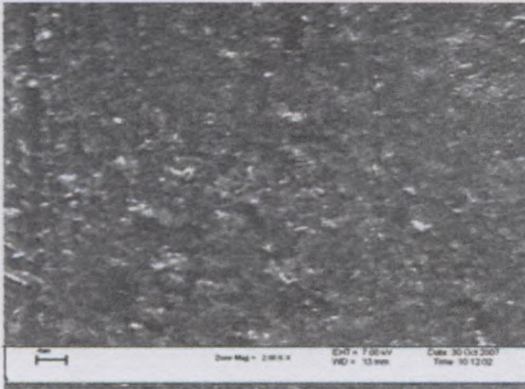
$$\text{Vitec}_{(\text{membrane})} = 2(\text{mg/L}) \times 0.40\% / 0.14\text{m}^2 \quad \text{Equation 4.1}$$

### 4.5.2.3 SEM analysis of scaled BW30-4040 membranes treated with commercial anti-scalant

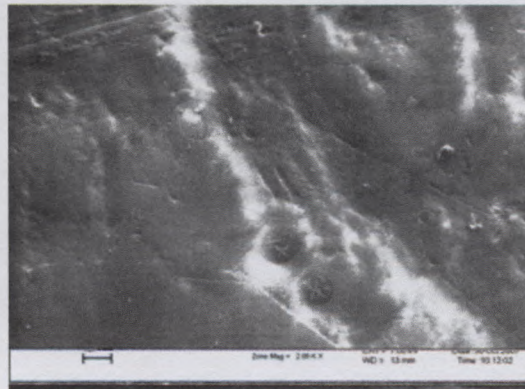
Figures 4.9 show SEM images of (Figure 4.9 A) membrane samples after anti-scaling when using 1 , 2 and 3 mg/L commercial anti-scalant in the feed solution (100 L), respectively, and (B) untreated membranes (Mag. 200x).

The crystal morphology was also consistent with the flux decline results.

(A)



(B)



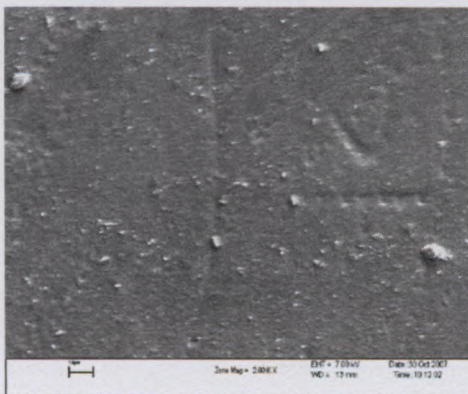
**Figure 4-9: SEM images of (A) a membrane sample BW30-4040 after anti-scaling by 1m g/L Vitec 3000 commercial anti-scalant and (B) a untreated membrane (Mag. 200x)**

The SEM images show the ability of the anti-scalant to modify the deposited particle sizes and crystal morphology. In Figure 4-10 B indicated that the crystallization of  $\text{CaCO}_3$  was highly reduced in the presence of anti-scalants and only minimal deposits were left on the membrane surface as white clusters. In the latter (Figure 4-10) scaling was minimal as observed in the SEM image on the untreated membrane, which means that the anti-scalant solution was successfully used to clean the scales off the membrane surface.

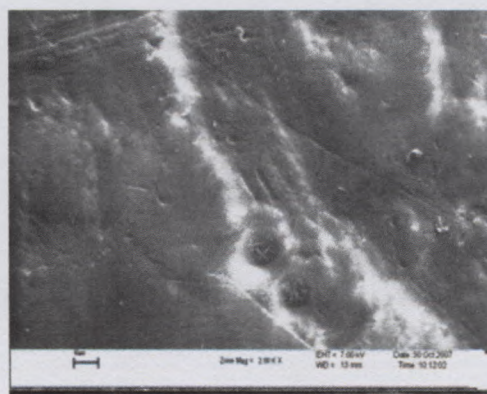
The absence of small crystals on the membrane indicated that the mechanism of scale inhibition by the anti-scalant was the control on the inception of  $\text{CaCO}_3$  and  $\text{CaSO}_4$  nuclei formation rather than on crystal growth. However, the general understanding demonstrates that the anti-scalant adsorbs onto the formed crystals or complexes with the incipient nuclei, thereby inhibiting salt crystal growth.

It is plausible that surface nucleation, adhesion and growth of surface salt crystals of the anti-scalant with mineral salt nuclei and crystal surfaces, as well as the membrane surface, are all affected by a complex interplay of membrane topology and surface chemistry.

(A)

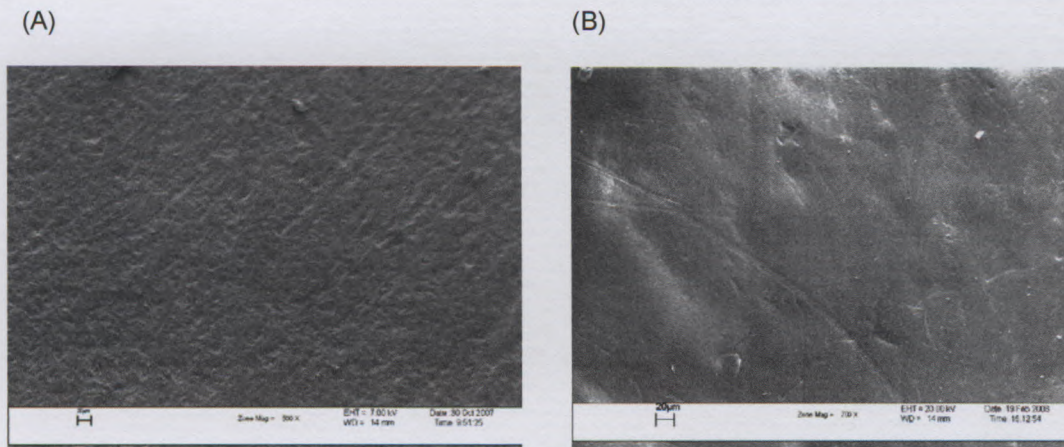


(B)



**Figure 4-10 : SEM images of (A) a membrane sample BW30-4040 after anti-scaling by 2 Vitec 3000 mg/L commercial anti-scalant and (B) untreated membrane (Mag. 200x)**

Figure 4-10 B shows that when 2mg/L of the commercial anti-scalant was used, the white spots/clusters were not as apparent as on the surface of the membrane as in Figure 4-9 B (when 1mg/L commercial anti-scalant was used). This is due to the use of a higher concentration of the commercial anti-scalant used.



**Figure 4-11: SEM images of (A) a membrane sample BW30-4040 after anti-scaling by 3 mg/L Vitec 3000 commercial anti-scalant and (B) untreated membrane (Mag. 500x).**

Figure 4.11 B shows the SEM image of the membrane surface after it has been treated with 3 mg/L of the commercial anti-scalant. A minimal number of material clusters on the membrane surface indicated that the anti-scalant was effective in reducing the precipitation of  $\text{CaCO}_3$ . A large area on the membrane surface was observed to be free from scale. The membrane surface was clear hence no deposits can be seen on the surface. Hence, it was concluded that the addition of 3mg/L of commercial anti-scalant to the feed solution resulted in better anti-scaling reduction than when 1 or 2mg/L of the ant-scalant was used.

## 4.6 SEM and OM analyses of scaled BW30-4040 membranes

### 4.6.1 Experimental

The same equipment as described in Section 4.3.2, and shown in Figure 4.5, was used. The only difference was that here the feed solution constituted a solution generating  $Zn^{2+}$  ions in two different concentrations: 0.06 and 0.12 mg/L.

### 4.6.2 Calculations of zinc ion concentration

The concentrations of the  $Zn^{2+}$  ions were determined by means of a mass balance on the RO test system (refer to Figure 4-1). Samples were taken from the brine and permeate, and with mass balancing the concentration on the membrane could be calculated.

The concentration of  $Zn^{2+}$  ions in the brine was found to be 75  $\mu\text{g/L}$  (see Appendix A 4.6.2).

The concentration of  $Zn^{2+}$  ions in the brine was found to be 120  $\mu\text{g/L}$  (see Appendix A 4.6.2).

### 4.6.3 SEM results

Unclear observations could be determined from the SEM images recorded at low magnifications. Deposits were however observed at high magnification (1500x), as shown in Figure 4-12 and Figure 4-13.

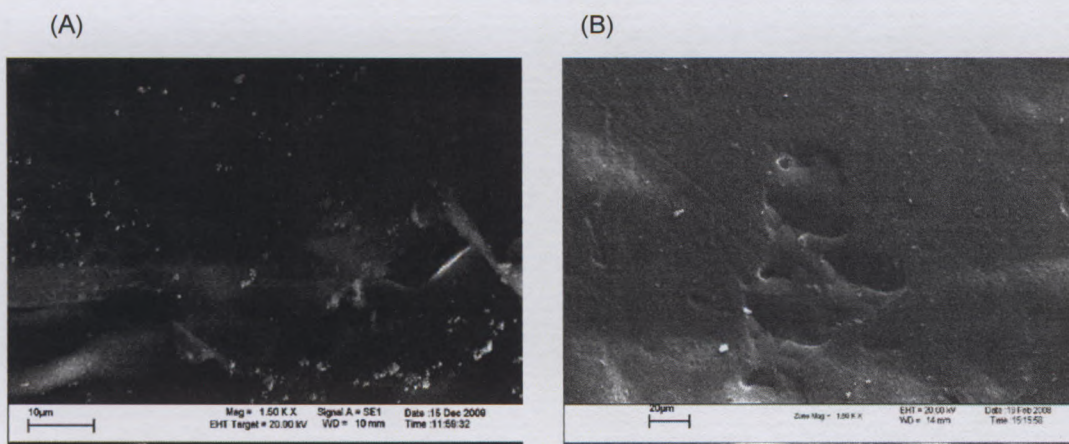
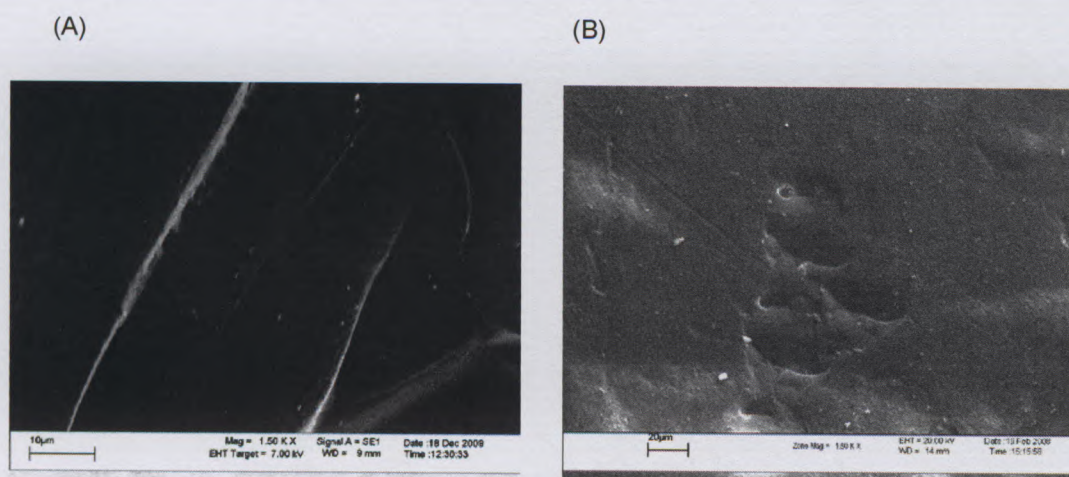


Figure 4-12: SEM images of (A) a BW30-4040 membrane after anti-scaling with 0.06 mg/L  $Zn^{2+}$  and (B) untreated membrane (Mag. 1500x)

Figure 4-12 shows that after treatment with a 0.06 mg/L  $Zn^{2+}$  ion solution only a slight deposit was observed on the surface of the membrane, as white clusters. Most of the area on the membrane was free from scale. The SEM image was taken from the position on the membrane where the density of the crystals was high. However, large particle deposits were less in number and were found to be very loose, dispersed and adhere less to the membrane surface compared to the particles formed in the absence of anti-scalant. Moreover, the particles were observed to be distorted such that the collection looked like well defined rhombohedral and rectangular crystals that are characteristic of calcite phase of  $CaCO_3$ . The minimal presence of grown crystals suggested that the mechanism of scale control by anti-scalant was mainly by the inhibition of crystal nuclei. This  $Zn^{2+}$  ion solution performed well as an anti-scalant in this case in terms of removing the scaling from the membrane surface.

Meyer (1984) studied the effect of additives on the growth speed of calcite, among which  $Zn^{2+}$  ions were to inhibit calcite formation, which proves that this element is a good inhibitor, more efficient than Cu ions. According to Meyer (1984) there was a reduction of the growth speed by 20% for  $Zn^{2+}$  concentration of  $5 \times 10^{-8}$  M, by 50% for  $10^{-7}$  M and by 80% for  $2 \times 10^{-7}$  M. Other researchers also noticed the disappearance of scaling on cooling installations in the presence of  $Zn^{2+}$  ions (Glasner et al (1980)).



**Figure 4-13: SEM images of (A) a BW30-4040 membrane sample after anti-scaling with 0.12 mg/L  $Zn^{2+}$  and (B) untreated membrane (Mag. 1500x)**

Figure 4-13 shows that the white spots/clusters on the surface of the membrane treated with 0.12 ppm zinc ion solution were not as apparent as on the surface of the membrane in Figure 4-12.

Glasner and Weiss (1980) showed that cations such as  $Zn^{2+}$  can co-precipitate with calcite. They also suggested the formation of a complex carbonate ion,  $[Zn(CO_3)_2]^{2-}$ , which would be used as the centre of nucleation for the crystallization of calcite. The inhibiting effect of zinc is significant according to the study concluded by Abouali et al., (1996) whereby inhibition of the germination of calcium carbonate was observed for  $Zn^{2+}$  concentrations from 0.02 mg/L. However, according to Yang (2006), the increase of  $Zn^{2+}$  concentration beyond 2mg/L diminished the inhibition effectiveness. Macadam and Parsons (2004) found that the best inhibitory effect on calcium carbonate precipitation was obtained by dosing 0.5 mg/L of zinc.

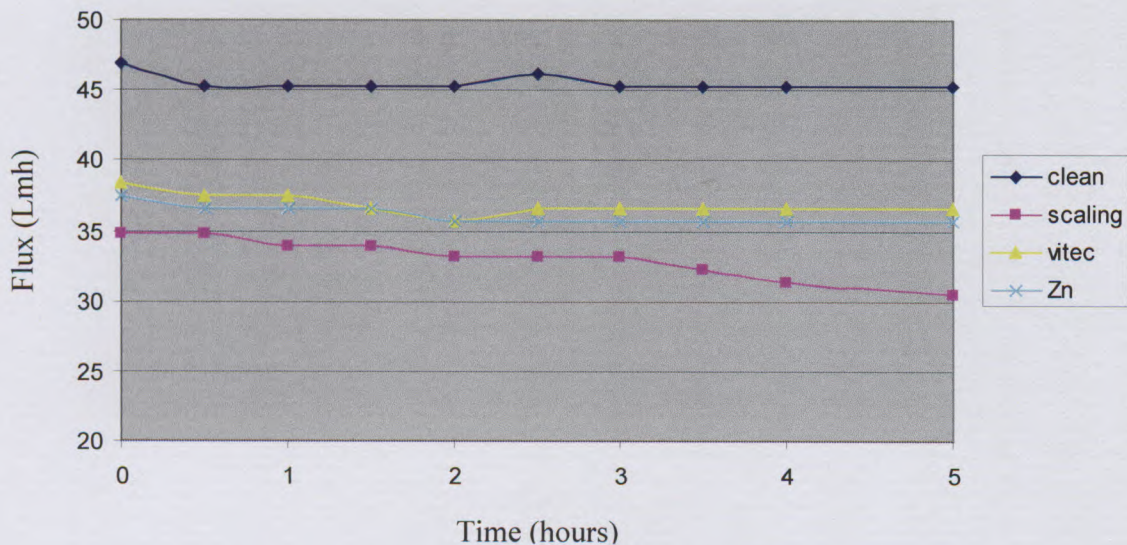
#### **4.7 Discussion**

RO membrane surfaces were scaled by adding  $CaCl_2$ ,  $MgSO_4$  and  $NaHCO_3$  to the feed solution in a RO test rig with flat cells. In some cases, complete fouling was achieved after 90 min by crystal structures of minerals forming on the membrane surface. The crystal structures were confirmed using SEM and OM. The RO performances, flux and rejection, of the scaled membranes were determined.

Then the effects of using two different types of anti-scaling agents, a commercial anti-scalant Vitec 3000 and  $Zn^{2+}$  ions, on the scaled membranes, was investigated. SEM and OM analyses showed that scaling was indeed reduced. The RO performances, flux and rejection, of the treated membranes were also determined.

RO results recorded for a untreated (clean) membrane, and scaled and treated membranes, are shown in Figure 4-14 (flux) and Figure 4-15 (rejection).





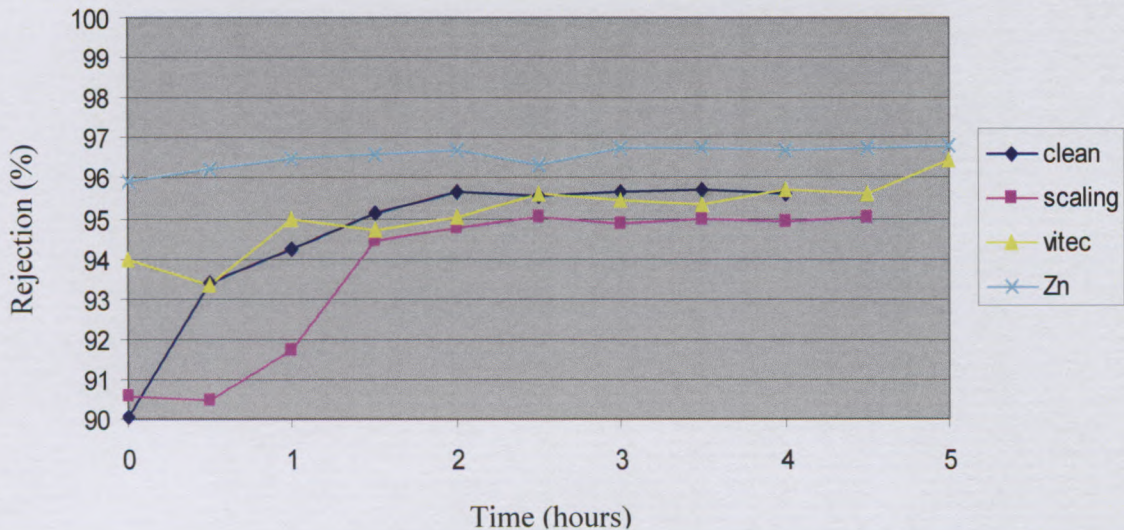
**Figure 4-14: RO results (flux) results recorded for unscaled (clean) membrane, a scaled membrane, and membranes treated with a commercial anti scalant and with  $Zn^{2+}$  0.12mg/L**

The flux rate of the unscaled membrane remained constant over the time but that of the scaled membrane decreased from 35 to 30.5 (Lmh) in less than 5 h. This was because the amount of deposited particles on the membrane surface increased with time.

When using the commercial anti-scalant there was initially a slight decrease in flux, but after 2 h the flux was stable at 36 (Lmh). When using  $Zn^{2+}$  ions (0.12mg/L) as anti-scalant, the flux stayed constant. The use of  $Zn^{2+}$  ions did however not improve the flux rate but seemed to prevent any additional deposition of particles on the membrane surface.

Kavanagh et al., (1990) noted the effects of metal ions which affect the growth of calcium carbonate by reducing the speed of nucleation and growth of the crystal, by deteriorating the morphology of the precipitate and, in certain cases, by causing the precipitation of a less stable phase (aragonite or vaterite) in place of calcite. The metal  $Zn^{2+}$  ions could be adsorbed on the crystals, and thus block active growth sites of the growing nuclei (Ghizellaoui et al., 2007,; Koutsoukos 1984).

In conclusion, the percentage of flux drop when we used commercial anti-scaling after 5 hours was around 6%, while it was 9% when Zinc ions were used. As the investigation of the potential of  $Zn^{2+}$  to inhibit calcium carbonate scaling under test conditions was part on this research, it good agreement with what is reported in literature. The flux of a scaled membrane was improved by using a commercial anti-scalant; it was more effective than the use of  $Zn^{2+}$  ions significance. In terms of the rejection, both types of anti-scalants appeared to have a positive effect on reversing scaling.

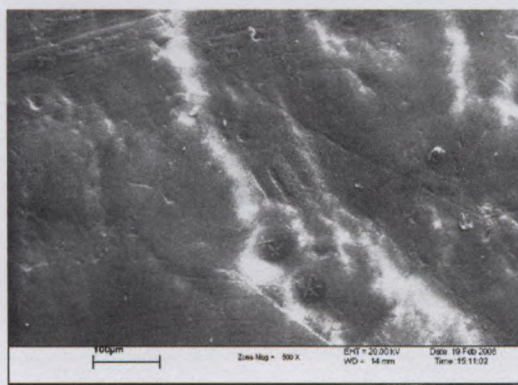


**Figure 4-15: RO results (rejection) results recorded for untreated (clean) membrane, a scaled membrane, and membranes treated with a commercial anti-scalant and with Zn<sup>2+</sup> ions at 0.12mg/L**

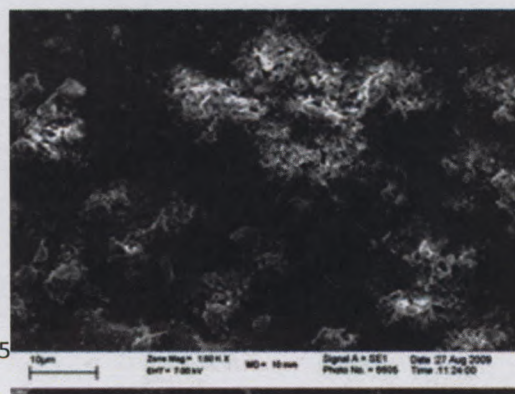
The compaction causes an increase in the time required for the reflection from the membrane surface, since compression moves the membrane–fluid interface away from the transducer. Compaction data are usually reported in terms of the compressive strain. In the case of a thin-film composite membrane such as the BW30-4040, most of the compaction is occurring in the thick support layer. Nonetheless, the strong relation between the compaction and permeation data in Figures 4.14 and 4.15 suggests that the high pressure is progressively changing either the functional layer of the membrane or the functional support interface region.

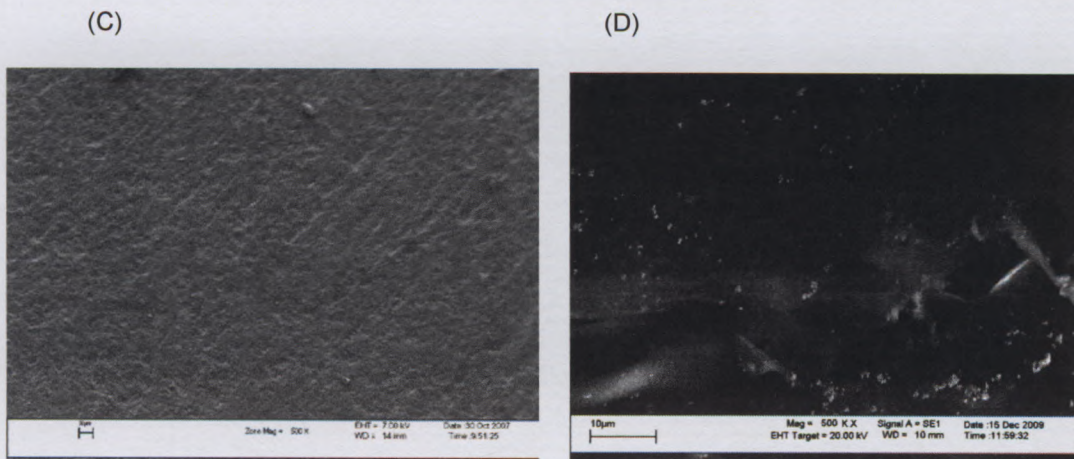
SEM's were used to detect the scaling, and the effects of the use of two different anti-scalants, on membrane surfaces. Figure 4-16 A shows the SEM image of smooth clean membrane surface, with no particles deposited on the surface. Figure 4-16 B shows the surface of a scaled membrane, with clusters, crystals and salt particles of different sizes and shapes deposited on the surface. Figure 4-16 C illustrates the surface of a scaled membrane after treatment with a commercial anti-scalant (3 mg/L).

(A)



(B)





**Figure 4-16: SEM images of the surface of (A) a untreated membrane, (B) a scaled membrane, (C) membrane after using a commercial anti-scalant, and (D) membrane after using  $Zn^{2+}$  ions at 0.12mg/L as anti-scalant (Mag. 500x)**

As the anti-scaling concentration increases the morphology of the membrane surface decreased. The membrane surface appeared smooth and clean. This was because the commercial anti-scalant disrupted the normal crystal growth (due to scaling) to produce an irregular crystal structure with poor scale-forming ability. This crystal distortion promotes the dispersion of deposits on the membrane surface and reduced the rate of crystal growth, and hence reduces membrane scaling. Figure 4-16 D illustrates the surface of a scaled membrane after treatment with  $Zn^{2+}$  ions 0.12mg/L as anti-scalant. Only some scaling has been removed.

### **Summary**

The above results were achieved in the laboratory scale and the effectiveness of the anti-scaling solutions was tested by using synthetic feed water. The following chapter will show these effects of anti-scalants on scaled membranes operated in RO pilot plant at Bitterfontein.

## Chapter 5

# Anti-scaling treatment of XLE 4040 RO membranes

### 5.1 Introduction

The previous chapter summarized the experimental investigations on the scale formation on the surface of membranes on a laboratory scale. Three types of salt solutions were used to create scaling on the membrane surface. Then a commercial anti-scalant (Vitec 3000) and  $Zn^{2+}$  ions were used, in separate experiments, as anti-scalants to reduce scaling on the membrane surface. The commercial anti-scalant was found to be more effective than the  $Zn^{2+}$  ions substantiated in Chapter 4.

In this part of the study similar investigations on the effect of anti-scalants was carried out on XLE4040 membranes that were in a RO pilot plant at Bitterfontein.

### 5.2 Objectives

1. Determine the RO performances of the XLE 4040 membranes (flux and rejection). Study the effect of scaling on membranes used in pilot plant.
2. Investigate the efficiency of two different anti-scalants and study the effect of commercial anti-scalant Vitec 3000 and zinc ions on RO XLE 4040 membrane performance.
3. To Autopsies the membranes and take samples from different locations on the selected membrane.
4. Analyses of membrane surfaces using electron microscopy (SEM) and optical microscope (OM) in order to study the morphology of the membrane surface after treatment of the scaled membrane, then compare these results to a surface of an untreated membrane (see Figures 5.11 and 5.13).
5. Compare the RO performances of treated membrane and untreated membrane without and with Vitec and  $Zn^{2+}$  ions anti-scaling by rejection and flux measurements as well as analyses of membrane surfaces (see Figures 5.14 and 5.15).

### 5.3 RO pilot plant

The required experiments to evaluate the performance and effectiveness of the spiral wrap membrane elements and the evaluation of the anti-scaling chemicals were undertaken on a mobile pilot RO plant. A pilot plant with three XLE4040 membranes was used in the

investigation, one membrane was (untreated), and the other two membranes were treated with different anti-scaling measures (a commercial anti-scalant and  $Zn^{2+}$  ions).

#### 5.4 The Scaled XLE 4040 membrane

Initially an autopsy of a XLE 4040 membrane was carried out on a used membrane, and then on another two membranes that were treated with different anti-scaling agents (a commercial anti-scalant and  $Zn^{2+}$  ions). The membranes were taken from an RO plant in operation at Bitterfontein. Autopsies were carried out on eighteen membrane samples taken from different locations on the membranes. The membranes that were autopsied had the following specifications:

Membrane type	Diameter cm	Membrane area $m^2$	Salt rejection %	Product flow rate $m^3/d$
XLE 4040	4	8.1	99.0	9.8

#### 5.5 Experimental: Autopsy procedure

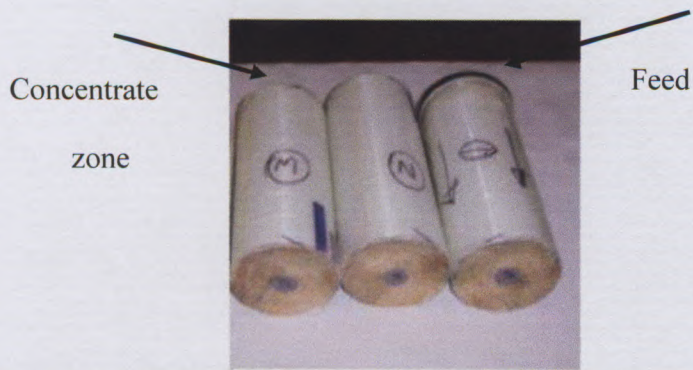
Autopsies were carried out on eighteen membrane samples taken from different locations on the selected membrane (Figure 5.1). The procedure of the autopsy was carried out at the same way as explained in Section 3.3.

##### 5.5.1 Membrane dissection

Each membrane element was divided it into three zones (Figure 5.2) and then opened by removing the ends and separating the fibreglass housing. Two samples were taken from each zone for analysis. One sample was taken close to the membrane shell and another sample was taken close to the core (see Figure 5.3). To distinguish between the samples, a number and a letter were assigned to each sample. For instance, the code 1S was given to the sample taken closer to the shell in part number 1, and 1C was given to the sample taken close to the core in part number 1. Both sides of the membrane for all samples were analysed using SEM.



**Figure 5-1: Photograph of the membrane to be autopsied**

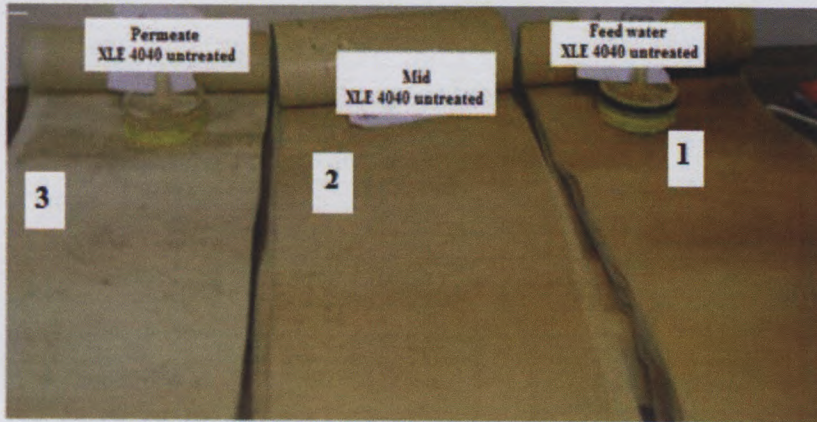


**Figure 5-2: Photograph of the membrane cut into three parts**



**Figure 5-3: A photograph of the autopsied part of the membrane**

RO membrane sheets were unrolled and the spacer carefully removed in the direction of cross flow, and was noted to identify swatch location (see Figure 5.4).



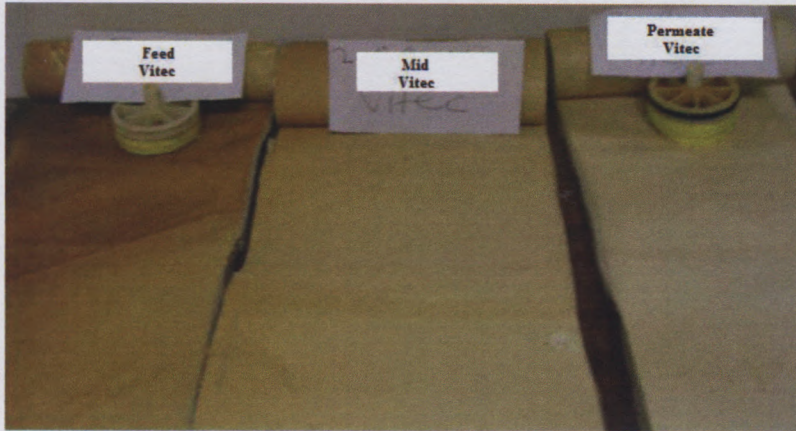
**Figure 5-4: Photograph of the unravelled membrane sheets, cut into three parts: permeate, mid, and feed**

Membrane swatches were recovered for analysis from the feed end, the middle and the permeate end of the RO membrane sheets.

Photographs of the membranes treated with  $Zn^{2+}$  and with the commercial anti-scalant, cut into three parts, are shown in Figure 5-4 and Figure 5-5.



**Figure 5-5: Photograph of membrane (treated with  $Zn^{2+}$  ions) cut into three parts**




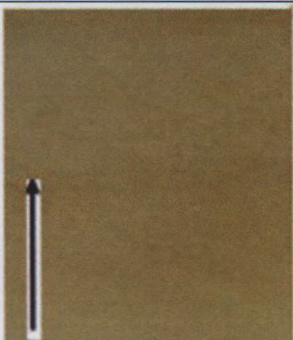
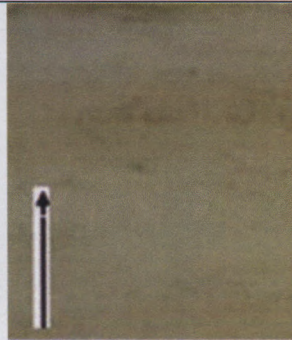
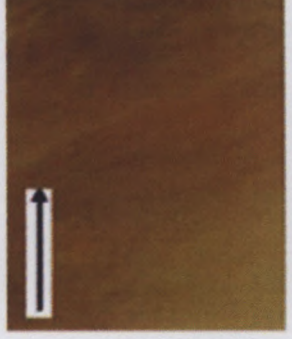
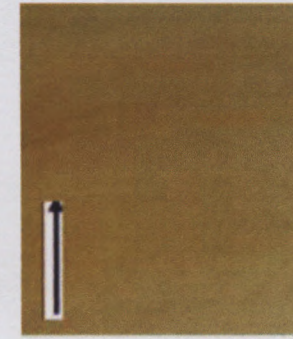



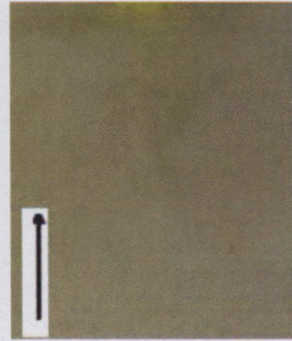
**Figure 5-6: Photograph of membrane (treated with commercial anti-scalant) cut into three parts**

## **5.6 Autopsy results**

### **5.6.1 Visual comparison**

For visual comparison, photos were taken for the three zones (feed, middle and permeate) of each XLE 4040 membrane (untreated, treated with  $Zn^{2+}$  and treated with commercial anti-scalant) and presented in Figure 5-7. The direction of the arrow in this figure illustrates the water flow direction.



Zone NO.	Anti-scalant		
1	 <p data-bbox="254 685 429 712">Feed untreated</p>	 <p data-bbox="611 685 771 712">Mid untreated</p>	 <p data-bbox="924 685 1142 712">Permeate untreated</p>
2	 <p data-bbox="283 1095 400 1123">Feed Zinc</p>	 <p data-bbox="647 1095 749 1123">Mid Zinc</p>	 <p data-bbox="939 1095 1113 1123">Permeate Zinc</p>
3	 <p data-bbox="298 1506 414 1534">Feed Vitec</p>	 <p data-bbox="618 1506 720 1534">Mid Vitec</p>	 <p data-bbox="953 1506 1128 1534">Permeate Vitec</p>

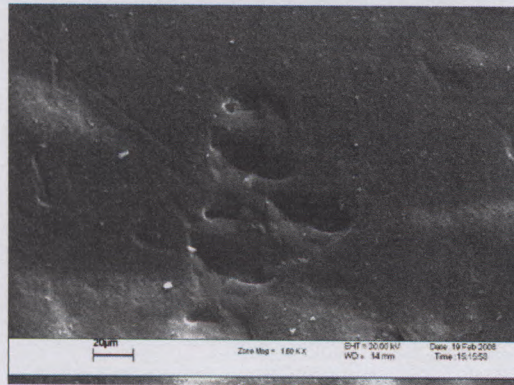
**Figure 5-7: Comparison between three XLE 4040 membranes: one membrane was untreated, and the other two membranes were treated with different anti-scaling measures.**

### 5.6.2 SEM results

The SEM images, of the samples (shell and core) are shown in Figure 5-9, Figure 5-10 and Figure 5-11. Note that in the case of SEM analyses the images of each sample were taken from both sides, namely the feed and permeate.

An untreated membrane was also analysed for comparison purposes. The autopsy results (SEM analysis) of the control were carried out at an earlier stage.

An SEM image showed in Figure 5-8 shows the surface of the XLE 4040 untreated membrane. No cracks or deposits were observed.



**Figure 5-8: An SEM image of the XLE 4040 untreated membrane**

SEM images in Figure 5-9, Figure 5-10 and Figure 5-11 showed that scaling had taken place after two hours. More deposits (evident as small white clusters) were observed on the surface of the untreated membrane for both the shell and core samples, as shown in Figure 5-9 fewer deposits seem to be observed on the surface of the treated membranes, especially in the case of membranes treated with the commercial anti-scalant, as shown in Figure 5-10.

5.6.2.1 Membrane treated with a commercial anti-scalant

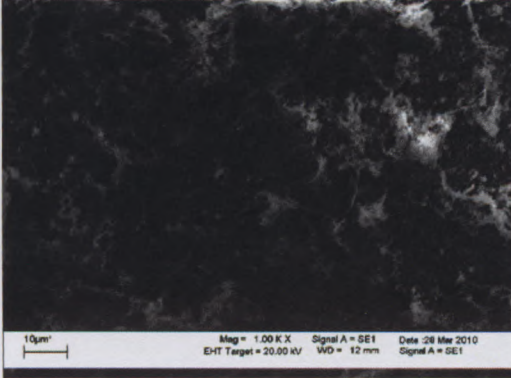
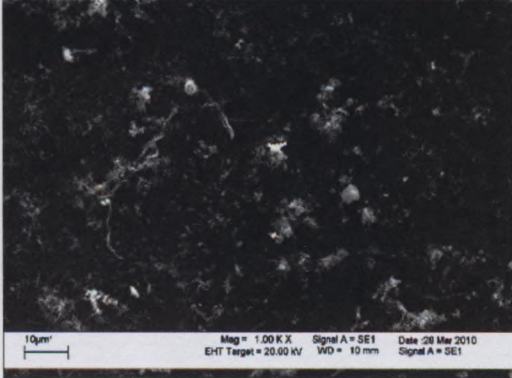

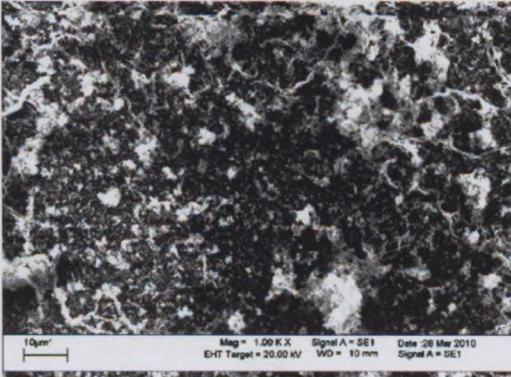
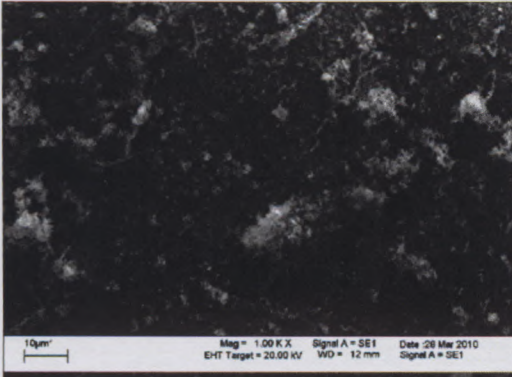
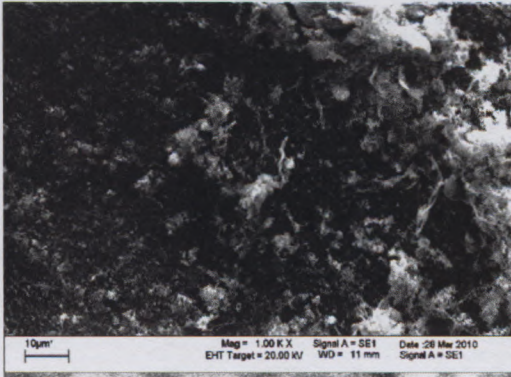
Zone no.	Shell-side	Core-side
1	 <p data-bbox="398 789 569 821">Feed samples</p>	 <p data-bbox="971 789 1141 821">Feed samples</p>
2	 <p data-bbox="394 1261 575 1293">middle sample</p>	 <p data-bbox="937 1261 1118 1293">middle sample</p>
3	 <p data-bbox="380 1740 592 1772">permeate sample</p>	 <p data-bbox="923 1740 1132 1772">permeate sample</p>

Figure 5-9: Comparison of SEM images of feed, middle and permeate side an untreated membrane (Mag. 1000x).

5.6.2.2 Membrane treated with a commercial anti-scalant

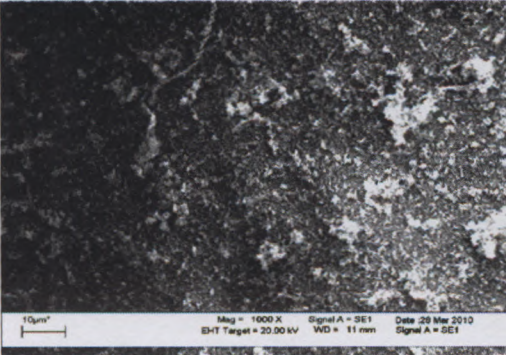
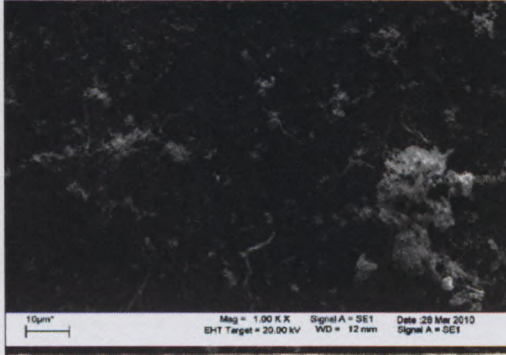
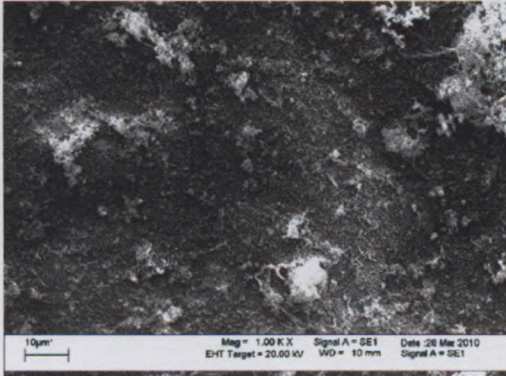
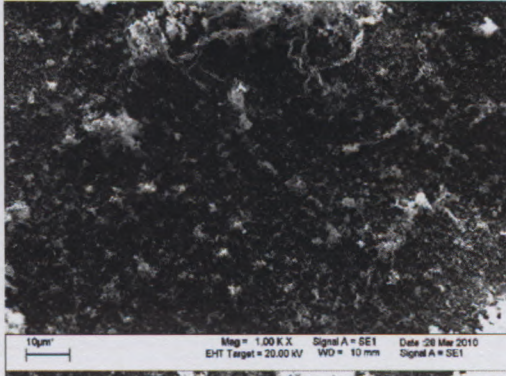
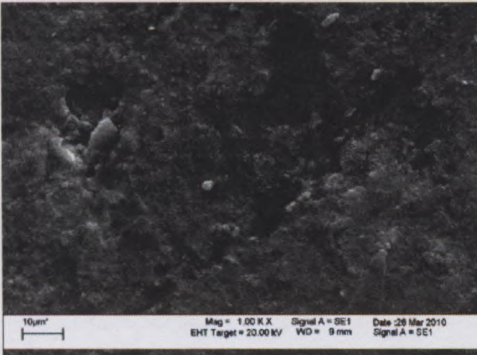
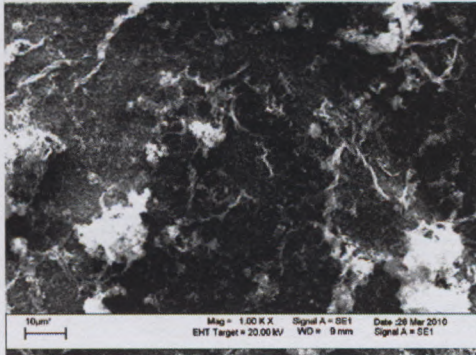
Zone no.	Shell-side	Core-side
1	 <p data-bbox="420 756 579 789">Feed sample</p>	 <p data-bbox="962 756 1121 789">Feed sample</p>
2	 <p data-bbox="413 1235 589 1267">Middle sample</p>	 <p data-bbox="955 1235 1131 1267">Middle sample</p>
3	 <p data-bbox="398 1698 607 1731">Permeate sample</p>	 <p data-bbox="937 1698 1145 1731">Permeate sample</p>

Figure 5-10: Comparison of SEM images of feed side, middle and permeate side an membrane treated with a commercial anti-scalant (Mag. 1000x).

### 5.6.2.3 Membranes treated with Zn<sup>2+</sup> ions

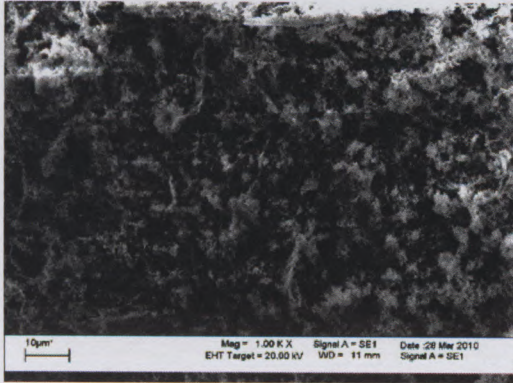
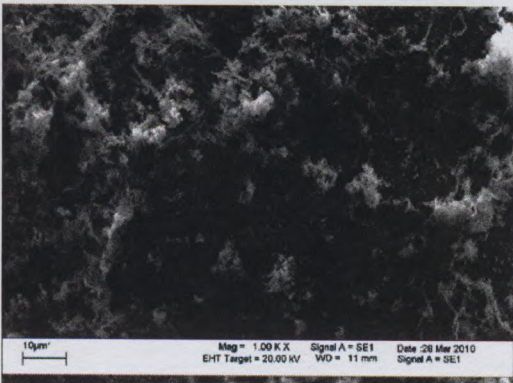
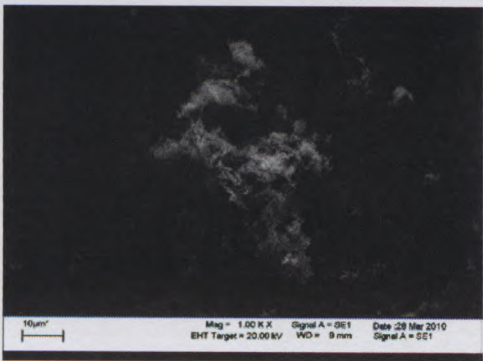
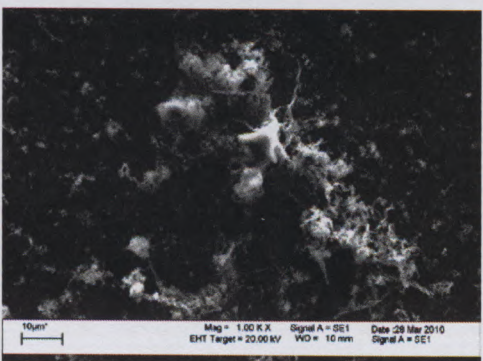
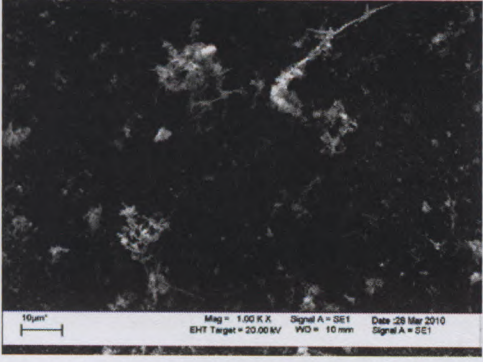
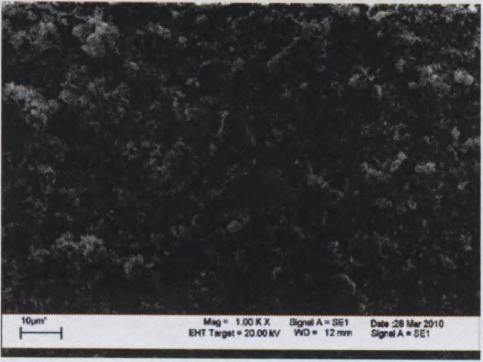
Zone no.	Shell-side	Core-side
1	 <p data-bbox="465 720 625 750">Feed sample</p>	 <p data-bbox="1014 720 1174 750">Feed sample</p>
2	 <p data-bbox="455 1181 636 1211">middle sample</p>	 <p data-bbox="999 1181 1180 1211">middle sample</p>
3	 <p data-bbox="439 1642 651 1673">permeate sample</p>	 <p data-bbox="984 1642 1195 1673">permeate sample</p>

Figure 5-11: Comparison of SEM images of feed side, middle and permeate of membrane treated with Zn<sup>2+</sup> ions (Mag. 1000x).

## 5.7 Discussion

SEM images showed significant differences on the surface of the membrane at the feed side, middle, and permeate side. Images of the untreated membrane in (Figure 5-9) showed that the deposited material was towards the core side than on the shell side. The deposited materials were concentrated in the middle of the core side especially at the feed and permeate areas of the membrane.

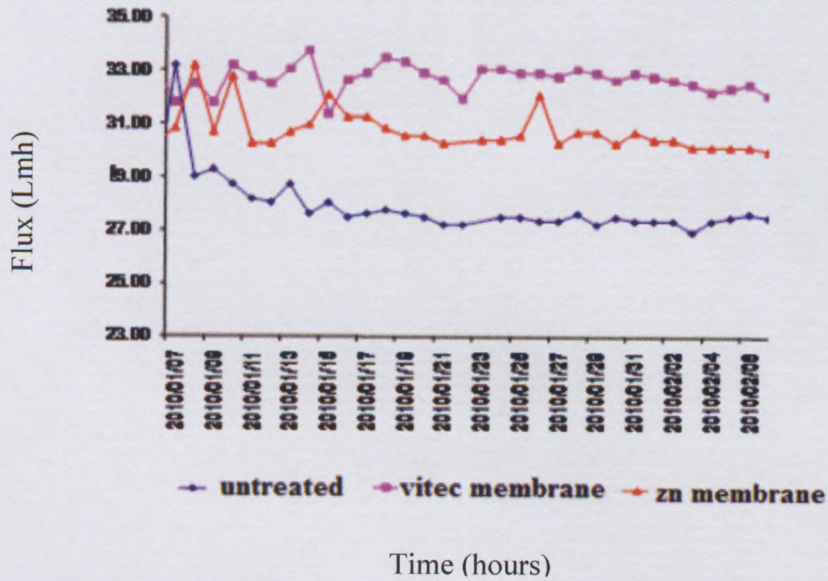
Although, macroscopically the RO membranes were covered rather uniformly by scale deposits, it was observed, microscopically, that the scale crystals are somehow larger close to the exit permeate compared with those close to the entry, apparently due to the existence of an increasing concentration polarization

SEM images of the surface of the membrane treated with commercial anti-scalant (Figure 5-10) showed that the deposits were distributed evenly in the three zones of the core side than in three zones of the shell side. This indicates that membrane surface at the shell side had less deposits. However, the commercial anti-scalant seems to disperse the deposit, and the remaining deposit sizes were smaller than the ones at the untreated membrane in Figure 5-9.

SEM images from the surface of membrane treated with  $Zn^{2+}$  ions (in Figure 5-11) showed that the deposits were prevalent than the deposits in the case of the membrane treated with the commercial anti-scalant, as shown in. Figure 5-9 and in Figure 5-10. This means the  $Zn^{2+}$  ions eliminate less scaling crystals than the commercial anti-scalant. This indicates that  $Zn^{2+}$  ions are less effective as an anti-scalant in comparison with commercial anti-scalant for large RO plants. in Figure 5-11 also indicated that the deposited materials were deposited on the shell and core side of the feed zone and the core of the permeate zone than other zones investigated.

Figure 5-12 Figure shows the flux rate of the following membranes: untreated, treated with  $Zn^{2+}$  ions, and treated with commercial anti-scalant. The flux of the untreated membrane (5-12, blue line) decreased over time. This supports the SEM results in Figure 5-9, which showed that the untreated membrane had more deposits accumulated on the membrane surface (than the treated membranes). After the addition of an anti-scalant to the system, the flux rate of the membranes improved (Figure Figure 5-12, pink and red lines). This indicated the effectiveness of the anti-scalants used, especially the commercial anti-scalant (pink line in Figure 5-12). This supports the SEM results in Figure 5-10 and Figure 5-11. Once again, the inhibition of crystal growth on the surface of the membrane seems to be pronounced in the case of the membrane treated with commercial anti-scalant in comparison with the membrane treated with  $Zn^{2+}$  ions and the untreated membrane. The

commercial anti-scalant interfered with the normal crystal growth, to produce an irregular crystal structure with poor scale-forming ability. Overall, the anti-scalant reduced the rate of crystal growth that inhibits/reduces the membrane performance thus causing membrane fouling.



**Figure 5-12: Flux results for an untreated membrane and membranes treated with different anti-scalants (commercial anti-scalant and Zn<sup>2+</sup>)**

The effectiveness of the two different anti-scalants was further assessed by determining the rejection of membranes exposed to the different treatments. Results are shown in Figure 5-12. The untreated membrane (Figure 5-12, blue line) had a lower rejection than the treated membranes. The rejection of the treated membranes (Figure 5-12, pink and yellow lines) was higher than that of the untreated membrane. The rejection of membrane treated with commercial anti-scalant was higher than that of the membrane treated with Zn<sup>2+</sup> ions. This was in agreement with SEM results taken: more deposits remained on the surface of the membrane treated with Zn<sup>2+</sup> ions than that treated with Vitec 3000 (see Appendix B).

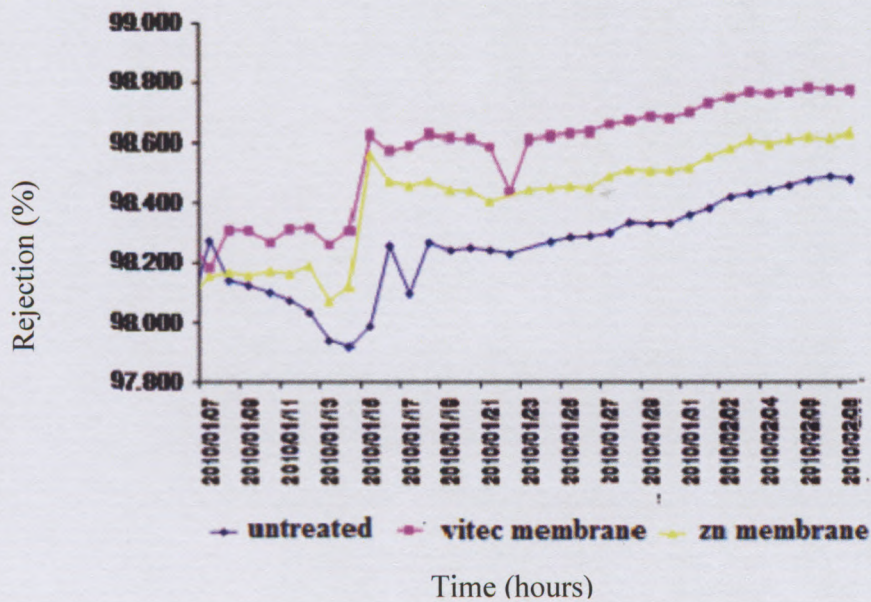


Figure 5-13: Rejection results for an untreated membrane and membranes treated with different anti-scalants (commercial anti-scalant and Zn<sup>2+</sup> ions)

### Summary

SEM analysis as well as OM analysis was done in this chapter to investigate the morphology of the membrane surface. The gained results from these investigations showed significant differences between the feed side, middle, and the permeate side. RO performances for both treated and untreated membrane were also studied in this chapter. Their results were in agreement with the observations obtained from the SEM analysis.



## Conclusions

The main findings of this study were the following:

1. The proposed autopsy procedure was successfully used in this study for the analysis of the compared RO membranes BW30-4040 and XLE 4040.
2. Laboratory and pilot plant scale experiments showed that the use of specific concentrations of  $Zn^{2+}$  ions can inhibit scale formation in RO feed water by changing the scale crystal structure. Laboratory experiments showed that  $Zn^{2+}$  at concentrations of 0.12 mg/L and 0.06 mg/L can inhibit the onset of scaling (i.e. no flux decline due to scaling), while pilot plant scale experiments showed that the addition of  $Zn^{2+}$  can improve the flux by up to 10% (compared to when no anti-scalant treatment is used).
3. Two different concentrations (0.12 mg/L and 0.06 mg/L) of  $Zn^{2+}$  ions were successfully generated in the lab using electrochemical cell.
4. Utilizing both SEM and OM were able to show the morphological changes on the surface of the membranes, compared to an untreated membrane. SEM analysis showed that the commercial anti-scalant Vitec 3000 was more effective than  $Zn^{2+}$  ions as fewer deposits were observed on a membrane surface treated with the former.
5. More effective anti-scaling was achieved when 3 mg/L of the commercial anti-scalant Vitec 3000 was used, compared to 1 and 2 mg/L.
6. Better anti-scaling was achieved when 0.12 mg/L  $Zn^{2+}$  ions was used compared to 0.06 mg/L, indicating that a higher concentration of  $Zn^{2+}$  ions reduced crystal formation, thus distorting calcite formation.
7. The SEM results, from the pilot plant images, showed more presence of deposits in the untreated membrane sample compared to that of the treated membrane samples. These deposits were more prevalent on the core side than on the shell side.
8. SEM images of the surface of a membrane treated with the scalant Vitec 3000 showed that the deposits were distributed evenly in the all three zones of both the core and the shell side, however, deposits in the core sides were more pronounced.

9. SEM images of the surface of a membrane treated with  $Zn^{2+}$  ions showed that the deposits were more prevalent than the deposits in the case of the membrane treated with the Vitec 3000. The deposited materials were prevalent on the shell and core side of the feed zone and permeate zone than other zones.
10. RO performance results (membrane flux and rejection) of the membranes confirmed the observations achieved with the SEM images. The flux and rejection of a membrane sample treated with the commercial anti-scalant was higher than in the case of a membrane samples treated with  $Zn^{2+}$  ions, including untreated membrane sample.  $Zn^{2+}$  does improve anti-scaling.

### **Recommendations and Future Work:**

The following issues may be recommended for the follow up of the works conducted in this thesis:

1. Additional analytical research is required to evaluate anti-scalant effects on membrane scaling. This is because fouling and scaling occurs differently depending on water quality and different mechanisms are required for each water quality used in the RO system. More information about the SEM is required to interpret the analysis clearly.
2. Scale inhibition capability of anti-scalants is related to chemical structure, molecular weight, active functional groups and solution pH. Therefore, other techniques can be used to investigate scaling and scale inhabitation in more details. Techniques such as EDS elemental analysis can be used to define the deposited salts.
3. A number of factors can be measured or monitored, such as the presence of other ions, the pH and Langelier Saturation Index which can be used to determine the efficiency of anti-scale treatments.
4. Optimization of  $Zn^{2+}$  concentrations in which the onset of scaling is inhibited and flux is improved.

## References

- Aboutali E., Jean O. and Lédion J., 1996. *J. Europ. d'Hydrologie*, 27: p.109–126.
- Alyson, S., Benny, F., 2002. *Fundamentals of Membranes for Water Treatment*, University of Austin, Texas.
- Avista Technologies, 2004. Vitec 3000: Antiscalant/Dispersant Product Datasheet. [www.avistatech.co.uk/html/anti/anti-pdf/vitec3000](http://www.avistatech.co.uk/html/anti/anti-pdf/vitec3000).
- AL-Rammah A (2002) The application of acid free anti-scalant to mitigate scaling in reverse osmosis membranes. *Desalination* 132 83–87.
- Baker, R.W., 2004. *Membrane Technology and Applications*. 2nd edition, Chichester, England: John Wiley & Sons. pp. 217-219.
- Binnig, G., Rohrer, H., and Gerber C., 1983. *Reconstruction on Si (111) resolved in real space*, *Phys. Rev. Lett.* 50: 120-123.
- Boubakri, A., Bouguecha. S., 2008. *Diagnostic and membrane autopsy of Djerba Island desalination station*, *Desalination*, 220: 403-441.
- Butt, F., Rahman, B., and Baduruthamal, U., 1995. *Identification of scale deposits through membrane autopsy*, *Desalination*, 101: 219-230.
- Butt, F., Rahman, H., and Baduruthamal, U., 1997. *Characterization of foulants by autopsy of RO desalination membranes*, *Desalination*, 114: 51-64.
- Cadotte, J., 1985. *Evaluation of composite reverse osmosis membrane*. In: *Materials Science of Synthetic Membranes*, D.R. Lloyd (ed.). Symposium series No. 296, American Chemical Society, Washington.
- Cadotte, J., King R., Majerle R., and Petersen, R., 1981. *Interfacial synthesis in the preparation of reverse osmosis membranes*. *Journal Micromole. Sci. Chem P.* 1 3: New York.
- Cadotte, J., Petersen, J., 1975. *Thin-film composite membranes: origin, development and recent advances*, *ACS Symposium Series*. p. 21-33.

- Cadotte, J., King R., Majerle R., and Petersen, R., 1982. *Interfacial synthesis in the preparation of Reverse Osmosis membranes*. Journal of macromolecular science p. 727.
- Chesters, S. P., Darton, E.G., and Vigo, F.D., 2007. *Theoretical and practical experience of calcium phosphate inhibition in RO waters*. IDA World Congress Desalination and Water Reuse Gran.
- Coetzee, P., Yacoby, M., Howell, S., and Mubenga, S., 1998. *Scale reduction and scale modification effects induced by Zn and other metal species in physical water treatment*, p: 77-84. University, PO Box 524, Johannesburg, South Africa.
- Coetzee PP, Yacoby M & Howall S. 1996. *The role of zinc in magnetic and other physical water treatment methods for the prevention of scale*. Water SA 22(4): p.319–326.
- Cengeloglua, A., Arslana, A., Tor, B., Kocak, A., and Dursun, C., 2008. *Removal of boron from water by using reverse osmosis*. Separation and Purification Technology 64: p. 141–146.
- Dalton, T., Annunziata, F., and Gallego, P., 2004. *Membrane autopsy helps to provide solutions to operational problems*, Desalination 167: p. 239-245.
- Darton, E., Fazel, M. 2002. *Performing a membrane autopsy*, Desalination and Water Reuse, 11: p. 40-46.
- Dudley, L., Darton, G., 1996. *Membrane autopsy a case study*, Desalination, 105: p. 135-141.
- Drak, A., Glucina, B., Busch, A., Hasson, A., Lame, B., and Semiat, A., 2000. *Laboratory technique for predicting the scaling propensity of RO feed water*.Desalination 132: p. 233-242 .
- Eun, G. Myong-jin, Y, Hee-kyong, and O.Yong-hun. 2003. *Fouling characteristics of NF and RO operated for removal of dissolved matter from ground water*, Water Research, 37: p. 2989-2997.
- Fay, I., Linossier, V., Langlois, D., Haras, K., and Vallee-Rehel, 2005. *SEM and EDX analysis: two powerful techniques for the study of antifouling paints*, Progress in Organic Coatings, 54: p. 216-223.

Gamal, M., Khedr, A., 1998. *A case study of RO plant failure due to membrane fouling analysis and diagnosis*. Desalination 120: p. 107-113.

Ghizellaoui S., Euvrard M., Ledion J., Chibani A., 2007. Desalination. *Inhabitation of scaling in the presence of copper and zinc by various chemical processes*. 206. pp. 185–197.

Glasner A. and Weiss D., Inorg J. 1980. Nucl. Chem., 42(5): p. 655–663.

Gloede, T., Melin, M., 2008. *Physical aspects of membrane scaling*, Desalination, 224: p. 71-75.

Goldie, I., Aziz, M., Apozrida, A., and Sanderson, R., 2008. Anti-scaling studies on high CaCO<sub>3</sub> waters in spiral-wrap membrane systems. Report to the Water Research Commission.

Hilal, A., Mohammad, B., Atkin, N., and Darwish, A., 2003. Desalination. *Using atomic force microscopy towards improvement in nanofiltration membranes properties for desalination pre-treatment: a review*. 157. pp. 137-144.

Hui, L., Chihpin, H., and Jill, R., 2008. Desalination. *Characteristics of RO foulants in a brackish water desalination plant*. 220 pp. 353-358.

Ismail, K., Mark, W., 2007. *Morphological variation of precipitated salts on NF and RO membranes*, Environmental Engineering Science, 24: p. 602-614.

Jefferies, M., Champion, R., 2009. *Membrane Autopsies: Techniques Utilized, and a Statistical Presentation of Results of 100 Autopsies*, Avista Technologies. [www.wisa-Mtcog.com/agen](http://www.wisa-Mtcog.com/agen).

John, S., Baker, S., Judd, J., and Simon, A., 1997. Desalination. *Anti scale magnetic pre-treatment of reverse osmosis feedwater*. 110. pp. 151-166.

Johnson, G., Culkin, M., 2002. *Kinetics of Mineral Scale Membrane Fouling: A Comparison of Conventional Crossflow Membranes and V-SEP, a Vibratory Membrane System*. Technical Article. p. 1-14.

Kavanagh A., Rayment T. and Price T., J. Chem. Soc. Faraday Trans., 86(6) (1990) 965–972.

Koros, W., Shimizu, T., 1996. *Terminology for membranes and membrane processes*, IUPAC Recommendations, 120: p. 149-159.

- Koutsoukos P. And Kontoyannis C. 1984. *Prevention and inhibition of calcium carbonate scale*, Jour. Of Crystal Growth, 69: P. 366-376.
- Leenheer, J., Crouc, J., Benjamin, G., Korshin, C., Hwang, A., Bruchet, G., and Aiken, G., 2000. *Comprehensive isolation of natural organic matter from water for spectral characterizations and reactivity testing*, ACS Symposium Series No. 761, American Chemical Society: Washington DC.
- Lisitsin, Q. Yang, D., and Hasson, R., 2005. Desalination. *Inhibition of CaCO<sub>3</sub> scaling on RO membranes by trace amounts of zinc ions*. 183. pp. 289-300.
- Lindsay, M., 2000. *The scanning probe microscope in biology*, in *Scanning Probe microscopy and Spectroscopy*, p. 290-330.
- Loeb, S., Sourirajan, 1963. *Sea water demineralization by means of an osmotic membrane in saline water conversion*, Advances in Chemistry Series No. 28, American Chemical Society, Washington, DC. p. 117-132.
- Lond Sourirajan, S., 1981. *Reverse Osmosis: A new field of applied chemistry and chemical engineering*, ACS Symposium Series. p. 11-62.
- Luo, M., Wang, Z. 2001. Desalination. *Complex fouling and cleaning in place of a reverse osmosis desalination system*. 141. pp. 15-22.
- Luo, Z., Wang, 2001. Desalination. *Complex fouling and cleaning-in-place of a reverse osmosis desalination system*. 141. pp. 15-22.
- Macadam, J. And Parsons, A. Water Science and Technology. *Calcium carbonate scale control, effect of material and inhibitors*. 153. pp. 153-159.
- Masahiko, H., Yoshihiro, M., and Yoshiyasu, K., 1997. Journal of Membrane Science. *The relationship between polymer molecular structure of RO membrane skin layers and their RO performances*. 123: p. 151-156.
- Maxime, P., Sophie, R., Anju, T., Jean, D., Valerie, J., and Jerome, L., 2005. Desalination. *Tools for membrane autopsies and antifouling strategies in sea water feeds*. 181: pp. 75-90.
- Menlo, P., 1997. Membrane Technology and Research, Inc. California, p. 578-663.
- Meyer HJ. 1984. *The influence of impurities on the growth rate of calcite*. J. Cryst. Growth 66: p. 639-646.

- Michaels, A., 1976. *Synthetic polymeric membranes: practical applications, past present and future*, Pure and Applied Chemistry, 46: p.193-204.
- Microscopy and Spectroscopy, edited by Dawn A. Bonnell. 2 nd ed new york : wiley. 290-330.
- Mulder, M., 1996. *Basic Principles of Membrane Technology*. Kluwer Academic: Dordrecht. pp. 299-305.
- Myzairah, B. 2007. "Low pressure reverse osmosis membrane for rejection of heavy metals". Master thesis, Universiti Teknologi Malaysia.
- Naidoo, P.D., van Ballegooyen, R., Pulfrich, A., and Steffani, N. 2008. *Environmental impact assessment: proposed reverse osmosis plant, iron-ore handling facility, Port of Saldanha*, Joint CSIR/Pisces report, CSIR/NRE/ECO/ER/2007/0149C.
- Nicolaisen, B., 2002. Desalination. *Developments in membrane technology for water treatment*. 153: pp. 355-360.
- Nkosikho, 2008. *The investigation to select an anti-scalant for desalination of brackish water through a reverse osmosis (RO) laboratory bench scale flat cell* Department of Chemical Engineering. Cape Town Campus Final Report. P. 1-30.
- Norman, n., Anthony, G., Fane, W.S., Winston, HO., and Matauura, T. 2008. *Advanced membrane technology and applicants*. Wiley. New Jersey, p. 1-17.
- Odhav, B., 2004. *Guidelines for routine monitoring of membrane performance for potable water production in small water treatment plant*. Report to the Water Research Commission, South Africa. pp. 9-11.
- Pearce, G., 2007. *Introduction to Membranes, Filtration and Separation*, 44: 24-27.
- Pernot B, Euvrard H, Remy F & Simon P. 1999. *Influence of Zn(II) on the crystallization of calcium carbonate application to scaling mechanisms*. J. Water SRT–Aqua 48(1): p.16–23.
- Pontie, A., Rapenne, B., Thekkedath, A., Duchesne, D., Jacquemet, C., Leparc, C., and Suty, C., 2005. Desalination. *Tools for membrane autopsies and antifouling strategies in seawater feeds: a review*. 181: p. 75-90.
- Roever, BE., Huisman, H., 2006. Desalination. *Microscopy as a tool for analysis of membrane failure and fouling*. 207: pp. 35–44.

Schippers, C., Verdouw, J., 1980. *The modified fouling index, a method of determining the fouling characteristics of water*, Desalination, 32: p. 137-148.

Scott, K., Hughes, R., 1996. *Industrial Membrane Separation Technology*. Chapman and Hall: Schneider, A., Ferreira, A., Binder, A., and Ramos, B., 2005. *Journal of Membrane Science. Analysis of foulant layer in all elements of an RO train*. 261: pp. 152–162.

Sheikholeslami, R., Tan S., 1999. *Desalination. Effects of water quality on silica fouling of desalination plants*. 126: pp.267-280.

Shon, H., Vigneswarana, S., Zareiea, M., Ben Aimb, R., Leec, J., Leec, J., and Choc, S., 2009. *Desalination. Physico-chemical pre-treatment to seawater reverse osmosis (SWRO): organic characterization and membrane autopsy*. 236: pp. 282–290.

Shun, D., 2007. *Water and Wastewater Calculations Manual*. 2<sup>nd</sup> edition.

Sourirajan, 1981. *Reverse Osmosis: A new field of applied chemistry and chemical engineering*, ACS symposium Series. P. 11-62.

Stergios, G., Yiantsios, J., and Karabela, S., 2002. *Desalination An assessment of the Silt Density Index based on RO membrane colloidal fouling experiments with iron oxide particles*. 151: pp. 229-238.

Tzotzi, A., Pahiadaki, B., Yiantsios, B., Karabelas, B., Andritsos, A., 2007. *Journal of Membrane Science. A study of CaCO<sub>3</sub> scale formation and inhibition in RO and NF membrane processes*. , 296: pp. 171-184.

Trana, B., Boltoa, S., Grayb, M., Hoanga, E., and Ostarcevicc, A., 2007. *Water research. An autopsy study of a fouled reverse osmosis membrane element used in a brackish water treatment plant*. 41: pp. 3915 -3923.

Thuy, T., Brian, B., Stephen, G., Manh, H., and Eddy, O., 2007. *Water Research. An autopsy study of a fouled reverse osmosis membrane element used in a brackish water treatment plant*. 41: pp. 3915-3923.

Ted, D., Dalton, a., Ursula, A., Fernando, A., del, P., and Silvia, G., 2004. *Membrane autopsy helps to provide solutions to operational problems*. Desalination 167: p. 239-245



Wilf, M., 2007. *The guide book to membrane desalination technology*. Italy: Balaban Desalination Publications.

Shih, A. Rahardianto, Ron-Wai Lee, Y. Cohen, 2005. *Journal of membrane science*. *Morphometric characterization of calcium sulphate dehydrate (gypsum) scale on reverse osmosis membranes*. 252: p. 253-263.

Yang, Q. 2006. *Inhibition of CaCO<sub>3</sub> Scalling in Reverse Osmosis system by Zinc Ion*, Chinese J. Chem. Eng., 14 : p. 178-183.

Yang, Q., Hasson, D., Semiat, R., and Lisitsin, D., 2005. *Inhibition of CaCO<sub>3</sub> scaling on RO membranes by trace amounts of zinc ions*, *Desalination*, 183: p. 289-300.

Yuan, A., Ning, b., Zhen-Min, A, and Raphael, C., 2009. *Electrostatic potential on anti-scalants*

*CaCO<sub>3</sub> (104) surface: A molecular simulation study*. *Desalination* 238: p. 246–256.

Zazouli, M., Nasser, S., Mahvi, H., Gholami, M., Mesdaghinia, R., and Younecian, M., 2008. *World Applied Sciences Journal*. *Studies on Rejection and Fouling of Polyamide Reverse Osmosis Membrane in the Treatment of Water Solutions Containing Humic Acids*. 3(3): p. 434-440.

Zeppenfeld K. 2010. *Prevention of CaCO<sub>3</sub> scale formation by trace amounts of copper (II) in comparison to zinc (II)*, *Desalination*, 252: p. 60-65.

## Appendices

### APPENDIX A: Flat cell test experimental results

**Table 1: Data of synthetic scaling water at 5 bars**

Conditions

DATA	
Length	0.145
Width	0.095
XS Area	0.013775
Time of flux	5

Date	11 November 2009
Experiment	AA1 Scaling
Conditions	
Conc (ppm)	N/a
Pressure	1000

DATA INPUT				
Time	Flow rate Permeate	Flow rate Permeate (L/hr)	Flux	Pump RPM (Hz)
8:10	40	0.48	34.84573503	26.3
8:40	40	0.48	34.84573503	26.1
9:10	39	0.468	33.97459165	25.6
9:40	39	0.468	33.97459165	26.2
10:10	38	0.456	33.10344828	25.9
10:40	38	0.456	33.10344828	25.1
11:10	38	0.456	33.10344828	25.3
11:40	37	0.444	32.2323049	25.1
12:10	36	0.432	31.36116152	23
12:40	35	0.42	30.49001815	24.5

DATA INPUT			
Time	EC FEED	EC PERMEATE	Rejection
8:10	1189	112	90.58032
8:40	1069	102	90.458372
9:10	1182	98	91.708968
9:40	1171	65	94.449189
10:10	1262	66	94.770206
10:40	1248	62	95.032051
11:10	1205	62	94.854772
11:40	1158	58	94.991364
12:10	1147	58	94.94333
12:40	1122	56	95.008913

**Table 2: Data of synthetic scaling water with vitec 3000 at 5 bars**

Conditions

DATA	
Length	0.145
Width	0.095
XS Area	0.013775
Time of flux	5

Date	30 November 2009
Experiment	AA4
Conditions	Vitec
Conc (ppm)	N/a
Pressure	1000

DATA INPUT				
Time	Flow rate Permeate	Flow rate Permeate (L/hr)	Flux	Pump RPM (Hz)
9:00	44	0.528	38.33030853	25.9
9:30	43	0.516	37.45916515	24.2
10:00	43	0.516	37.45916515	25.3
10:30	42	0.504	36.58802178	25
11:00	41	0.492	35.7168784	25.6
11:30	42	0.504	36.58802178	25.8
12:00	42	0.504	36.58802178	24.9
12:30	42	0.504	36.58802178	24.8
13:00	42	0.504	36.58802178	25.3
13:30	42	0.504	36.58802178	26.5
14:00	42	0.504	36.58802178	25.6

DATA INPUT			
Time	EC FEED	EC PERMEATE	Rejection
9:00	1369	82.2	93.995617
9:30	1275	84.5	93.372549
10:00	1018	51.3	94.960707
10:30	1110	58.9	94.693694
11:00	1066	53.2	95.009381
11:30	945	41.4	95.619048
12:00	1096	49.8	95.456204
12:30	1068	49.8	95.337079
13:00	1103	47.4	95.702629
13:30	960	42.1	95.614583
14:00	1203	42.6	96.458853

**Table 3: Data of synthetic scaling water with zinc at 5 bars**

Conditions

DATA	
Length	0.145
Width	0.095
XS Area	0.013775
Time of flux	5

Date	08 December 2009
Experiment	AA5
Conditions	Zn
Conc (ppm)	0.06
Conc (mg/L)	60
Pressure	1000

DATA INPUT					
Time	Flow rate Permeate	Flow rate Permeate (L/hr)	Flux	Pump RPM (Hz)	Zn Conc in feed line (mg/L)
9:00	43	0.516	37.45916515	25.1	0
9:30	42	0.504	36.58802178	25.4	0
10:00	42	0.504	36.58802178	25.6	0
10:30	42	0.504	36.58802178	25.6	0
11:00	41	0.492	35.7168784	25.2	0
11:30	41	0.492	35.7168784	24.7	100
12:00	41	0.492	35.7168784	24.9	60
12:30	41	0.492	35.7168784	25.3	30
13:00	41	0.492	35.7168784	25.4	60
13:30	41	0.492	35.7168784	24.8	60
14:00	40	0.48	34.84573503	24.7	140
<b>Average</b>					<b>75</b>

DATA INPUT			
Time	EC FEED	EC PERMEATE	Rejection
9:00	1239	50.8	95.899919
9:30	1198	45.3	96.218698
10:00	998	34.8	96.513026
10:30	1098	37.1	96.621129
11:00	1002	33.1	96.696607
11:30	1363	50.3	96.309611
12:00	1274	41.3	96.758242
12:30	1273	41.5	96.739984
13:00	1248	41.4	96.682692
13:30	1236	40.3	96.739482
14:00	1245	39.7	96.811245

**Table 4: Data of synthetic scaling water with zinc at 5 bars**

DATA	
Length	0.145
Width	0.095
XS Area	0.013775
Time of flux	5

Date	10 December 2009
Experiment	AA7
Conditions	Zn
Conc (ppm)	0.12
Conc (mg/L)	120
Pressure	1000

DATA INPUT						
Time	Flow rate Permeate	Flow rate Permeate (L/hr)	Flux	Pump RPM (Hz)	Zn Conc in feed line (mg/L)	Zn Conc in Permeate (mg/L)
7:30	44	0.528	38.33030853	25.6	0	0
8:00	43	0.516	37.45916515	25.2	0	0
8:30	43	0.516	37.45916515	25.6	0	0
9:00	42	0.504	36.58802178	24.9	0	0
9:30	41	0.492	35.7168784	26.4	0	0
10:00	41	0.492	35.7168784	25.6	100	0
10:30	42	0.504	36.58802178	25.6	110	0
11:00	41	0.492	35.7168784	26.4	150	0
11:30	41	0.492	35.7168784	25.6	130	0
12:00	41	0.492	35.7168784	25.3	210	0
12:30	41	0.492	35.7168784	25.1	150	0
<b>Average</b>					<b>141.67</b>	

DATA INPUT			
Time	EC FEED	EC PERMEATE	Rejection
7:30	1238	72.1	94.17609
8:00	1224	66.4	94.575163
8:30	1248	60.6	95.144231
9:00	1379	61.9	95.51124
9:30	1151	50.5	95.612511
10:00	1369	59.7	95.639153
10:30	1168	48.1	95.881849
11:00	1260	49.9	96.039683

11:30	1120	44.3	96.044643
12:00	1066	41.3	96.125704
12:30	1270	49	96.141732

#### 4.6.2 The procedure of calculations of Zinc ion concentrations

Feed rate = 25.95 RPM = 118 L/h

Permeate flux = 0.511 L/h (0.40%)

Brine flow = 117.489 L/h (99,60%)

Zinc dosing rate (before pumping commences) = 2.52 L/h

Permeate flux rate = 0.001008 L/h (0.40%)

Brine flow rate = 2.518992 L/h (99,60%)

#### The amount of Zn<sup>2+</sup> ions on the membrane

$$\text{Zn}^{2+}_{(\text{membrane})} = \text{Conc}_{\text{brine}} \times \text{Permeate}_{\text{flow}}$$

$$\text{Zn}^{2+}_{(\text{membrane})} = 75\mu\text{g} / \text{L} \times 0.511\text{L} / \text{hr}$$

$$\text{Zn}^{2+}_{(\text{membrane})} = 38.325\mu\text{g} / \text{hr}$$

$$\text{Zn}^{2+}_{(\text{membrane})} = \text{Conc}_{\text{brine}} \times \% \text{Permeate}_{\text{flow}}$$

$$\text{Zn}^{2+}_{(\text{membrane})} = 75\mu\text{g} / \text{L} \times 0.004$$

$$\text{Zn}^{2+}_{(\text{membrane})} = 0.3\mu\text{g} / \text{L} \div 0.14\text{m}^2$$

$$\text{Zn}^{2+}_{(\text{membrane})} = 21.42\mu\text{g} / \text{L.m}^2$$

$$\text{Zn}^{2+}_{(\text{membrane})} = \text{Conc}_{\text{brine}} \times \text{Permeate}_{\text{flow}}$$

$$\text{Zn}^{2+}_{(\text{membrane})} = 120\mu\text{g} / \text{L} \times 0.511\text{L} / \text{hr}$$

$$\text{Zn}^{2+}_{(\text{membrane})} = 61.32\mu\text{g} / \text{hr}$$

$$\text{Zn}^{2+}_{(\text{membrane})} = \text{Conc}_{\text{brine}} \times \% \text{Permeate}_{\text{flow}}$$

$$\text{Zn}^{2+}_{(\text{membrane})} = 120\mu\text{g} / \text{L} \times 0.004$$

$$Zn^{2+}_{(membrane)} = 0.48\mu g / L \div 0.14m^2$$

$$Zn^{2+}_{(membrane)} = 34.29\mu g / L.m^2$$

### Appendix B: Pilot plant experimental results

Table 1: Shows the sequence of the experimental tests and the results as well as the quantity of salt added in each experiment of operating the RO pilot plant during the period

10/02/2009 till 3/03/2010:

DATE	FEED		PERM		TOTAL PRESS Kpa	Flux	Rejection
	FLOW L/HR	COND µ/SCH	COND µ/SCH	FLOW L/HR			
10/2/2009	1105.2	6861	489	276	900	38.33	92.873
10/3/2009	1128.3	6725	500	282	900	39.17	92.565
10/4/2009	1120.1	6767	492	284	900	39.44	92.729
10/5/2009	1125.4	6742	491	288	900	40.00	92.717
10/6/2009	1131.9	6760	479	292	900	40.56	92.914
10/7/2009	1128.5	6764	473	285	900	39.58	93.007
10/7/2009	1102.8	6714	458	281	900	39.03	93.178
10/8/2009	1129.9	6724	439	284	900	39.44	93.471
10/9/2009	1132.1	6713	430	282	900	39.17	93.595
10/10/2009	1123.4	6722	440	239	900	33.19	93.454
10/11/2009	1129.3	6711	434	283	900	39.31	93.533
10/12/2009	1129.1	6635	408	279	900	38.75	93.851
10/13/2009	1115.43	6568	404	284	900	39.44	93.849
10/14/2009	1115.1	6651	309	282	900	39.17	95.354
10/15/2009	1115.9	6567	307	282	980	39.17	95.325
10/16/2009	1115.2	6567	304	282	980	39.17	93.325
10/17/2009							
10/18/2009							
10/19/2009							
10/20/2009							
10/21/2009							
10/22/2009	1109.3	6487	294	291	1000	38.06	38.06
10/23/2009	1105.4	6440	265	289	999	36.81	36.81
10/24/2009	1115.2	6434	259	289	1000	39.86	39.86
10/25/2009	1118.9	6466	236	289	1000	41.25	41.25
10/26/2009	1162.2	6470	233	286	1000	32.22	32.22
10/27/2009	1118.3	6488	236	244	1000	40.42	40.42
10/28/2009	1118.6	6524	216	241	1003	40.14	40.14
10/29/2009	1122.3	6488	211	235	1005	40.14	40.14
10/30/2009	1125.3	6476	207	235	1005	39.72	39.72
10/31/2009	1120.4	6524	206	235	920	33.89	33.89
11/12/2009	992	6170	185.3	245	920	33.47	33.47
11/13/2009	979	6180	165	245	940	32.64	32.64
11/14/2009	973	6327	154.9	211	999	32.64	32.64

11/15/2009	991	6337	146.3	216	999	32.64	32.64
11/16/2009	958	6414	142.7	207	1000	34.03	34.03
11/17/2009	956	6446	146.7	206	1000	34.17	34.03
11/18/2009			146.3		1000	34.86	97.712
11/19/2009	960	6387	143.6	251	1000	34.31	97.712
11/20/2009	962	6401	147.3	247	1000	34.31	97.752
11/21/2009	975	6374	149.5	241	1000	33.47	97.699
11/22/2009	966	6444	147.3	249	1000	34.58	97.655
11/23/2009	971	6402	150.3	245	1000	34.03	97.714
11/24/2009	966	6381	149.5	249	1000	34.58	97.652
11/25/2009	985.4	6441	152.8	244	1000	33.89	97.628
11/26/2009							
11/27/2009							
11/28/2009	973	6430	149.6	230	999	31.39	97.679
11/29/2009	972	6423	149.1	226	999	31.25	97.702
11/30/2009	955	6385	146.7	225	999	31.39	97.751
12/1/2009	968	6392	145.9	226	999	34.94	97.756
12/2/2009	960	6382	143.5	231	999	31.39	97.759
12/3/2009	968	6364	142.8	228	999	31.25	97.704
12/4/2009	958	6362	142.6	228	999	31.39	97.655
12/5/2009	971	6312	144.9	224	999	32.08	97.670
12/6/2009	975	6400	150.1	236	999	31.67	97.676
12/7/2009	971	6325	147.4	226	999	31.67	97.721
12/8/2009	977	6335	147.2	221	999	31.11	97.686
12/9/2009	972	6348	144.7	224	995	32.78	97.706
12/10/2009	984	6236	144.3	219	998	31.39	97.518
12/11/2009	947	6159	141.3	215	998	30.69	97.538
12/12/2009	957	5797	143.9	217	995	31.11	97.538
12/13/2009	965	6085	149.8	215	999	30.42	97.538
12/14/2009							
12/15/2009	963	6059	114.7	222	994	30.83	98.12
12/16/2009	976	6084	115.4	223	999	30.97	98.07
12/17/2009	966	6043	116.3	223	995	30.97	98.09
12/18/2009	971	6016	117.3	223	995	30.97	98.06
12/19/2009	968	5991	116.5	225	997	31.25	98.08
12/20/2009	972	5994	116.3	236	998	32.78	98.08
12/21/2009	956	6119	117.6	223	995	30.97	98.10
12/22/2009	977	6253	119	222	998	30.83	98.12
12/23/2009	974	6039	116.9	223	998	30.97	98.12
12/24/2009	982	5956	114.7	225	995	31.25	98.11
12/25/2009	963	5963	107.4	243	998	33.75	97.91
12/26/2009	974	5965	109.9	224	999	31.11	98.21
12/27/2009	970	5952	108.3	224	999	31.11	98.23
12/28/2009	965	5963	107.1	219	999	30.42	98.30
12/29/2009	979	5952	107	219	999	30.42	98.30
12/30/2009	975	5947	107.2	215	999	29.86	98.34
12/31/2009	993	5930	109.4	213	999	29.58	98.35
1/1/2010	971	5941	111.1	213	999	29.58	98.35
1/2/2010	971	5841	114.2	214	999	29.72	98.03
1/3/2010	967	5921	116.7	207	999	28.75	98.35
1/4/2010	970	6430	149.6	230	998	28.61	98.38
1/5/2010	975	6423	149.1	229	998	28.61	98.36
1/6/2010	973	6385	146.7	234	998	34.17	
1/7/2010	978	6392	145.9	229			98.18
1/8/2010	975	6382	143.5	239	998	31.81	98.31
1/9/2010	959	6364	142.8	236	999	32.50	98.31
1/10/2010	973	6362	142.6	234	999	31.81	98.27



1/11/2010	978	6312	144.9	238	1000	33.19	98.31
1/12/2010	961	6400	150.1	243	1000	32.78	98.32
1/13/2010		6325	147.4	226	1000	32.50	98.26
1/14/2010		6335	147.2	235		33.06	98.31
1/15/2010		6348	144.7	237		33.75	98.62
1/16/2010		6236	144.3	241		31.39	98.57
1/17/2010		6159	141.3	240		32.64	98.59
1/18/2010		5797	143.9	237		32.92	98.63
1/19/2010		6085	149.8	235		33.47	98.62
1/20/2010				230		33.33	98.61
1/21/2010		6059	114.7	238		32.92	98.59
1/22/2010		6084	115.4	238		32.64	98.44
1/23/2010		6043	116.3	237		31.94	98.61
1/24/2010	971	6016	117.3	237	1000	33.06	98.62
1/25/2010	975	5991	116.5	229	1000	33.06	98.63
1/26/2010	971	5994	116.3	234	1000	32.92	98.64
1/27/2010	972	5874	99.8	197	1000	27.36	98.66
1/28/2010	976	5884	97.9	199	1000	27.64	98.67
1/29/2010	979	5857	97.7	196	1000	27.22	98.69
1/30/2010	977	5881	98.1	198	1050	27.50	98.68
1/31/2010	971	5847	95.8	197	1050	27.36	98.70
2/1/2010	969	5866	94.8	197	1050	27.36	98.73
2/2/2010	978	5890	99.8	197	1050	27.36	98.75
2/3/2010	964	5898	97.9	194	1050	26.94	98.77
2/4/2010	974	5866	97.7	197	1050	27.36	98.76
2/5/2010	975	5859	98.1	198	1050	27.50	98.77
2/6/2010	977	5862	95.8	199	1050	27.64	98.78
2/7/2010	978	5870	94.8	198	1050	27.50	98.78
2/8/2010	968	5854	93	195	1050	27.08	98.77
2/9/2010	971	5852	92.4	190	1010	26.39	98.66
2/10/2010	976	5935	91.2	188	1010	26.11	98.69
2/11/2010	971	5934	90.2	188	1010	26.11	98.67
2/12/2010	956	5917	89.2	188	1010	26.11	98.70
2/13/2010	986	5905	88.6	189	1050	26.25	98.71
2/14/2010	971	5915	88.8	187	1050	25.97	98.70
2/15/2010	974	5892	98.1	189	1070	26.25	98.74
2/16/2010	977	5921	97.6	186	1090	25.83	98.75
2/17/2010	980	5902	98.2	187	1090	25.97	98.76
2/18/2010	970	5837	96.8	186	1090	25.83	98.80
2/19/2010	981	5874	91.5	184	1090	25.56	98.78
2/20/2010	978	5782	95.1	203		28.19	98.73
2/21/2010	983	5732	95.7	203	1090	28.19	98.64
2/22/2010	970	5762	85	196	1060	27.22	
2/23/2010	970	5778	87.2	196	1050	27.22	98.88
2/24/2010	969	5733	87.2	191	1040	26.53	98.89
DATE	FEED		PERM		TOTAL PRESS Kpa	Flux	Rejection
	FLOW L/HR	COND μ/SCH	COND μ/SCH	FLOW L/HR			
10/2/2009	1111.2	6809	544	273	900	37.92	98.78
10/3/2009							
10/4/2009	1127.2	6783	542	277	900	38.47	98.85
10/5/2009	1129.9	4741	483	283	900	39.31	98.83
10/6/2009	1121.7	6740	476	286	900	39.72	98.83
10/7/2009	1125.6	6761	517	273	900	37.92	98.12
10/8/2009	1118.8	6745	505	273	900	37.92	98.07
10/9/2009	1130.3	4717	483	276	900	38.33	98.09
10/10/2009	1131.2	4701	473	275	900	38.19	98.06
10/11/2009	1134.7	6711	426	282	900	39.17	98.08

10/12/2009	1133.5	6674	457	278	900	38.61	98.08
10/13/2009	1117.4	6595	447	274	900	38.06	98.10
10/14/2009	1129.5	6601	405	288	900	40.00	98.12
10/15/2009	1129.4	6662	343	276	900	38.33	98.12
10/16/2009							
10/17/2009							
10/18/2009							
10/19/2009							
10/20/2009							
10/21/2009							
10/22/2009	1113.3	6588	298	293	1000	40.69	98.34
10/23/2009	1109.4	6437	263	290	999	40.28	98.35
10/24/2009	1117.4	6442	261	295	1000	40.97	98.35
10/25/2009	1114.5	6470	237	284	1000	39.44	98.03
10/26/2009	1123.2	6474	236	291	1000	40.42	98.35
10/27/2009	1128.4	6473	226	292	1000	40.56	98.38
10/28/2009	1113.3	6508	208	289	1003	40.14	98.36
10/29/2009	1128.8	6409	199.7	289	1003	40.14	98.36
10/30/2009	1116.4	6505	193.9	290	1005	40.28	98.18
10/31/2009	1114.2	6509	202	219	810	30.42	98.31
11/12/2009	971	6171	181	247	910	34.31	98.31
11/13/2009	979	6173	168.8	233	920	32.36	98.27
11/14/2009	962	6325	158.3	233	940	32.36	98.31
11/15/2009	939	6351	152.3	231	999	32.08	98.32
11/16/2009	995	6364	151.6	231	990	32.08	98.26
11/17/2009	966	6425	155.4	241	1000	33.47	98.31
11/18/2009	968	6391	155.9	242	1000	33.61	98.62
11/19/2009	979	6337	154.5	247	1000	34.31	98.57
11/20/2009	979	6370	155.1	245	1000	34.03	98.59
11/21/2009	979	6403	147.3	247	1000	34.31	98.63
11/22/2009	949	6454	149.1	247	1000	34.31	98.62
11/23/2009	978	6366	137.3	247	1000	34.31	98.61
11/24/2009	952	6377	158.9	244	1000	33.89	98.59
11/25/2009	958	6445	156.5	246	1000	34.17	98.44
11/26/2009							
11/27/2009							
11/28/2009	951	6377	145.8	242	999	33.61	98.63
11/29/2009	955	6410	142.1	241	999	33.47	98.64
11/30/2009	958	6396	139.6	240	999	33.33	98.66
11/31/2009	959	6387	137.1	241	999	33.47	98.67
12/1/2009	959	6369	137.4	241	999	33.47	98.69
12/2/2009	978	6378	135.2	244		33.89	98.68
12/3/2009							
12/4/2009	971	6297	164.1	211	990	29.31	98.73
12/5/2009	959	6406	144.5	244	990	33.89	98.75
12/6/2009	973	6313	132.5	249	999	34.58	98.77
12/7/2009	971	6302	132.5	247	996	34.31	98.76
12/8/2009	970	6317	127.1	250	997	34.72	98.77
12/9/2009						34.72	98.78
12/19/2009	971	5541	155	207	995	28.75	98.78
12/20/2009	941	5910	120.8	253	999	35.14	98.77
12/21/2009	974	6036	120.7	259	999	35.97	98.66
12/22/2009						35.14	98.69
12/23/2009	968	6050	113.9	232	995	32.22	98.67
12/24/2009	961	6024	116	233	999	32.36	98.70
12/25/2009	967	6053	115.8	233	995	32.36	98.71
12/26/2009	984	5993	116.1	234	995	32.50	98.70
12/27/2009	977	5964	114.4	236	994	32.78	98.74

12/28/2009	966	5963	114.6	220	996	30.56	98.75
12/29/2009	973	6107	116.2	235	995	32.64	98.76
12/30/2009	979	6209	116.5	234	998	32.50	98.80
12/31/2009	973	6044	113.8	235	997	32.64	98.78
1/1/2010	965	5953	112.5	237	995	32.92	98.73
1/2/2010	982	5914	123.8	219	999	30.42	98.64
1/3/2010	979	5933	106.2	248	999		
1/4/2010	982	5935	105.1	239	999	33.19	98.88
1/5/2010	982	5941	101.1	243	999	33.75	98.89
1/6/2010	976	5895	100.4	241	999	33.47	98.91
1/7/2010	972	5937	98.6	241	999	33.47	98.91
1/8/2010	974	5918	97.8	241	999	33.47	98.78
1/9/2010	970	5893	97.4	245	999	34.03	98.89
1/10/2010	974	5899	116.5	210	999	29.17	98.85
1/11/2010	982	5913	97.4	244	999	33.89	98.83
1/12/2010	974	5909	95.5	246	998	34.17	98.83
1/13/2010	967	5879	96.6	246	998	34.17	98.12
1/14/2010						34.17	98.07
1/15/2010	971	5940	107.9	229	998	31.81	98.09
1/16/2010	971	5978	101	234	999	32.50	98.06
1/17/2010	972	6048	102.3	229	999	31.81	98.08
1/18/2010	971	5976	103.5	239	1000	33.19	98.08
1/19/2010	985	6066	102.3	236	1000	32.78	98.10
1/20/2010	971	6109	102.8	234	1000	32.50	98.12
1/21/2010		6005	104.4	238	1000	33.06	98.12
1/22/2010	914	5958	100.8	243	1000	33.75	98.11
1/23/2010	973	5876	80.8	226	1000	31.39	97.91
1/24/2010	986	5845	83.3	235	1000	32.64	98.21
1/25/2010	970	5700	80.3	237	1000	32.92	98.23
1/26/2010	972	5678	77.9	241	1000	33.47	98.30
1/27/2010	968	5780	80	240	1000	33.33	98.30
1/28/2010	972	5850	81.2	237	1030	32.92	98.34
1/29/2010	971	5856	82.7	235	1050	32.64	98.35
1/30/2010	978	5869	91.5	230	1050	31.94	98.35
1/31/2010	914	5848	81.2	238	1000	33.06	98.03
2/1/2010	973	5857	80.7	238	1000	33.06	98.35
2/2/2010	986	5868	80.4	237	1000	32.92	98.38
2/3/2010	970	5859	79.9	237	1000	32.92	98.36
2/4/2010	972	5869	78.7	236	1000	32.78	98.18
2/5/2010	968	5833	77.5	238	1000	33.06	98.18
2/6/2010	972	5865	77	237	1000	32.92	98.31
2/7/2010	971	5853	77.3	235	1030	32.64	98.31
2/8/2010	978	5831	75.8	237	1050	32.92	98.27
2/9/2010	979	5847	74.1	236	1050	32.78	98.31
2/10/2010	978	5834	73	235	1050	32.64	98.32
2/11/2010	972	5874	72.3	234	1050	32.50	98.26
2/12/2010	971	5842	72.3	232	1050	32.22	98.31
2/13/2010	972	5832	71.8	233	1050	32.36	98.62
2/14/2010	974	5823	70.9	234	1050	32.50	98.57
2/15/2010	969	5809	71.1	231	1050	32.08	98.59
2/16/2010	963	5843	71.6	230	1050	31.94	98.63
2/17/2010	974	5832	78.2	223	1010	30.97	98.62
2/18/2010	986	5982	78.1	221	1010	30.69	98.61
2/19/2010	960	5872	78.2	222	1010	30.83	98.59
2/20/2010	984	5918	76.7	222	1010	30.83	98.44
2/21/2010	974	5909	76.2	221	1050	30.69	98.61
2/22/2010	973	5904	76.9	218	1050	30.28	98.62
2/23/2010	981	5886	74.1	223	1070	30.97	98.63

2/24/2010	966	5913	73.8	221	1090	30.69	98.64
2/25/2010	976	5839	72.2	222		30.83	98.66
2/26/2010	972	5838	70.3	222		30.83	98.67
2/27/2010	965	5787	70.5	222	1090	30.83	98.69
2/28/2010	981	5736	72.9	210	1050	29.17	98.68
3/1/2010	978	5741	78.1	224	1090	31.11	98.70
3/2/2010	971	5768		225	1050	31.25	98.73
3/3/2010	967	5810	64.9	225		31.25	98.75